Published in final form in Molecular Psychiatry
Accessible at http://www.nature.com/mp/journal/v20/n3/full/mp201421a.html

Astrocytic abnormalities and global DNA methylation patterns in depression and suicide.

Corina Nagy, B.Sc.[1,2], Matthew Suderman, Ph.D.[45] Jennie Yang , M.Sc.[1], Moshe Szyf, Ph.D.[5,6] Naguib Mechawar, Ph.D.[1,2,3], Carl Ernst, Ph.D.[1,3], Gustavo Turecki, M.D, Ph,D.[1,2,3].

Affiliations at McGill University:

1. McGill Group for Suicide Studies, Douglas Mental Health University Institute

2. Integrated Program in Neuroscience

3. Department of Psychiatry

4. McGill Centre for Bioinformatics

5. Sackler Program for Epigenetics & Developmental Psychobiology

6. Department of Pharmacology and Therapeutics

Correspondance**:**

Gustavo Turecki MD PhD
McGill Group for Suicide Studies,
Douglas Mental Health University Institute
6875 Lasalle boul.
Montreal, Qc
H4H 1R3
Canada

Abstract

Astrocytes are glial cells specific the central nervous system involved in numerous brain functions including regulation of synaptic transmission and of immune reactions. There is mounting evidence suggesting astrocytic dysfunction in psychopathologies such as major depression, however, little is known about the underlying etiological mechanisms. Here we report a two-stage study investigating genome-wide DNA methylation associated with astrocytic markers in depressive psychopathology. We first characterized prefrontal cortex samples from 121 individuals (76 who died during a depressive episode and 45 healthy controls) for the astrocytic markers *GFAP, ALDH1L1*, *SOX9, GLUL, SCL1A3, GJA1*, and *GJB6*. A subset of 22 cases with consistently downregulated astrocytic markers was then compared to 17 matched controls using MBD2-sequencing followed by validation with high resolution melting and bisulfite Sanger sequencing. With these data, we generated a genome-wide methylation map unique to altered astrocyte-associated depressive psychopathology. The map revealed differentially methylated regions (DMRs) between cases and controls, the majority of which displayed reduced methylation levels in cases. Among intragenic DMRs, *GRIK2* and *BEGAIN* were the most significant, and also significantly correlated with genes expression. Cell sorted fractions were investigated and demonstrated an important non-neuronal contribution of methylation status in *BEGAIN.* Functional cell assays revealed promoter and enhancer-like properties in this region, which were markedly decreased by methylation. Furthermore, a large number of our DMRs overlapped known ENCODE identified regulatory elements. Taken together, our data indicate significant differences in the methylation patterns specific to astrocytic dysfunction associated with depressive psychopathology, providing a potential framework for better understanding this disease phenotype.

Keywords: Astrocytes, mental Health, DNA methylation, epigenomics, genetics, depression.

Introduction

Glial cells account for at least 75% of brain cells [1], and are implicated in a range of psychiatric disorders, including alcoholism [2], schizophrenia [3], depression[4] and suicide [5, 6]. In particular, astrocytic dysfunction is evident in depressive psychopathologies, including suicide[4]. Astrocytes are multifaceted cells with numerous functions, including regulation of blood flow, synaptic communication and plasticity, immune regulation [7] and maintenance of neuronal functioning[8]. These - and other - physiological roles are likely impacted in depression and suicide given evidence from postmortem and animal studies showing altered astrocytic morphologies [5] and persistently decreased expression of astrocyte-specific genes, such as glial fibrillary acidic protein (GFAP) [9], glutamine synthetase (GLUL)[10], the glial high affinity transporters, SLC1A2 and SLC1A3 [10], aquaporin 4 (AQP4) [11] and the connexin genes Cx30 and Cx43 [6].

Despite consistent reports, little is known about the underlying etiological mechanisms linking astrocytic dysfunction to depression and suicide. These could involve epigenetic factors such as DNA methylation, which stably modulates gene expression. Indeed, DNA methylation changes at specific genomic loci are associated with increased risk of psychopathology [12, 13]. The purpose of the current study was to identify DNA methylation patterns associated with astrocytic alterations in depression and suicide. To this end, we characterized expression of astrocytic markers *GFAP, ALDH1L1, SLC1A3, GJA1, GJB6*, *GLUL* and *SOX9* in the dorsolateral prefrontal cortex of individuals having died by suicide and sudden death controls. For all subjects with consistent and pronounced down-regulation of astrocytic markers, we conducted methylation binding domain (MBD) enrichment coupled with next-generation sequencing. Our results suggest a framework to better understand how astrocyte dysfunction impacts depression and suicide.

Materials and Methods

Brain samples, clinical characterization and group composition

Brain tissue was obtained from the Douglas-Bell Canada Brain Bank (DBCBB; http://www.douglas.qc.ca/page/brain-bank). The DBCBB recruits suicide cases and sudden death control subjects. To avoid prolonged agonal states, both cases and controls recruited to the bank cannot undergo resuscitation procedures or medical intervention. Brain tissue for the DBCBB is collected after consent is obtained from next-of-kin. Families are recontacted after approximately 4 months to undergo a series of structured interviews, known as psychological autopsies, with the person best acquainted with the deceased, as described elsewhere [14]. Interviews are supplemented with information from archival material obtained from hospitals, the Coroner's office or social services. Following the interviews, clinical vignettes are produced and assessed by a panel of clinicians to generate DSM-IV diagnoses. This is a well-accepted and valid procedure to obtain clinical information on deceased individuals through proxy-based interviews[15, 16].

Cases in this study were individuals who died by suicide as determined by the Coroner, and following psychological autopsies met criteria for major depressive disorder or had no axis I, but with evidence of depressive symptoms at the moment of death. Controls were individuals who died suddenly in motor vehicle accidents or by cardiac arrest, and did not have evidence of axis I disorders. For preliminary screening, we included 121 brain samples (76 cases) and tested two cortical brain regions. Low expressors were identified using tissue from Brodmann area (BA) 10 then replicated in tissue from BA 8/9. Only tissue from the left hemisphere (grey matter only) was used. These cortical regions are consistently implicated in depression [17-20] and are involved in higher order functioning such as decision-making, that is impaired in suicide [21].

The second part of this study used expression profiles to define the case group. Specifically, at least 5 of the 7 genes investigated had to be in the lowest quartile (n=22) of expression (SI Figure 1-3). Controls were selected based on age, gender and PMI to group match the suicide group; gene expression was not used to select controls. The average PMI (± S.E.M) for controls was 18.8 (± 2.91) and cases 17.7 (±4.48). The average age of controls was 41.3 (±5.87) and suicides 41.0 (±2.64) and the average RIN for controls was 6.2 (±0.16) and suicide 6.4 (±0.16). There was no significant difference between groups for any of these variables. This study was approved by the Douglas Institute Research Ethics Board.

Methods for histological sectioning, gene expression analysis, methylation binding domain protein sequencing (MBD-Seq), sequencing analysis, ENCODE analysis, high resolution melting and site-specific bisulfite sequencing, fluorescence assisted cell sorting (FACs), and functional cell assays can be found in the online supplemental information (SI Methods).

Results

Identification of cases with low expression of astrocyte-related genes

To identify subjects with potential astrocytic dysfunction, we screened prefrontal cortical (PFC) samples obtained from the DBCBB for expression levels of genes exclusively or primarily expressed in astrocytes. This initial screen was conducted on 121 subjects (87 males), including 76 individuals who died by suicide, and 45 sudden death controls. We selected the following 7 genes for screening based on their high expression in astrocytes: *GFAP*, *ALDH1L1*, *SOX9*, *GLUL*, *SCL1A3*, *GJA1,* and *GJB6,* all showing significantly decreased expression in cases compared to controls (Figure 1). To demonstrate that these results specifically reflected a decrease in astrocyte gene expression, we examined the level of NeuN (aka *RBFOX3*), a well-known marker of neurons [22] and found no significant difference between cases and controls (Figure 1h).

Epigenetic factors are known to regulate gene expression and may contribute to the astrocytic dysfunction observed in our cases. Specifically, we hypothesized that DNA methylation patterns differ between groups. To test this, we conducted a genome-wide methylation sequencing study focusing on individuals with the most severe molecular phenotype. We selected cases showing the lowest mRNA expression levels of the astrocyte marker genes used for screening, and operationally defined extreme cases by expression levels in the bottom quartile for at least 5 of the 7 genes; 22 cases met these criteria (SI Figures 1-5, SI Tables 1-2). Cases were compared with 17 psychiatrically normal controls grouped-matched according to age, RIN, post-mortem interval and gender. To decrease variability, all subjects included in the analysis were males.

Generation of high quality genome-wide MBD2-seq profiles

We performed genome-wide DNA methylation analysis by isolating fragmented DNA using biotinylated-MBD2. The MBD2 protein specifically targets densely methylated CpGs [23] and does not target hydroxymethylated cytosines [23, 24] thus sequencing MBD2-enriched DNA identifies methylated regions from the whole genome. Comparing the number of sequenced reads matching each region enabled us to identify methylation differences between cases and controls. Many quality control steps where preformed to insure high quality (SI Figures 6-7 SI Table 3)

In total, we obtained nearly 450 million reads, and mean read counts were similar between groups (Student T test, p=0.85) (SI Table 4). Our reads provided 20x coverage per base for the MBD enrichment (SI Figure 8). We assessed our data for genomic metrics, irrespective of disease status. First, we assessed the consistency of sequencing data by measuring overall methylation levels at specific genomic features. DNA methylation levels were consistent with expectations at all genomic loci assessed: CpG islands showed the least amount of methylation, first exons showed less methylation than other exons and imprinted regions showed increased levels of methylation (Figure 2a, Wilcoxin rank-sum, p< 2E10-22).

Second, to validate the enrichment of methylated reads and to confirm bioinformatic processing, we selected regions of the genome identified in sequencing data as either highly methylated or poorly methylated and re-performed MBD2 enrichment reactions using identical DNA samples as the initial sequencing reaction. We found that levels identified as highly methylated in the sequencing reaction gave the lowest Ct values in qRT-PCR analysis, and the opposite was found in genomic regions with low methylation (region 1: r=-0.81, t=0.025; region 2 r=-0.74, t=0.047; region 3: r= -0.61, t=0.09) (SI Figure 9).

Differentially methylated regions in cases and controls

After ensuring quality and accuracy of MBD2 enrichment, we assessed case and control group differences. There were 115 differentially methylated regions (DMRs) across the genome. Of these, 33.91% (N = 34) were found in genes, almost all intragenic and falling within introns (N= 31; 31.3%). Nearly 11% (N=14) of DMRs were within promoters, defined as sequences up to 5Kb upstream of transcription start sites (Figure 2b). However, the majority of DMRs were found in intergenic regions 56.6% (N=66).

As expected, the number of reads mapping back to each chromosome strongly correlated with their size (spearman r=0.83, p< 0.0001), while there was no difference in the contribution of each group to chromosome coverage (SI Figure 10a,b). We found no relationship between chromosome size and location of DMR, i.e., DMRs were independent of size and read count (Spearman r= -0.15, p=0.48) (SI Figure 10c).

Most DMRs were hypomethylated in cases. There was considerable decrease in methylation within the gene body of cases; 58.8% of the within gene DMRs were less methylated in cases compared to controls, and these results were consistent in the intergenic regions, where a similar percentage of DMRs were hypomethylated (57.6%) (Figure 2c).

We observed two genomic regions enriched with DMRs clusters: one on chromosome 10 and another on the X chromosome (Fisher's exact test, FDR < 0.05; SI Table 5 and SI Figure 11). The DMRs in these two regions overlapped strongly with ENCODE elements suggesting potentially important regulatory roles [25].

Functional relevance of DMRs derived from ENCODE data

Using publically available data from the Encyclopedia of DNA elements (ENCODE), we performed an in-silico assessment of the regulatory potential of each DMR by identifying overlaps with ENCODE features. Altogether, we assessed 41 ENCODE features which include histone modifications and DNA binding proteins known to influence gene transcription. Our analysis showed enrichment for 37 of the 41 features in hypomethylated regions (Fisher's exact test average $p < 4.82E-03$, SI Table 6); however, there was no enrichment in hypermethylated sites. Nearly half the DMRs contained at least one ENCODE feature (Figure 3a). Histone 3 lysine 4 trimethylation (H3K4me3), a chromatin modification enriched in gene promoters and most often associated with euchromatin and active transcription[26], and DNase I hypersensitivity sites (DHSs) which are associated with many *cis*-regulatory elements including promoters, enhancers, insulators, silencers and locus control regions[27], overlapped most frequently with the DMRs (Figure 3b). Both features overlapped with 22.6% of DMRs. As DHSs have been shown to precede promoter regions marked by H3K4me3 [27], it was not surprising that most DHS sites overlapped with H3K4me3. We found 4 DMRs with an impressive overlap of 20 or more ENCODE features. These regions were found in the pericentromeric region of 4 different chromosomes (4,7,16 and 21). One of the most conserved functions of DNA methylation is stabilizing pericentromeric repeats by inhibiting their latent transcriptional potential [28]. Moreover, decondensing of these heterochromatic regions can result in illegitimate rearrangements [29], therefore hypomethylation in these regions often lead to notable consequences.

To assess the permissive or inhibitory relationship of the ENCODE data with our data, we grouped the ENCODE features into active or repressive marks based on their known function (SI Tables 6-8). The distribution of DMRs falling into each category was

comparable, with 45% overlapping repressive elements and 55% overlapping active elements.

Differentially methylated astrocytic genes

As our subjects were selected based on astrocytic expression patterns, we were interested in potential associations between DMRs and astrocyte and/or astrocyte-regulatory genes. To assess whether these genes were associated with DMRs, we conducted gene ontology analyses focusing on genes highly expressed in astrocytes and genes coding for regulatory factors of astrocytic expression. There were 4 astrocyte-associated genes coded within regions of differential methylation (Table 1), containing multiple sites of differential methylation. These represented 21% of the gene-associated DMRs.

Gene specific validation of DMRs showed inverse correlation to gene expression levels.

We validated the most significant DMRs, focusing on the DMRs related to astrocytic function (Table 1) and the complete intragenic DMRs (SI Table 10). These DMRs were, respectively, in *GRIK2* and *BEGAIN* (Figure 4a-b). *GRIK2* is implicated in astrocytic function and has been associated with mood disorders [30-33], whereas *BEGAIN* is associated with cellular communication[34]. For validation, we performed both bisulfite cloning (Bs-Cloning) and High Resolution Melting analysis (HRM). In both cases, DMRs were consistent with the MBD-seq analysis, though as expected, HRM showed less sensitivity. HRM results are presented in figure 4c and 4g, and show significant differences for both GRIK2 (Student T-test, $p=0.02$) and *BEGAIN* (Student t-test, $p=0.007$) in the same direction observed with the MBD-Seq data. With Bs-cloning, we achieved base-pair resolution of methylation levels for *GRIK2* and *BEGAIN,* which strongly supported the MBD-Seq data. (Figures 4d, h and SI Table 9a and b). Next, we measured expression levels for each gene, finding an increase in *GRIK2* expression

in cases (Figure 4f, p=0.012). For *BEGAIN,* there are two major transcripts with little known about their expression patterns. We investigated brain and peripheral tissues, and found that variant 1 has increased expression in the brain (Figure 4j). When we assessed expression of *BEGAIN* transcripts, we observed a marked decrease of variant 1 in cases (2.3 fold decrease, p<0.0001), while variant 2 remained unchanged (Figure 4k-l). Analysis of cluster CpGs methylation and expression showed a significant inverse correlation for both *GRIK2* (Figure g, r=-0.37, p<0.05) and *BEGAIN* (Figure 4n, r=-0.37, p<0.05), suggesting a role for methylation regulating expression in these genes.

Non-Neuronal cells from case samples drive methylation difference in *BEGAIN*

As DNA methylation is known to be cell-type specific, we used fluorescence assisted cell sorting to separate tissue homogenates into neuronal and non-neuronal fractions. While it is currently methodologically challenging to isolate astrocytic fractions from frozen tissue, the non-neuronal fraction is primarily composed of astrocytes as they make up the bulk of non-neuronal cells of the human brain. We collected nuclei marked with NeuN and unmarked nuclei for all samples. DNA from each fraction was directly bisulfite converted, then subjected to cloning and Sanger sequencing as for validation of brain homogenates. For *GRIK2,* we observed no difference in methylation across cell types (SI Figure 14d), however, for *BEGAIN* we observed a marked increase of methylation for cases in the non-neuronal fraction, suggesting that the sizeable difference in methylation between cases and controls was largely driven by non-neuronal cells (Figure 4j, one-way anova, $F(3, 32) = 10.74$, $P < 0.0001$).

DNA methylation in DMR represses transcription

Considering the strong increase of methylation detected in both the homogenate and non-neuronal cellular fraction of BEGAIN, we decided to assess this region in a functional cell

assay to determine the direct consequences of methylation. As suggested by the CHROMHMM from ENCODE (SI Figure 15), this region of *BEGAIN* has both promoter and enhancer capabilities, therefore the 474bp amplicon was inserted into 2 separate CpG-free vectors, one containing no endogenous promoter (Figure 5a) to test potential promoter activity and a second under the control of the human EF-1α promoter to test enhancer-like activity (Figure 5b). The inserted amplicons were either fully methylated or fully unmethylated, the report assays were performed in quintuplicate and repeated twice independently. This 474bp region of *BEGAIN* clearly showed promoter activity, which was fully repressed by methylation (Figure 5c Kruskal Wallis =19.94, d.f, 3, $p<0.0001$, SI Figure 15a-b). Equally, when this region of *BEGAIN* was inserted in an enhancer position next to the human EF-1α promoter, methylation caused complete loss of reporter gene expression (Figure 5d, Kruskal Wallis= 22.15, d.f, 3, $p<0.0001$, SI Figure 15c-d). These results indicate a potent effect of DNA methylation on this region of BEGAIN and suggest a potentially causative role of methylation in the downregulation of the *BEGAIN* variant 1 we observed in cases with astrocytic dysfunction.

Discussion

In this study, we investigated genomic DNA methylation patterns that may contribute to astrocyte dysfunction in depression and suicide. First, we characterized groups for their expression profile of several astrocyte-associated genes in the prefrontal cortex. Subsequently, we conducted MBD-Seq focusing on cases with clear astrocytic dysfunction at a molecular level. The profiles generated in our study revealed differential DNA methylation at multiple loci, including ENCODE associated regulatory sequences. In following-up our top intragenic DMRs we were able to replicate our findings using two independent techniques, and in addition, we found that the methylation differences correlated with gene expression changes. Furthermore we demonstrated that in cases, non-neuronal cells drive methylation changes observed in *BEGAIN.* Lastly, we showed through functional cell assays that methylation of our isolated region in *BEGAIN* almost completely abolishes reporter gene expression in vitro. This is, to our knowledge, the first study using next-generation sequencing to investigate genome-wide differential methylation associated with depression and suicide.

Most DNA methylation studies use candidate approaches; among the strengths of the current study is the genome-wide approach coupled by DNA sequencing. Studies in rats and humans have shown discrete regions of hypermethylation associated with behavioural phenotypes and transcriptional regulation [35, 36]. These studies used candidate gene approaches or were focused on promoter sequences [37]. In the present study, we avoided restricting our analyses to promoter regions, and provided an unbiased view of DNA methylation associated with depressive psychopathology and suicide. About 90% of the DMRs were found in non-promoter regions where the relationship with expression is variable. We found many DMRs in gene bodies, where methylation is commonly associated with active transcription [38]. Our results are consistent with a regulatory mechanism for

repressing transcription in these regions. For example, a reduction of gene body methylation can result in *de novo* histone modifications [39] that decrease transcription. As many of the DMRs in this study were found within gene bodies and intergenically, hypomethylation may result in gene repression.

Our study provides valuable information about often-overlooked regions of the genome [40]. In support of our findings, most variability in methylation occurs in gene bodies and intergenic regions, rather than promoters and upstream regulatory regions [41]. We identified two cluster regions, on chromosome 10 and the X chromosome, where DMRs fell primarily on short (SINEs) and long interspersed element (LINEs). DNA methylation maintains the stability of the genome by silencing these mobile elements [42]. Decreased methylation and increased expression of these elements could disrupt gene transcription. In addition, reduced methylation in these clusters could alter associated chromatin [43]. Moreover, four of the DMRs that we found within pericentromeric regions overlapped with over 20 ENCODE elements, representing regions under extensive epigenetic control. Abnormal methylation in these regions is implicated in developmental disorders [44] suggesting important functional consequences [45] .

Among intragenic DMRs, we selected two according to significance for additional work: GRIK2 and BEGAIN. GRIK2 codes for glutamate ionotropic kainate receptor, which is a ligand-gated cation channel. This channel is associated with grey and white matter astrocytes [30], and altered calcium signaling in response to antidepressants[32]. *GRIK2* has been previously associated with psychiatric or neurological disorders[30-32, 49], including with depression[30-32]. Our combined data showed that *GRIK2* is hypomethylated in intron 13 in cases as compared to controls, and we suspect that this intronic region of hypomethylation

may influence alternative splicing of GRIK2 [50], potentially favoring the protein isoform with reduced permeability calcium signaling, however additional work is required to explore this hypothesis.

BEGAIN (brain-enriched guanylate kinase-associated protein), on the other hand, showed on average a 3-fold increase in methylation in cases, representing one of the strongest changes reported to date in psychiatric phenotypes. *BEGAIN*, is poorly studied in humans, but has been associated with diabetes and autoimmune disorders [51] an interesting finding considering the growing evidence for the inflammatory basis of depression[52, 53] and the role of astrocytes in the regulation of neuroinflammation [54].In addition, a study in rats has shown increased *BEGAIN* expression in the frontal pole in response to prenatal stress as a paradigm for the etiology of schizophrenia. [55]. BEGAIN is highly associated to the postsynaptic density proteins, and particularly to the postsynaptic density 95 (PSD95)[34, 56, 57], having 90% co-localization with PSD95 [56], and a role in sustaining the structure of this scaffolding protein [58]. PSD95 is the protein found in the postsynapic dendritic heads of excitatory synapses, and has been implicated in the coordination of the downstream communication of glutamate receptors, including GRIK2, through the binding of PSD95 to its guanylate kinase domains [59]. Recently, it has been shown that the astrocytes forming part of this excitatory synapse may play an important role in regulating the excitatory/inhibitory balance of neurons through PSD95 [60]. The epigenetic alterations to *BEGAIN* and *GRIK2* and their association to astrocytically mediated PSD95, suggests possible defective synaptic communication and/or synaptic plasticity [57].

Interestingly, our two top hits are involved in synaptic communication and regulation [34, 61]. Whereas GRIK2 is known to be expressed in astrocytes and to be directly involved in astrocyte-mediated responses to antidepressant drugs [31, 32, 49], *BEGAIN* has no known association to astrocytes. However, as the primary contribution of methylation was found in

non-neuronal cells, it appears that astrocytes have a functional role in the regulation of this gene via methylation alterations. Otherwise, this would not be the first time that changes to genes in astrocytes at an epigenetic level are seen to influence normal neuronal function. For instance, Tao and colleagues showed that selectively knocking-out Dicer in astrocytes leads to neuronal dysfunction and degeneration [62]. Thus far BEGAIN has been investigated and localized in nuclei and synapses of neurons [56], but there is no information on its relation to astrocytes. Much like GRIK2, BEGAIN could play an important role in both cell types. Since BEGAIN is thought to maintain the structure of the post-synaptic density it would be interesting to see if the strong reduction of its transcript results in altered dendritic morphology as has become one of the emerging theories of autism, schizophrenia and Alzheimer's [63]. This study has opened the door to this and many other questions.

Our study is not without limitations. MBD2 has a higher affinity to densely methylated CpGs than antibody-based approaches; therefore we may be missing single base pair differences. Conversely, MBD is able to discriminate between 5' hydroxymethylcytosine and 5' methylcytosine [24] with greater efficiency than the monoclonal antibody directed against 5-methylcytidine [64]. Regarding our sample selection, altered transcription is often used as a marker for astrocytic dysfunction [6, 9, 10], however, astrocyte dysfunction can be defined in many ways and may not be reflected by gene expression differences. Finally we limited this study to DNA methylation changes and thus did not examine other epigenetic mechanism that may be involved in gene regulation. Despite these limitations, our study produced a list of differentially methylated regions showing clear evidence of astrocytic dysfunction in individuals who were depressed and died by suicide. Furthermore we identified two genes involved in synaptic communication, *GRIK2* and *BEGAIN,* which appear to be regulated by DNA methylation in cases with astrocytic dysfunction. Each DMR identified here provides

avenues for further investigation of the pathophysiological mechanisms underlying astrocytic dysfunction in mood disorders.

Acknowledgments: We thank the members of the next generation sequencing platform at Genome Quebec, and acknowledge the expert help of the DBCBB staff. C.N is supported by a scholarship from the FRQS. CE is supported by the Canada Research Chairs program. NM is a CIHR New Investigator and Bell Senior Fellow in Mental Health. GT is a national researcher from FRQS. This study was funded by a CIHR operating grant (MOP# 119429).

Supplementary information is available at Molecular Psychiatry's website

References

1. **Kettenmann H, Ransom BR. *Neuroglia*. 2nd edn. Oxford University Press: New York, 2005, xix, 601 p.pp.**

2. **Hercher C, Parent M, Flores C, Canetti L, Turecki G, Mechawar N. Alcohol dependence-related increase of glial cell density in the anterior cingulate cortex of suicide completers. *Journal of psychiatry & neuroscience : JPN* 2009; 34(4): 281-288.**

3. **Bernstein H-G, Steiner J, Bogerts B. Glial cells in schizophrenia: pathophysiological significance and possible consequences for therapy. *Expert review of neurotherapeutics* 2009; 9(7): 1059-1071.**

4. **Rajkowska G, Stockmeier CA. Astrocyte pathology in major depressive disorder: insights from human postmortem brain tissue. *Curr Drug Targets* 2013.**

5. **Torres-Platas S, Hercher C, Davoli M, Maussion G, Labonté B, Turecki G *et al.* Astrocytic hypertrophy in anterior cingulate white matter of depressed suicides. *Neuropsychopharmacology : official publication of the American College of Neuropsychopharmacology* 2011; 36(13): 2650-2658.**

6. **Ernst C, Nagy C, Kim S, Yang J, Deng X, Hellstrom I *et al.* Dysfunction of astrocyte connexins 30 and 43 in dorsal lateral prefrontal cortex of suicide completers. *Biological psychiatry* 2011; 70(4): 312-319.**

7. **Oberheim N, Goldman S, Nedergaard M. Heterogeneity of astrocytic form and function. *Methods in molecular biology (Clifton, NJ)* 2012; 814.**

8. **Sidoryk-Wegrzynowicz M, Wegrzynowicz M, Lee E, Bowman AB, Aschner M. Role of astrocytes in brain function and disease. *Toxicologic pathology* 2011; 39(1): 115-123.**

9. **Si X, Miguel-Hidalgo J, O'Dwyer G, Stockmeier C, Rajkowska G. Age-dependent reductions in the level of glial fibrillary acidic protein in the prefrontal cortex in major depression. *Neuropsychopharmacology : official publication of the American College of Neuropsychopharmacology* 2004; 29(11): 2088-2096.**

10. **Choudary P, Molnar M, Evans S, Tomita H, Li J, Vawter M *et al.* Altered cortical glutamatergic and GABAergic signal transmission with glial involvement in depression. *Proceedings of the National Academy of Sciences of the United States of America* 2005; 102(43): 15653-15658.**

11. **Bernard R, Kerman IA, Thompson RC, Jones EG, Bunney WE, Barchas JD *et al.* Altered expression of glutamate signaling, growth factor, and glia genes in the locus coeruleus of patients with major depression. *Mol Psychiatry* 2011; 16(6): 634-646.**

12. **Turecki G, Ernst C, Jollant F, Labonte B, Mechawar N. The neurodevelopmental origins of suicidal behavior. *Trends Neurosci* 2012; 35(1): 14-23.**

13. **Nagy C, Turecki G. Sensitive periods in epigenetics: bringing us closer to complex behavioral phenotypes. *Epigenomics* 2012; 4(4): 445-457.**

14. **Dumais A, Lesage AD, Alda M, Rouleau G, Dumont M, Chawky N *et al.* Risk factors for suicide completion in major depression: a case-control study of impulsive and aggressive behaviors in men. *Am J Psychiatry* 2005; 162(11): 2116-2124.**

15. **Arsenault-Lapierre G, Kim C, Turecki G. Psychiatric diagnoses in 3275 suicides: a meta-analysis. *BMC Psychiatry* 2004; 4: 37.**

16. **Isometsa ET. Psychological autopsy studies--a review. *Eur Psychiatry* 2001; 16(7): 379-385.**

17. **Sequeira A, Morgan L, Walsh DM, Cartagena PM, Choudary P, Li J *et al.* Gene expression changes in the prefrontal cortex, anterior cingulate cortex and nucleus accumbens of mood disorders subjects that committed suicide. *PloS one* 2012; 7(4): e35367.**

18. **Kang H, Voleti B, Hajszan T, Rajkowska G, Stockmeier C, Licznerski P *et al.* Decreased expression of synapse-related genes and loss of synapses in major depressive disorder. *Nature medicine* 2012; 18(9): 1413-1417.**

19. **Goswami D, Jernigan C, Chandran A, Iyo A, May W, Austin M *et al.* Gene expression analysis of novel genes in the prefrontal cortex of major depressive disorder subjects. *Progress in neuro-psychopharmacology & biological psychiatry* 2012; 43C: 126-133.**

20. **Underwood M, Kassir S, Bakalian M, Galfalvy H, Mann J, Arango V. Neuron density and serotonin receptor binding in prefrontal cortex in suicide. *The international journal of neuropsychopharmacology / official scientific journal of the Collegium Internationale Neuropsychopharmacologicum (CINP)* 2012; 15(4): 435-447.**

21. Kim S, Lee D. Prefrontal cortex and impulsive decision making. *Biol Psychiatry* 2011; 69(12): 1140-1146.

22. Dent M, Segura-Anaya E, Alva-Medina J, Aranda-Anzaldo A. NeuN/Fox-3 is an intrinsic component of the neuronal nuclear matrix. *FEBS letters* 2010; 584(13): 2767-2771.

23. Li N, Ye M, Li Y, Yan Z, Butcher L, Sun J *et al.* Whole genome DNA methylation analysis based on high throughput sequencing technology. *Methods (San Diego, Calif)* 2010; 52(3): 203-212.

24. Mellén M, Ayata P, Dewell S, Kriaucionis S, Heintz N. MeCP2 Binds to 5hmC Enriched within Active Genes and Accessible Chromatin in the Nervous System. *Cell* 2012; 151(7): 1417-1430.

25. Tomilin N. Regulation of mammalian gene expression by retroelements and non-coding tandem repeats. *BioEssays : news and reviews in molecular, cellular and developmental biology* 2008; 30(4): 338-348.

26. Koch C, Andrews R, Flicek P, Dillon S, Karaöz U, Clelland G *et al.* The landscape of histone modifications across 1% of the human genome in five human cell lines. *Genome research* 2007; 17(6): 691-707.

27. Thurman RE, Rynes E, Humbert R, Vierstra J, Maurano MT, Haugen E *et al.* The accessible chromatin landscape of the human genome. *Nature* 2012; 489(7414): 75-82.

28. Lehnertz B, Ueda Y, Derijck AA, Braunschweig U, Perez-Burgos L, Kubicek S *et al.* Suv39h-mediated histone H3 lysine 9 methylation directs DNA methylation to major satellite repeats at pericentric heterochromatin. *Curr Biol* 2003; 13(14): 1192-1200.

29. Dejardin J. How chromatin prevents genomic rearrangements: locus colocalization induced by transcription factor binding. *Bioessays* 2012; 34(2): 90-93.

30. Brand-Schieber E, Werner P. AMPA/kainate receptors in mouse spinal cord cell-specific display of receptor subunits by oligodendrocytes and astrocytes and at the nodes of Ranvier. *Glia* 2003; 42(1): 12-24.

31. Li B, Zhang S, Li M, Zhang H, Hertz L, Peng L. Down-regulation of GluK2 kainate receptor expression by chronic treatment with mood-stabilizing anti-

convulsants or lithium in cultured astrocytes and brain, but not in neurons. *Neuropharmacology* 2009; 57(4): 375-385.

32. Li B, Zhang S, Zhang H, Hertz L, Peng L. Fluoxetine affects GluK2 editing, glutamate-evoked Ca(2+) influx and extracellular signal-regulated kinase phosphorylation in mouse astrocytes. *Journal of psychiatry & neuroscience : JPN* 2011; 36(5): 322-338.

33. Li H, Durbin R. Fast and accurate long-read alignment with Burrows-Wheeler transform. *Bioinformatics (Oxford, England)* 2010; 26(5): 589-595.

34. Deguchi M, Hata Y, Takeuchi M, Ide N, Hirao K, Yao I *et al.* BEGAIN (brain-enriched guanylate kinase-associated protein), a novel neuronal PSD-95/SAP90-binding protein. *The Journal of biological chemistry* 1998; 273(41): 26269-26272.

35. Weaver IC, Diorio J, Seckl JR, Szyf M, Meaney MJ. Early environmental regulation of hippocampal glucocorticoid receptor gene expression: characterization of intracellular mediators and potential genomic target sites. *Ann N Y Acad Sci* 2004; 1024: 182-212.

36. Labonte B, Yerko V, Gross J, Mechawar N, Meaney MJ, Szyf M *et al.* Differential glucocorticoid receptor exon 1(B), 1(C), and 1(H) expression and methylation in suicide completers with a history of childhood abuse. *Biol Psychiatry* 2012; 72(1): 41-48.

37. Labonte B, Suderman M, Maussion G, Navaro L, Yerko V, Mahar I *et al.* Genome-wide epigenetic regulation by early-life trauma. *Arch Gen Psychiatry* 2012; 69(7): 722-731.

38. Meissner A, Mikkelsen T, Gu H, Wernig M, Hanna J, Sivachenko A *et al.* Genome-scale DNA methylation maps of pluripotent and differentiated cells. *Nature* 2008; 454(7205): 766-770.

39. Hahn MA, Wu X, Li AX, Hahn T, Pfeifer GP. Relationship between gene body DNA methylation and intragenic H3K9me3 and H3K36me3 chromatin marks. *PloS one* 2011; 6(4): e18844.

40. Gerstein M, Kundaje A, Hariharan M, Landt S, Yan K-K, Cheng C *et al.* Architecture of the human regulatory network derived from ENCODE data. *Nature* 2012; 489(7414): 91-100.

41. **Consortium EP, Dunham I, Kundaje A, Aldred S, Collins P, Davis C *et al.* An integrated encyclopedia of DNA elements in the human genome. *Nature* 2012; 489(7414): 57-74.**

42. **Carnell AN, Goodman JI. The long (LINEs) and the short (SINEs) of it: altered methylation as a precursor to toxicity. *Toxicological sciences : an official journal of the Society of Toxicology* 2003; 75(2): 229-235.**

43. **Chueh AC, Northrop EL, Brettingham-Moore KH, Choo KH, Wong LH. LINE retrotransposon RNA is an essential structural and functional epigenetic component of a core neocentromeric chromatin. *PLoS Genet* 2009; 5(1): e1000354.**

44. **Xu GL, Bestor TH, Bourc'his D, Hsieh CL, Tommerup N, Bugge M *et al.* Chromosome instability and immunodeficiency syndrome caused by mutations in a DNA methyltransferase gene. *Nature* 1999; 402(6758): 187-191.**

45. **Smith ZD, Meissner A. DNA methylation: roles in mammalian development. *Nat Rev Genet* 2013; 14(3): 204-220.**

46. **Sundaram SK, Huq AM, Sun Z, Yu W, Bennett L, Wilson BJ *et al.* Exome sequencing of a pedigree with Tourette syndrome or chronic tic disorder. *Annals of neurology* 2011; 69(5): 901-904.**

47. **Scharf JM, Miller LL, Mathews CA, Ben-Shlomo Y. Prevalence of Tourette syndrome and chronic tics in the population-based Avon longitudinal study of parents and children cohort. *Journal of the American Academy of Child and Adolescent Psychiatry* 2012; 51(2): 192-201 e195.**

48. **Grupe A, Li Y, Rowland C, Nowotny P, Hinrichs A, Smemo S *et al.* A scan of chromosome 10 identifies a novel locus showing strong association with late-onset Alzheimer disease. *American journal of human genetics* 2006; 78(1): 78-88.**

49. **Li B, Dong L, Fu H, Wang B, Hertz L, Peng L. Effects of chronic treatment with fluoxetine on receptor-stimulated increase of [Ca2+]i in astrocytes mimic those of acute inhibition of TRPC1 channel activity. *Cell calcium* 2011; 50(1): 42-53.**

50. **Wan J, Oliver VF, Zhu H, Zack DJ, Qian J, Merbs SL. Integrative analysis of tissue-specific methylation and alternative splicing identifies conserved**

transcription factor binding motifs. *Nucleic Acids Res* 2013; 41(18): 8503-8514.

51. Wallace C, Smyth D, Maisuria-Armer M, Walker N, Todd J, Clayton D. The imprinted DLK1-MEG3 gene region on chromosome 14q32.2 alters susceptibility to type 1 diabetes. *Nature Genetics* 2010; 42(1): 68-71.

52. Miller AH, Maletic V, Raison CL. Inflammation and its discontents: the role of cytokines in the pathophysiology of major depression. *Biol Psychiatry* 2009; 65(9): 732-741.

53. Raedler TJ. Inflammatory mechanisms in major depressive disorder. *Current opinion in psychiatry* 2011; 24(6): 519-525.

54. Kritz Jasna. Neuron-Astrocyte Interactions in Neuroinflammatin. In: Suzumura Akio KI (ed). *Neuron-Glia Interaction in Neuroinflammation*. Springer: New York, 2013, pp 75-90.

55. Kinnunen A, Koenig J, Bilbe G. Repeated variable prenatal stress alters pre- and postsynaptic gene expression in the rat frontal pole. *Journal of neurochemistry* 2003; 86(3): 736-748.

56. Yao I, Iida J, Nishimura W, Hata Y. Synaptic and nuclear localization of brain-enriched guanylate kinase-associated protein. *The Journal of neuroscience : the official journal of the Society for Neuroscience* 2002; 22(13): 5354-5364.

57. Xu W. PSD-95-like membrane associated guanylate kinases (PSD-MAGUKs) and synaptic plasticity. *Current opinion in neurobiology* 2011; 21(2): 306-312.

58. Deguchi M, Hata Y, Takeuchi M, Ide N, Hirao K, Yao I *et al.* BEGAIN (brain-enriched guanylate kinase-associated protein), a novel neuronal PSD-95/SAP90-binding protein. *J Biol Chem* 1998; 273(41): 26269-26272.

59. Garcia E, Mehta S, Blair L, Wells D, Shang J, Fukushima T *et al.* SAP90 binds and clusters kainate receptors causing incomplete desensitization. *Neuron* 1998; 21(4): 727-739.

60. Wang C-C, Chen P, Hsu C-W, Wu S-J, Lin C-T, Gean P. Valproic acid mediates the synaptic excitatory/inhibitory balance through astrocytes - A preliminary study. *Progress in neuro-psychopharmacology & biological psychiatry* 2012; 37(1): 111-120.

61. **Lerma J, Marques JM. Kainate receptors in health and disease. *Neuron* 2013; 80(2): 292-311.**

62. **Tao J, Wu H, Lin Q, Wei W, Lu XH, Cantle JP *et al.* Deletion of astroglial Dicer causes non-cell-autonomous neuronal dysfunction and degeneration. *J Neurosci* 2011; 31(22): 8306-8319.**

63. **Penzes P, Cahill M, Jones K, VanLeeuwen J-E, Woolfrey K. Dendritic spine pathology in neuropsychiatric disorders. *Nature neuroscience* 2011; 14(3): 285-293.**

64. **Jin S-G, Kadam S, Pfeifer G. Examination of the specificity of DNA methylation profiling techniques towards 5-methylcytosine and 5-hydroxymethylcytosine. *Nucleic acids research* 2010; 38(11).**

Table 1: The list of astrocyte associated genes within the dataset.

These genes were selected based on functions such as cation homeostasis, response to oxidative stress, and glutamatergic synaptic transmission. Genes were supplemented by the addition of genes described by Cahoy et al. [30] as enriched in astrocytes. Some genes have multiple windows of methylation differences; altogether this list represents 7 DMRs of the previously described 34 gene based DMRs (~21%). *Meth status* refers to whether the regions show an increase (↑) or decrease (↓) in methylation. *ENCODE overlap* refers to either DHS or H3K4me3, both or no overlap with the DMR. *Region* describes the general genomic region where the DMR is found for that gene. *Strand* refers to the location of the genes, either on the sense (+) or antisense (−) strand. *Avg log_2 fold change* is the absolute difference of methylation at that site, it is averaged to account for the multiple windows (DMRs) found in the gene. *Avg Adj p value* is the significance of the fold change adjusted to correct for multiple testing, averaged as before. *# of win* is the number of windows found within that gene; a window represents a differentially methylated region. *Function* is a brief functional description of the gene. The list is ranked by DMR containing windows, and then lowest avg adj p value and avg log_2 fold change. * This DMR is technically not in the primary variant of *ROPN18.*

Chr	Gene Name	Meth Status	ENCODE Overlap	Regions	Strand	Avg Log_2 Fold change	Avg Adj P value	# of Win	Function
6	*GRIK2*	↓	None	intronic	+	1.44	0.09	2	Glutamate ionotropic kianate receptor
10	*NEBL*	↓	None	intronic	-	2.00	0.11	2	Actin-binding related protein
3	*PVRL3*	↑	None	intronic	+	2.96	0.08	1	Adhesion molecule at adhesion junctions
*3	ROPN1B	↑	Both	downstream of TES	-	1.04	0.01	2	signal transduction

Figure Legends

Figure 1: **Screening cases and controls for astrocytic genes.**

Strong decrease in expression of astrocyte markers in BA 10 from cases and controls (N=121) using quantitative PCR a) GFAP (mean ± SEM), case (1.17 ± 0.13), control (2.27 ± 0.40) p=0.0068 and b) ALDH1L1 case (1.12 ±0.13), control (2.08 ± 0.31), p=0.0023 c) SOX9 case (1.48± 0.22), control (2.41 ±0.64) p=0.03, d) GLUL case (1.02 ± 0.12), control (1.46 ± 0.21), p=0.01, e) SCL1A3 case (1.63 ± 0.28), control (2.12 ± 0.52), p=0.04, f) GJA1 case (1.17 ± 0.14), p=0.03, g) GJB6 case (1.48 ± 0.23), control (2.41 ± 0.64), p=0.05., h) Expression of RBFOX3 (aka NeuN, a standard marker for mature neuronal identity) shows no difference between groups (p=0.86). (Tests performed were either Student T-test or Mann Whitney, depending on the distribution of the data)

Figure 2: Estimated methylation levels across the genome and level of methylation in case relative to controls.

a) Comparison of DNA methylation levels between cases and controls reveals region specific effects in the human genome. The overall methylation levels were estimated from region read counts. The Wilcoxin rank-sum test was used to determine significance of methylation differences between pairs of region types. Only introns were not different than 3' regions, all other pairs of regions types were significantly differentially methylated (p< 2E10-22). TSS, transcription start site; TES, transcription end site, imprinted genes are based on geneimprint.com, CpG islands are defined as regions with an expected CpG frequency of greater than 60%, a GC content of greater than 50% and a length greater than 200bp. b) the percentage summary of DMRs in known genome regions. c) cases with decreased expression of astrocyte associated genes show a genome-wide pattern of hypomethylation. 63.5% of DMRs were hypomethylated in cases compared to controls.

Figure 3: DMRs overlap with ENCODE data

Strong overlap of DMRs with ENCODE data. a) 44% of DMRs overlap with at least one regulatory feature. a) the breakdown of DMRs overlapping multiple ENCODE features b) the proportion of all queried regulatory features represented within our sample. c) the breakdown of DMRs overlapping with active or repressive regulatory marks.

Figure 4: Gene specific validation of DMRs shows inverse correlation to gene expression levels and FAC sorting shows specific non-neuronal contribution.
Schematic diagrams of each gene highlighting region of methylation difference, the size of amplicon and the number and distribution of CpGs for each a) *GRIK2* and b) *BEGAIN*, respectively. c) HRM results for GRIK2 show a decreased methylation in cases (Unpaired t test, p=0.025). d) Bs-cloning supports MDB-Seq and HRM results showing a cluster of the first 9 CpGs as significantly less methylated in cases (n=21, avg. 17 clones/sample) than controls (n=20, avg. 17 clones/sample) mixed model regression analysis was perform to assess significance of methylation at each CpG, *p<0.05, **p<0.01, ***p<0.001 exact values for pairwise comparison are in SI table 9a and cluster analysis in 9b). e) *GRIK2* expression as measured by relative quantitation using TAQMAN probes shows an increasing in expression in cases (student t-test p= 0.012). f) GRIK2 expression correlates with the cluster of significantly differentially methylated CpGs (average methylation at each CpG, spearman r= -0.37, p=0.012). g) HRM results for *BEGAIN* show more methylation in cases compared to controls with (Unpaired t test with Welch's correction, p=0.007). h) Bs-cloning for BEGAIN shows striking increase in methylation of cases (n=17, avg. 11 clones/sample) compared to controls (n=18, avg. 11 clones/sample) mixed model regression analysis was perform to assess significance of methylation at each CpG, *p<0.05, **p<0.01, #p<0.00, ϕ trend 0.053, exact values for pairwise comparison are in SI table 9c and cluster analysis in 9d). Cases showed on average a three-fold increase in methylation within cluster on *BEGAIN*. i) *BEGAIN* FAC sorted samples show a strong contribution of methylation from the non-neuronal cell fraction in case samples, whereas there is no difference in controls sample methylation between the two fractions (n=9 for all groups, avg. 17 clones/sample, one-way Anova F (3.32)=10.74, p<0.0001, Tukey's pos-hoc, *p<0.05, ***p<0.001, ****p<0.0001). j) Analysis of *BEGAIN* variant expression in brain and blood. Experiment was independently repeated 3 times with 2 endogeneous controls per experiment, geometric mean of endogenous control was calculated and expression was normalized to this value. We qualitatively show that variant 1 is more expressed in brain and almost not present in blood, while we still detect variant 2 in blood. k) The astrocytic dyfunction group show a 2.3 fold decrease in the expression of *BEGAIN* Variant-1 compared to controls (Mann Whitney test p<0.0001), l) whereas variant-2 shows no change (Student t-test, p=0.26) m) The decrease in variant-1 expression correlates with the significantly differentially methylated cluster of CpGs in *BEGAIN* (average methylation at each CpG, spearman r=-0.37, p=0.019).

Figure 5: Promoter and enhancer properties repressed by DNA methylation in BEGAIN 474bp amplicon

Schematic diagram of CpG free lucia reporter vector with a) no endogeneous promoter and b) behind the human EF-1α promoter and placement of 474bp insert into multiple cloning site c) The unmethylated insert shows promoter activity which is completely abolished by methylation (10 replicates/ group, One-way Anova $F(2,27)=106.8$, $p<0.0001$, Tukey's post-hoc ****$p<0.0001$). d) Placed in front of the promoter, the 474 bp insert showed enhancer activity again showing complete repression of activity by methylation (10 replicates/group, One-way Anova $F(2,23)=17.80$, $p<0.0001$, Holm-Sidak's post-hoc, ***$p<0.001$ ****$p<0.0001$).

Figure 1

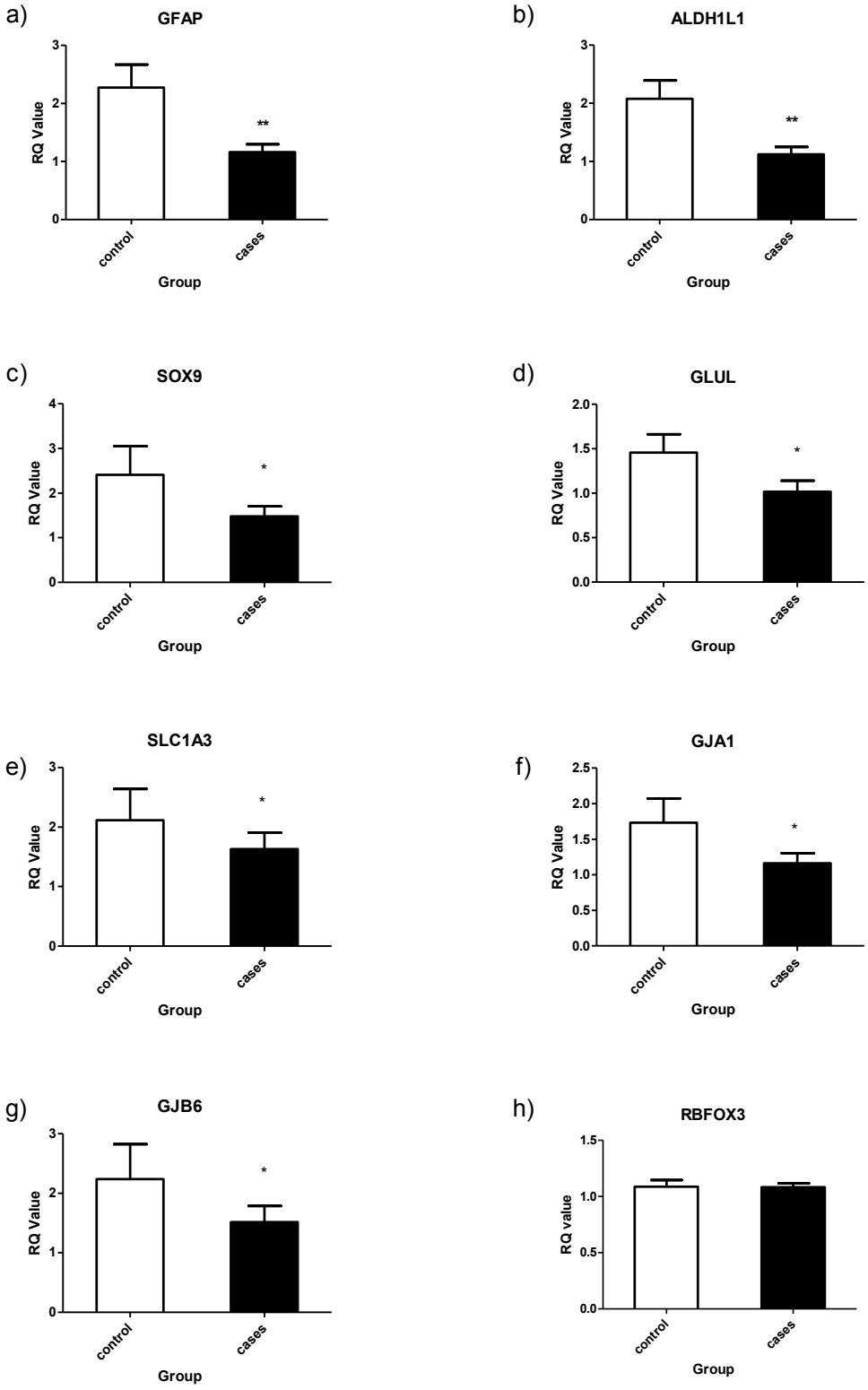
a)
GFAP
RQ Value
3
2
1
0
**
control
cases
Group
b)
ALDH1L1
RQ Value
3
2
1
0
**
control
cases
Group
c)
SOX9
RQ Value
4
3
2
1
0
*
control
cases
Group
d)
GLUL
RQ Value
2.0
1.5
1.0
0.5
0.0
*
control
cases
Group
e)
SLC1A3
RQ Value
3
2
1
0
*
control
cases
Group
f)
GJA1
RQ Value
2.5
2.0
1.5
1.0
0.5
0.0
*
control
cases
Group
g)
GJB6
RQ Value
3
2
1
0
*
control
cases
Group
h)
RBFOX3
RQ value
1.5
1.0
0.5
0.0
control
cases
Group

Figure 2

a)

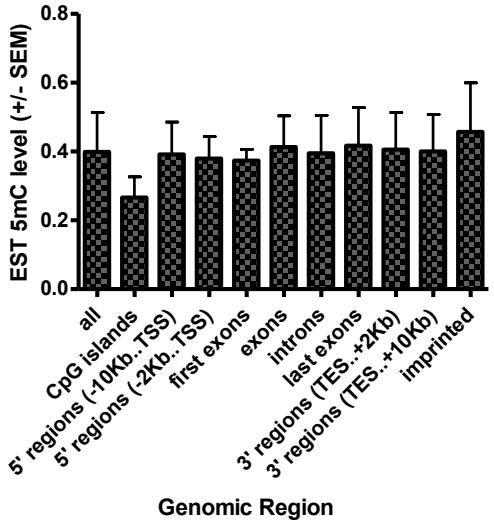

b)

Genomic region of DMR	% of DMRs (115)
first exon	0.87%
exon	2.61%
gene	33.91%
intron	31.30%
-5000bp..TSS	10.43%
TES..+5000bp	6.09%
Intergenic	56.52%

c)

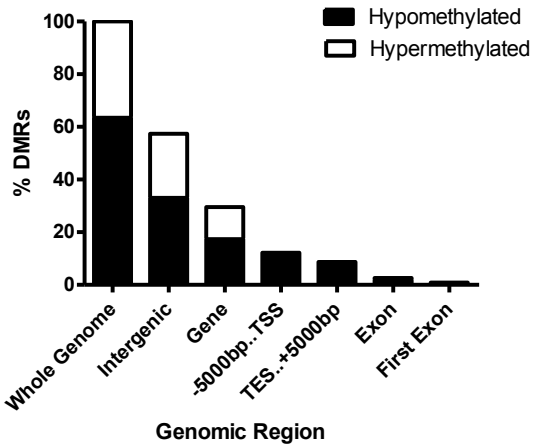

Figure 3

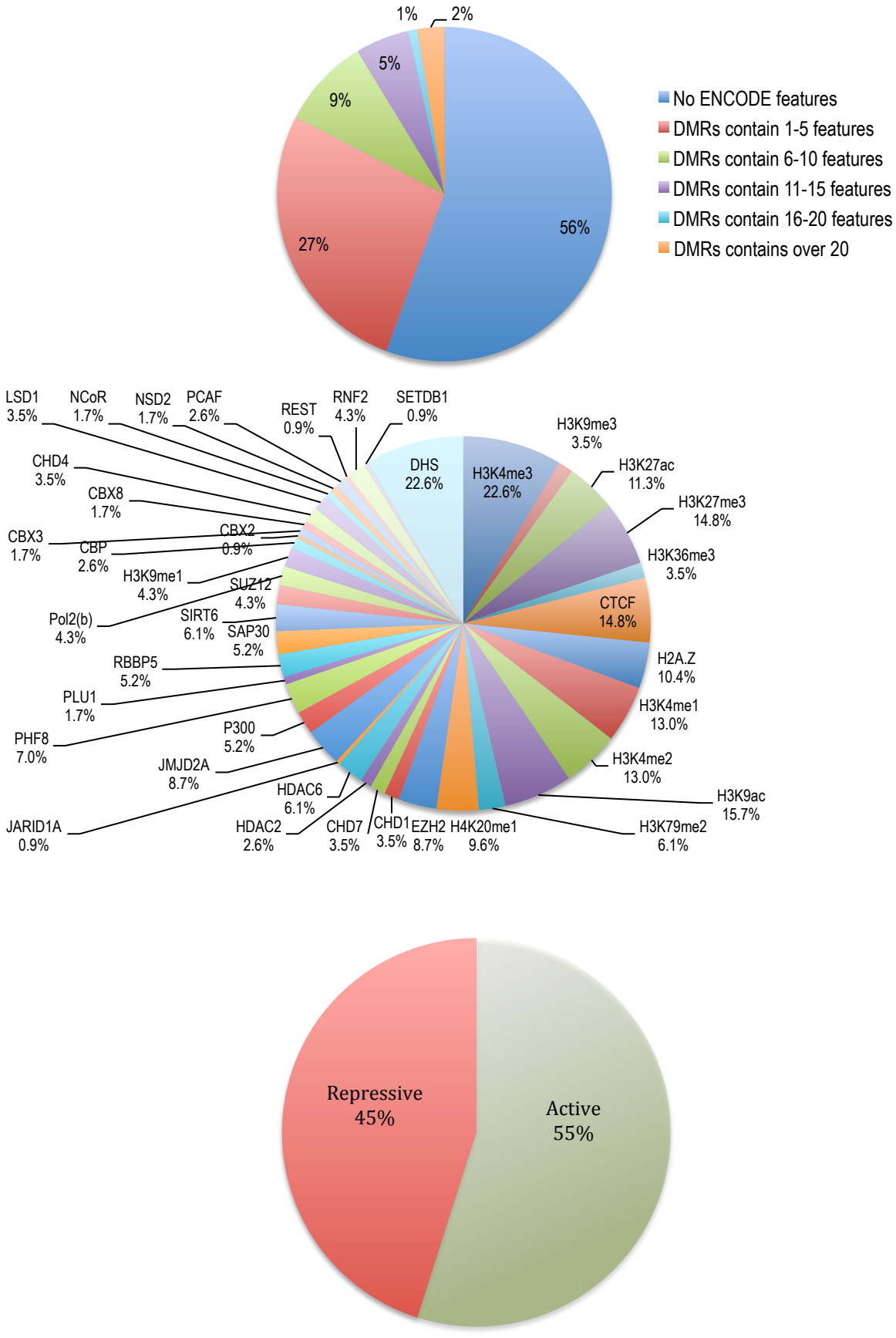
1%
2%
5%
9%
27%
56%
No ENCODE features
DMRs contain 1-5 features
DMRs contain 6-10 features
DMRs contain 11-15 features
DMRs contain 16-20 features
DMRs contains over 20
LSD1 3.5%
NCoR 1.7%
NSD2 1.7%
PCAF 2.6%
REST 0.9%
RNF2 4.3%
SETDB1 0.9%
CHD4 3.5%
CBX8 1.7%
CBX3 1.7%
CBX2 0.9%
CBP 2.6%
H3K9me1 4.3%
SUZ12 4.3%
Pol2(b) 4.3%
SIRT6 6.1%
SAP30 5.2%
RBBP5 5.2%
PLU1 1.7%
PHF8 7.0%
P300 5.2%
JMJD2A 8.7%
HDAC6 6.1%
JARID1A 0.9%
HDAC2 2.6%
CHD7 3.5%
CHD1 3.5%
EZH2 8.7%
H4K20me1 9.6%
H3K79me2 6.1%
H3K9ac 15.7%
H3K4me2 13.0%
H3K4me1 13.0%
H2A.Z 10.4%
CTCF 14.8%
H3K36me3 3.5%
H3K27me3 14.8%
H3K27ac 11.3%
H3K9me3 3.5%
H3K4me3 22.6%
DHS 22.6%
Repressive 45%
Active 55%

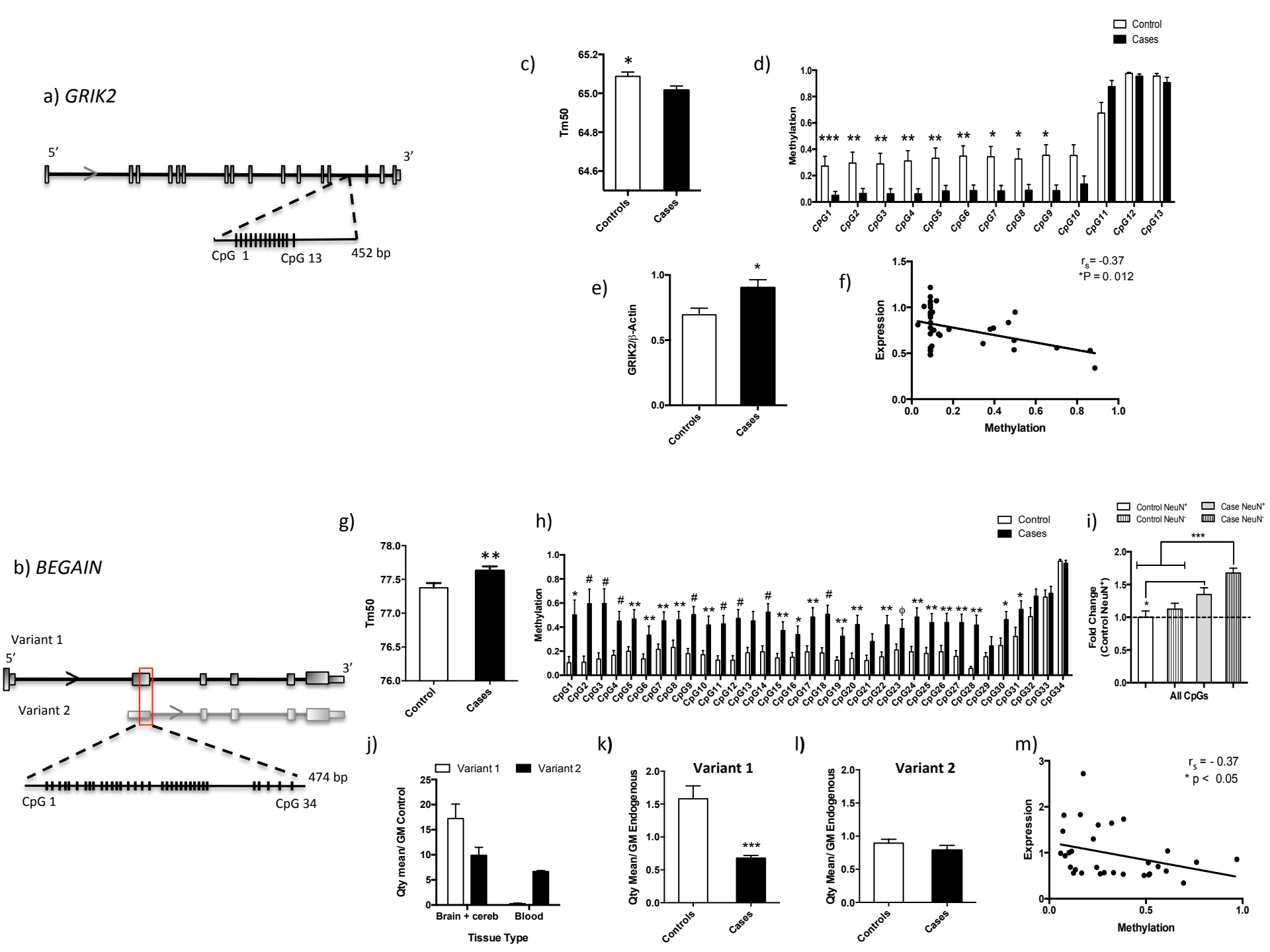
a) GRIK2
5′
3′
CpG 1
CpG 13
452 bp
b) BEGAIN
Variant 1
Variant 2
5′
3′
474 bp
CpG 1
CpG 34
c)
Tm50
Controls
Cases
d)
Control
Cases
Methylation
CpG1 CpG2 CpG3 CpG4 CpG5 CpG6 CpG7 CpG8 CpG9 CpG10 CpG11 CpG12 CpG13
e)
GRIK2/β-Actin
Controls
Cases
f)
r_s = -0.37
*P = 0. 012
Expression
Methylation
g)
Tm50
Control
Cases
h)
Control
Cases
Methylation
i)
Control NeuN+
Control NeuN-
Case NeuN+
Case NeuN-
Fold Change (Control NeuN+)
All CpGs
j)
Variant 1
Variant 2
Qty mean/ GM Control
Brain + cereb
Blood
Tissue Type
k)
Variant 1
Qty Mean/ GM Endogenous
Controls
Cases
l)
Variant 2
Qty Mean/ GM Endogenous
Controls
Cases
m)
r_s = - 0.37
* p < 0.05
Expression
Methylation

a)

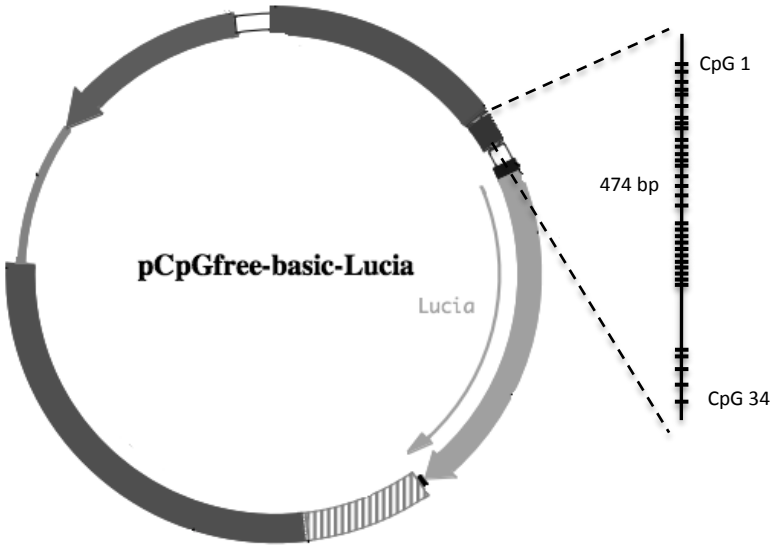
pCpGfree-basic-Lucia
Lucia
CpG 1
474 bp
CpG 34

b)

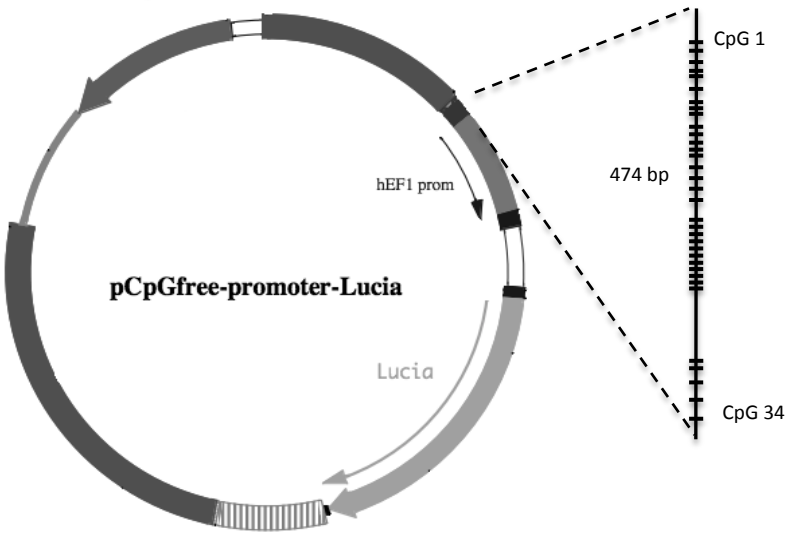
pCpGfree-promoter-Lucia
hEF1 prom
Lucia
CpG 1
474 bp
CpG 34

c)

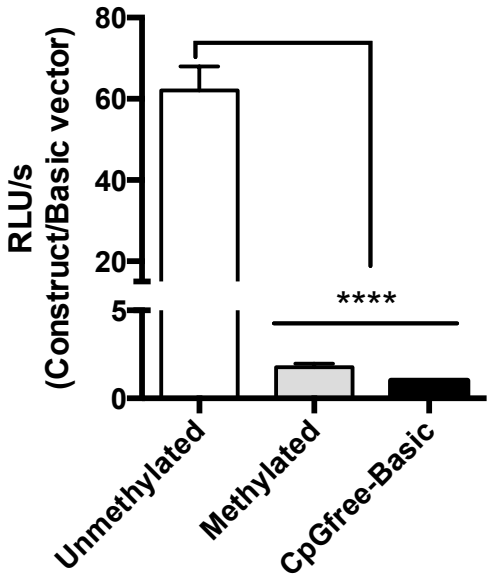
CpG Free Basic Luciferase Assay
RLU/s
(Construct/Basic vector)
80
60
40
20
5
0
****
Unmethylated
Methylated
CpGfree-Basic

d)

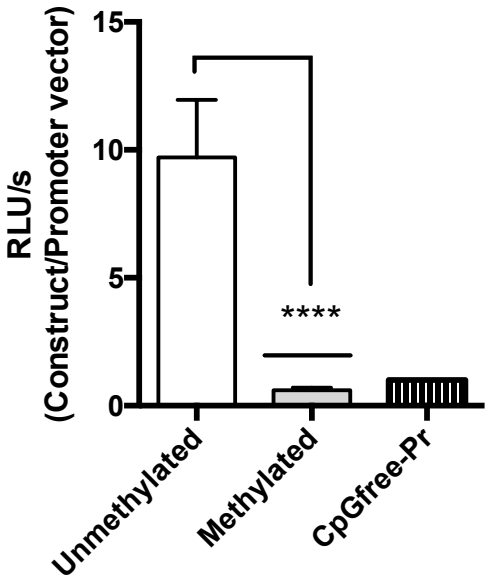
CpG Free Enhancer Luciferase assay
RLU/s
(Construct/Promoter vector)
15
10
5
0
****
Unmethylated
Methylated
CpGfree-Pr

Online Supplemental Information

I) Screening for astrocytic dysregulation

Figure 1 is a representative graph for 1 (GJA1) of the 7 genes used as a marker for astrocytic expression showing the variable distribution of expression between the groups. Only cases in the bottom quartile of expression were selected for MBD-sequencing.

Figure 1: Sample selection based on low expression

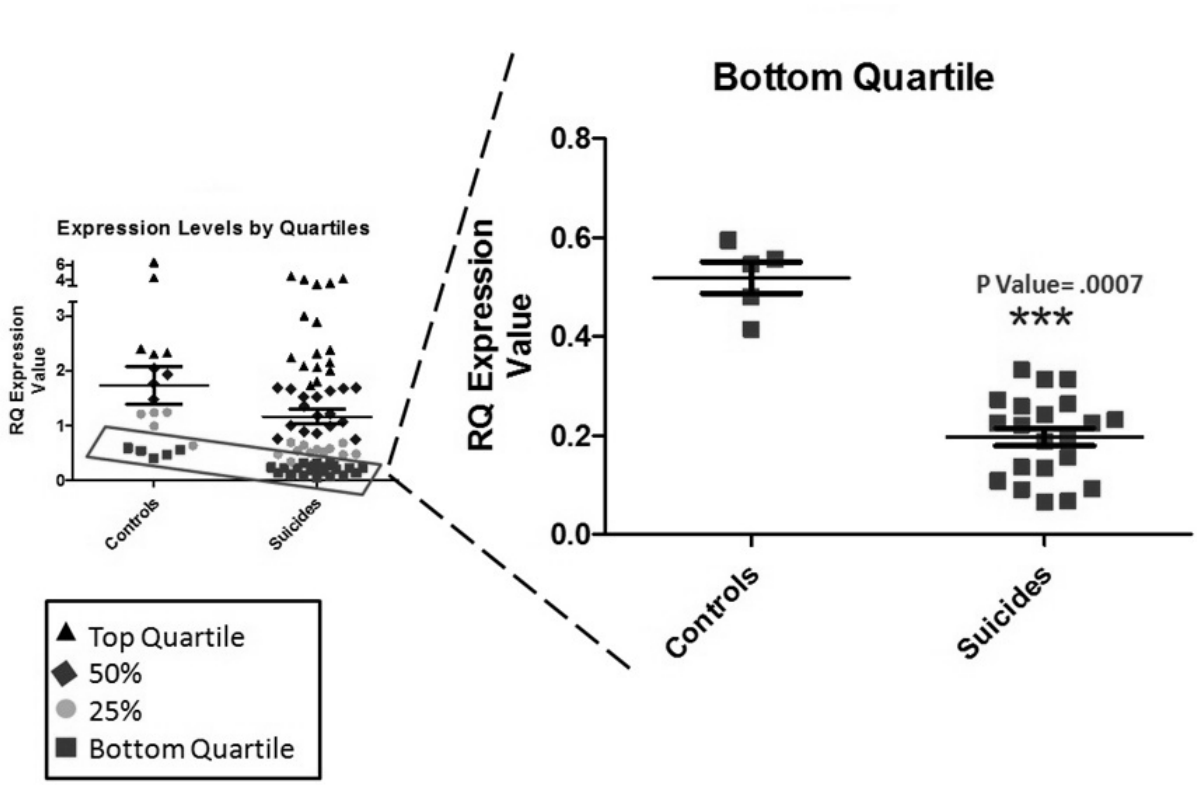

The graphs below show only subjects in the bottom quartile of expression for the controls and cases. When the controls are separate from the cases for each gene, the bottom quartile of expression in the suicide completers is significantly reduced compared to the controls. P values for Mann Whitney are shown on the graph.

Figure 2: Sample represented within the first quartile of expression level

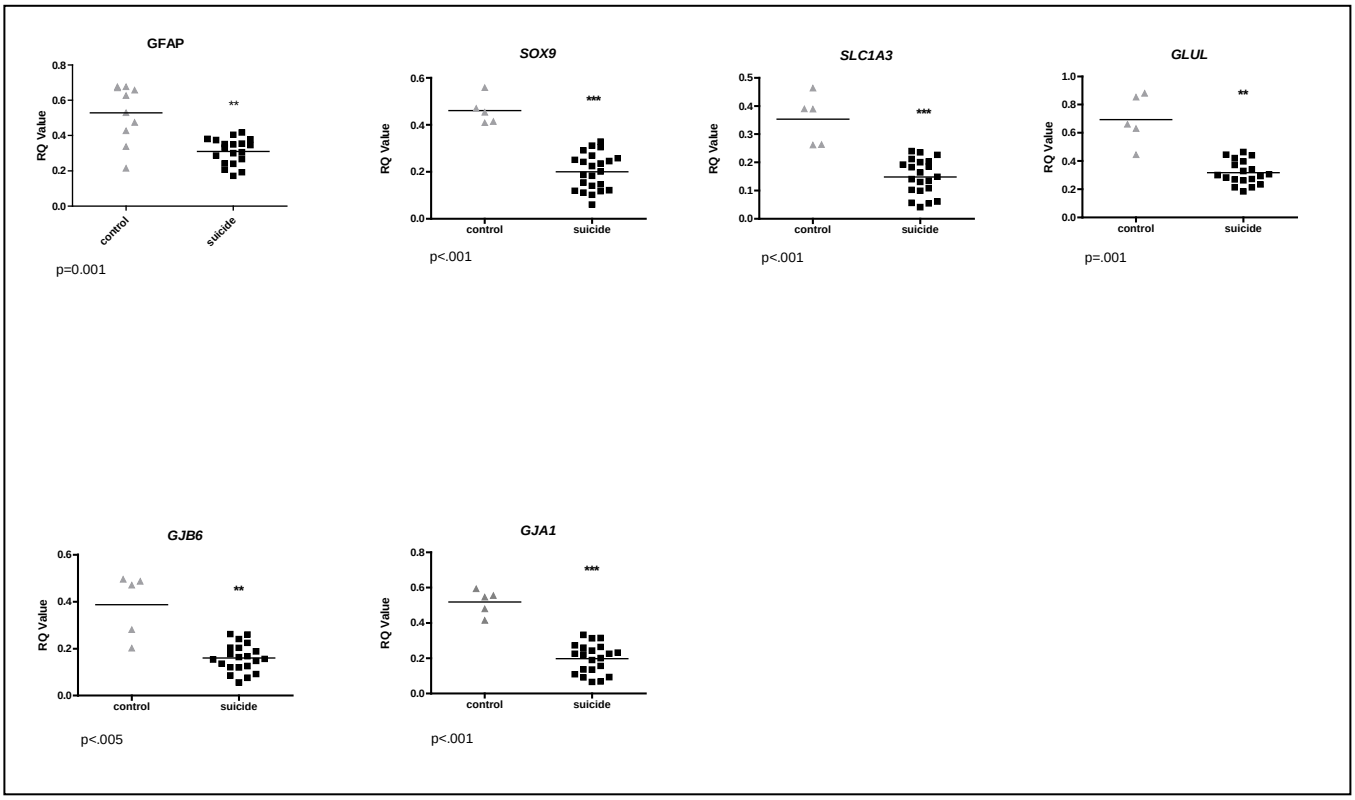

If we look specifically at the two genes most enriched in astrocytes, comparing the bottom quartile of expression to all controls quarried, we see how pronounced this decrease is. Testing the same parameters in a gene expressed exclusively in neurons (c) shows no difference. a) GFAP ($p < 0.0001$) and b) ADLH1L1 ($p < 0.0001$ show a dramatic decrease in expression in the suicide group compared to the controls, however expression of the neuronal marker gene c) RBFOX3 ($p = 0.210$) shows no difference between groups.

Figure 3: Relative quantities of astrocyte specific markers within the selected LX subgroup

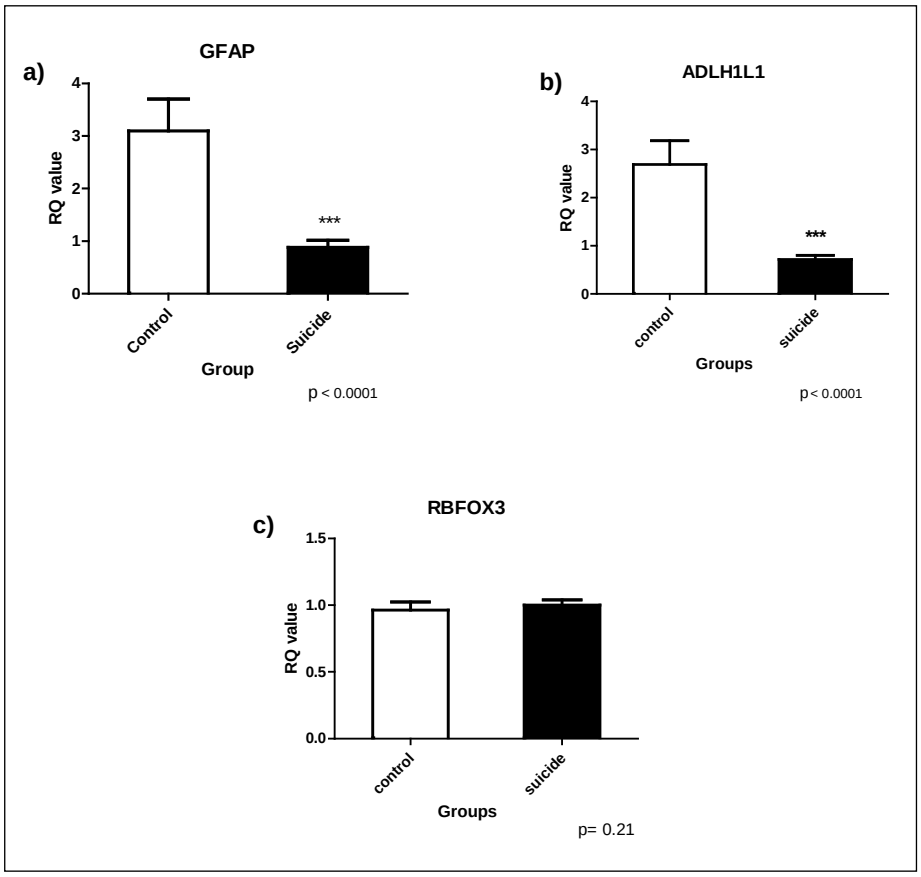

Our low expressing group was selected based on cases having bottom quartile expression levels for the majority of the genes tested, therefore, at least 5 of the 7 genes investigated. In order to be consistent, females where removed for the analysis so that selected samples would be male only.

Table 1: Summary of low Expressers that fit the criteria.

Sample	ALDH1L1	GFAP	CX43	CX30	SOX-9	GLUL	SLC1A3
6	X	X	X	X	X	X	X
37	X	X	X	X	X	X	X
48	X	X	X	X	X	X	X
58	X	X	X	X	X	X	X
84	X	X	X	X	X	X	X
118	X	X	X	X	X	X	X
119	X	X		X	X	X	X
142	X		X	X	X		X
145	X		X	X	X	X	
156	X		X	X	X	X	
167	X	X	X	X	X	X	X
174	X	X	X	X	X	X	X
184	X	X	X	X	X	X	X
199	X	X	X	X	X	X	X
200	X	X	X	X	X	X	X
202	X	X	X	X	X	X	X
204	X	X	X	X	X	X	X
213	X	X	X	X	X	X	X
214	X	X	X	X	X	X	X
220	X	X	X	X	X	X	X
225	X		X	X	X	X	X
226	X	X		X	X	X	X

We then looked to see how well these so called “astrocytic markers” correlated with each other within the low expressor subgroup. We found that for the most part the relationship is very strong with the exception of the glutamate transporter SLC1A3, which did not significantly correlate with any of the other genes quarried. However, there was also a strong overlap of cases that fell in the bottom quartile for this gene (91%). We also looked at the neuronal marker NeuN and found no correlation with any of the astrocytic genes.

Below are examples of correlations between queried genes, SOX9 is very closely associated with GJB6 showing 91% correlation between expression levels. This tight relationship is consistent with recent data showing that SOX9 acts as a transcription factor for GJB6 [1]. Table 3 shows a full summary for correlation between all genes. (*rs*; Spearman correlation coefficient.)

Figure 4: Correlation of Astrocyte genes in low expression cases

a) Correlation between two astrocytic genes.

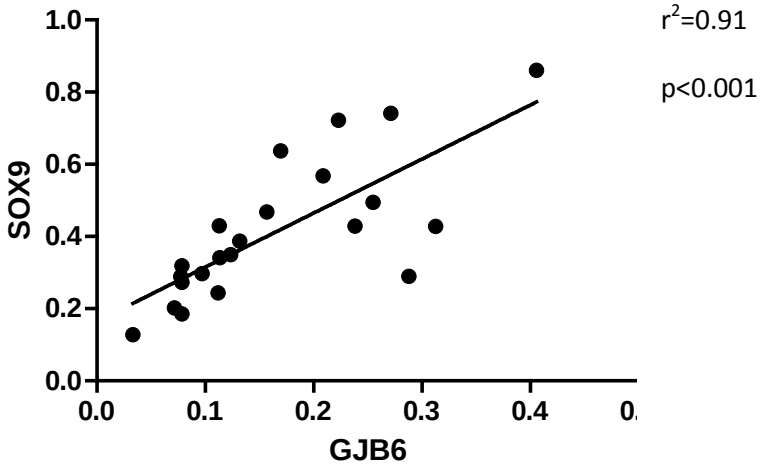

b) Correlation between astrocytic gene and Neuronal gene.

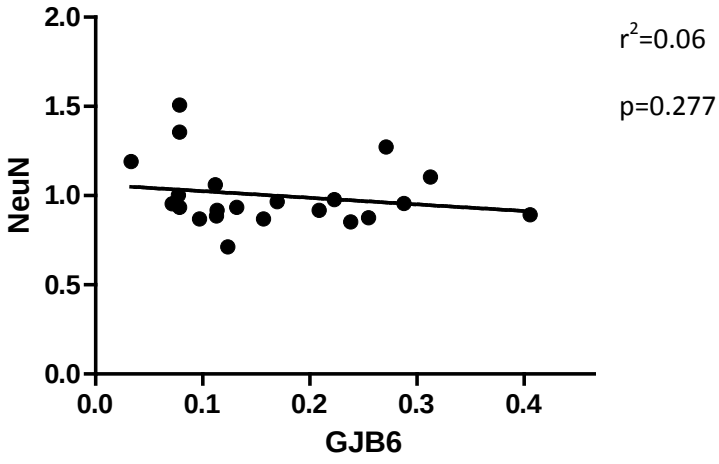

Table 2: Correlation of the bottom quartile of all genes for cases

	GJB6		GJA1		SOX9		GLUL		SLC1A3		GFAP		ALDH1L1		NeuN	
	rs	p value	*rs*	p value	*rs*	p value	*rs*	p value	*rs*	p value	*rs*	p value	*rs*	p value	*rs*	p value
GJB6			0.85	(0.000)	0.91	(0.000)	0.77	(0.000)	0.22	(0.321)	0.67	(0.001)	0.67	(0.001)	-0.24	(0.277)
GJA1	0.85	(0.000)			0.77	(0.000)	0.64	(0.001)	0.15	(0.506)	0.67	(0.001)	0.80	(0.000)	-0.12	(0.597)
SOX9	0.91	(0.000)	0.77	(0.000)			0.85	(0.000)	0.41	(0.059)	0.79	(0.000)	0.65	(0.001)	-0.31	(0.165)
GLUL	0.77	(0.000)	0.64	(0.001)	0.85	(0.000)			0.53	(0.011)	0.71	(0.000)	0.61	(0.002)	-0.28	(0.214)
SLC1A3	0.22	(0.321)	0.15	(0.506)	0.41	(0.059)	0.53	(0.011)			0.25	(0.259)	0.13	(0.559)	-0.38	(0.079)
GFAP	0.67	(0.001)	0.67	(0.001)	0.79	(0.000)	0.71	(0.000)	0.25	(0.259)			0.75	(0.000)	-0.27	(0.221)
ALDH1L1	0.67	(0.001)	0.80	(0.000)	0.65	(0.001)	0.61	(0.002)	0.13	(0.559)	0.75	(0.000)			0.07	(0.747)
NeuN	-0.24	(0.277)	-0.12	(0.597)	-0.31	(0.165)	-0.28	(0.214)	-0.38	(0.079)	-0.27	(0.221)	0.07	(0.747)		

II) Selected Samples for MBD-Sequencing

Extensive statistics were preformed on the final group used for sequencing. After removing the 3 suicide subjects and 1 control whose sequencing did not meet quality standards, we preformed Mann Whitney tests on all clinical variables. No differences were found between groups for RNA integrity number RIN, age, PMI and sex, since all subjects were male.

Using the clinical variables as possible covariates, we analysed the main effect of the groups for each gene. The ANCOVAs revealed that PMI, pH have no effect on any of the genes, however an effect was seen for GFAP and age ($F=4.91$, $p=0.03$). In line with the literature, our results show that GFAP expression increases with age [2-4]. This positive relationship between age and GFAP can be seen in the graphs below. Splitting the cases and controls shows a trend toward this relationship (a,b). When the groups are combined we reach the power to detect this relationship (c) $p= 0.047$.

Figure 5: Relationship of age on GFAP

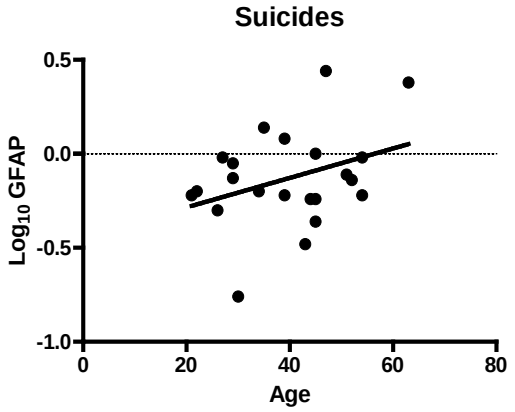

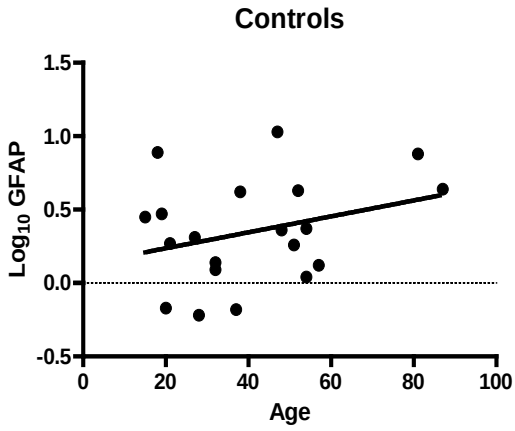

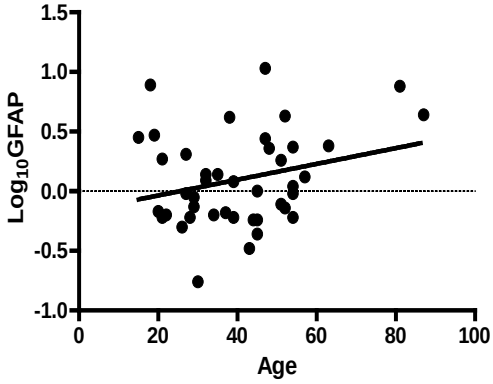

III) Generation of high quality genome-wide MBD2-seq profiles

DNA extracted from the PFC of the 39 samples was quality tested and prepared for Illumina libraries. For all subjects, MBD2-enriched DNA fragments had ideal size distributions between 200 and 500bp and an input quantity between 20 to 70ng/ul for Illumina ChIP-Seq library preparations, 2-7x greater than the specified starting amount in the Illumina protocol. The resulting DNA libraries produced high quality bioanalyser traces and passed all quality control standards. We rigorously tested MBD2 pulldown assays (eFigure 6), and optimized the procedure to ensure enrichment for methylated DNA, and to reduce the number of duplicate reads.

Illumina GAIIx 36 base-pair single end sequencing was completed for 39 samples (22 cases and 17 controls) (DNA quality details; eFigure 7) on a single lane per subject without indexing. After sequencing, reads were mapped to the reference human genome (hg19) using BWA [5] and extended 400bp (initial QC statistics; eTable 3). Five subjects (3 cases and 2 controls) were removed due to low quality sequencing scores resulting in few usable reads. The final sample set consisted of 19 cases and 15 controls.

Figure 6: Sample Quality Control for MBD-pulldown and next generation Sequencing.

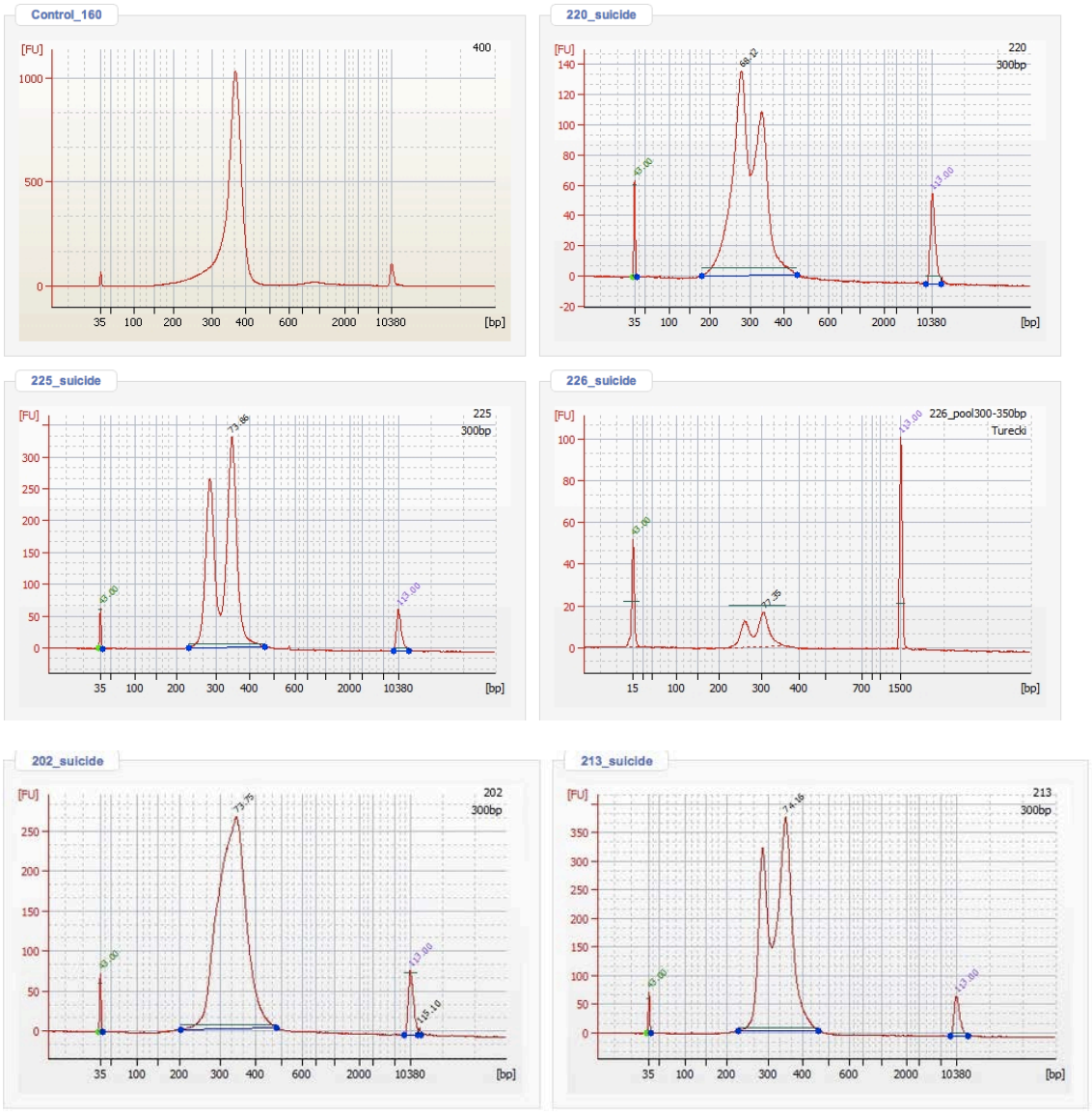

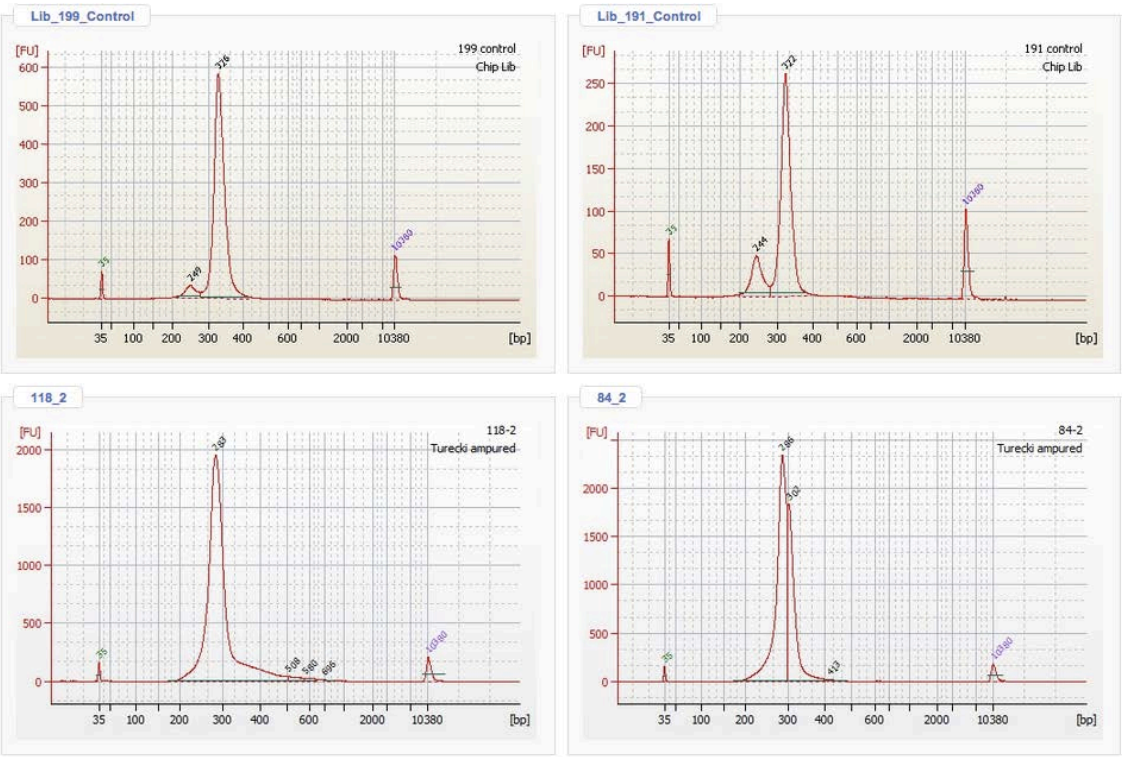

The eletrophoretograms from figure 6 show a representation of the library constructions prior to sequencing. Some libraries were constructed more than once, if they did not meet the required concentration and or profile the library preparation was repeated. Equally, before starting any library preparations, all sheared genomic DNA was assessed for quality and concentration with the Agilent Biolanalyser DNA 1000 chips. A representation of the profiles can be seen in figure 7 and the associated summary table. We required 4µg or more starting material within a range of 200-500bp to adequately perform the MBD enrichment protocol.

Figure 7: DNA qualities for library preps bioanalyser traces

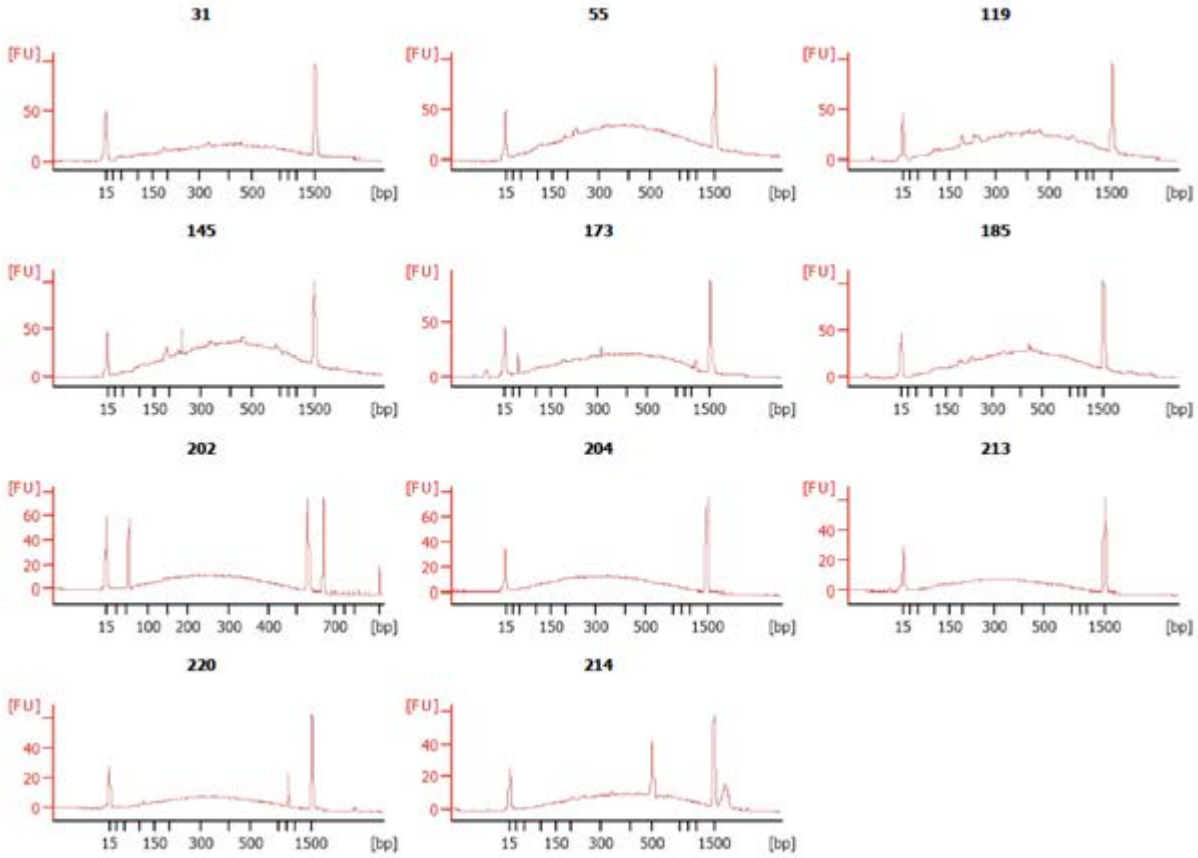

Sample Name	Avg size (bp)	Concentration (ng/ul)	Volume (µl)	Total amount (µg)
31	413	22.41	200	4.5
55	408	45.07	200	9.0
119	423	34.35	200	6.9
145	437	41.12	200	8.2
173	410	36.01	200	7.2
185	443	34.37	200	6.9
202	272	39.93	200	8.0
204	372	21.65	200	4.3
220	392	21.09	200	4.2
214	423	27.71	200	5.5

Table 3: Initial QC statistics for each subject

Name	Alias	Pooled Sample	Source	Volume	Conc	Quantity	Number of Bases	Number of Reads GA
104_control	1	No	Library	23.3	5.53	128.85	1,205,532,672	32,702,160
104_control	1	No	Library	10	0.058	0.58	0	0
118_2	2	No	Library	7.68	5.1	39.17	563,382,288	15,649,508
118_Suicide	2	No	Library	13	1.32	17.16	1,450,924,032	39,358,800
119_suicide	3	No	Library	17.9	9.19	164.5	1,262,610,432	34,250,520
119_suicide	3	No	Library	10	1.04	10.4	0	0
11_2	4	No	Library	12.47	1.31	16.34	692,662,176	19,240,616
11_Control	4	No	Library	9.6	0.57	5.47	1,477,822,464	40,088,400
135_control	5	No	Library	11.9	2.06	24.51	1,211,502,592	32,864,040
142_suicide	6	No	Library	10	0.722	7.22	0	0
145_suicide	7	No	Library	10	0.275	2.75	0	0
145_suicide	7	No	Library	16.5	8.84	145.86	1,479,092,224	40,122,960
150_control	8	No	Library	9.7	3.09	29.97	1,294,344,192	35,111,280
156_suicide	9	No	Library	10	0.63	6.3	0	0
164_control	10	No	Library	21.8	3.87	84.37	1,246,988,288	33,826,680
16_2	11	No	Library	11.23	0.88	9.88	624,958,236	17,359,951
16_Control	12	No	Library	1.7	0.19	0.32	1,487,496,192	40,350,840
173_control	13	No	Library	17.1	11.51	196.82	1,426,915,328	38,707,560
185_control	14	No	Library	17.8	12.69	225.88	1,342,143,488	z
202_suicide	15	No	Library	13.9	3.06	42.53	1,243,244,544	33,725,160
204_suicide	16	No	Library	17.6	12.47	219.47	1,401,980,928	38,031,120
213_suicide	17	No	Library	20.1	3.57	71.76	1,237,928,960	33,580,920
214_suicide	18	No	Library	18	14.55	261.9	1,396,595,712	37,885,080
220_suicide	19	No	Library	12.9	2.44	31.48	1,229,227,008	33,344,880
225_suicide	20	No	Library	19.2	3.05	58.56	1,191,550,976	32,322,840
226_suicide	21	No	Library	21.6	3.69	79.7	1,267,936,256	34,394,880
sample #20	Pilot	No	ChIP	999	1000	999000	1,009,142,784	27,374,760
sample #37	Pilot	No	ChIP	999	1000	999000	2,161,926,144	58,646,040
31_control	22	No	Library	16.7	258	4308.6	1,393,129,472	37,791,000
36_2	23	No	Library	12.26	1.28	15.69	651,756,852	18,104,357
36_Control	23	No	Library	8.9	0.48	4.27	1,491,125,248	40,449,360
37_2	24	No	Library	10.83	0.91	9.86	659,671,452	18,324,207
46_control	25	No	Library	10	0.775	7.75	0	0
48_2	26	No	Library	8.11	5.53	44.85	594,841,716	16,523,381
48_Suicide	27	No	Library	12.5	1.21	15.13	1,453,995,008	39,442,080
55_control	28	No	Library	16.7	10.32	172.34	1,382,639,616	37,506,480
55_control	28	No	Library	10	0.488	4.88	0	0

Name	Alias	Pooled Sample	Source	Volume	Conc	Quantity	Number of Bases	Number of Reads GA
6_2	29	No	Library	7.59	0.44	3.34	778,951,764	21,637,549
6_Suicide	29	No	Library	10.6	0.71	7.53	1,327,632,384	37,256,160
7_Control	30	No	Library	12.4	1.26	15.62	1,434,203,136	38,905,200
84_2	31	No	Library	10.09	7.69	77.59	630,909,252	17,525,257
84_Suicide	31	No	Library				1,401,570,304	38,019,960
94_control	32	No	Library	10	0.464	4.64	0	0
Control_160	33	No	Library	14.55	8.93	129.93	4,123,968,512	37,603,200
Lib_100_Control	34	No	Library	9.3	1.6	14.88	1,249,261,568	34,173,120
Lib_142	6	No	Library	14	5.42	75.88	1,522,832,384	41,309,400
Lib_156	9	No	Library	16.7	6.5	108.55	1,241,379,840	33,674,520
Lib_158_Control	35	No	Library	22.8	8.69	198.13	1,292,882,944	35,071,680
Lib_167	36	No	Library	16.5	2.64	43.56	1,282,243,584	34,783,080
Lib_174_Suicide	37	No	Library	7.7	2.09	16.09	1,107,919,872	30,054,240
Lib_182	38	No	Library	16.5	5.43	89.59	1,291,252,736	35,321,760
Lib_184_Suicide	39	No	Library	12.1	3.54	42.83	1,168,619,520	31,700,760
Lib_191_Control	3	No	Library	12	1.31	15.72	1,102,090,240	29,896,080
Lib_196	40	No	Library	16.5	5.42	89.43	1,285,022,720	34,858,440
Lib_199_Control	41	No	Library	15.4	2.54	39.12	844,188,672	22,900,080
Lib_200_Suicide	42	No	Library	20.1	5.29	106.33	1,197,045,760	32,471,880
Lib_46	25	No	Library	22.1	4.23	93.48	1,170,615,296	31,754,880
Lib_58	44	No	Library	16.8	6.51	109.37	1,348,204,544	36,879,720
Lib_94	32	No	Library	16.5	2.65	43.73	1,286,644,736	34,902,480

After samples were removed for either low quality scores or other technical issues the breakdown of samples and read counts can be found in table 6. There is no significant difference in the mean number of reads per group (p=0.85) and despite the unequal number of subjects per group, the reads for each group provided adequate coverage.

Table 4: The table shows all reads included in the analysis of differential methylation between groups.

Sample	group	reads
11	control	6,322,140
31	control	16,631,026
36	control	6,941,715
46	control	14,604,966
55	control	13,831,695
94	control	16,890,070
104	control	11,944,644
135	control	10,777,773
150	control	14,395,354
158	control	14,182,876
160	control	12,801,866
173	control	16,340,532
182	control	13,498,218
185	control	16,329,490
191	control	14,216,509

Sample	group	reads
48	suicide	9,824,749
58	suicide	15,725,715
84	suicide	7,528,187
118	suicide	9,454,514
119	suicide	13,900,619
142	suicide	17,212,977
145	suicide	14,680,445
156	suicide	13,418,423
167	suicide	16,843,024
174	suicide	13,001,935
184	suicide	13,284,744
199	suicide	7,916,222
200	suicide	14,461,724
204	suicide	17,845,704
213	suicide	13,174,954
214	suicide	18,592,343
220	suicide	8,813,984
225	suicide	10,080,189
226	suicide	13,086,627

Total control reads use **199,708,874**

Total suicide reads use **248,847,079**

IV) Sequencing Coverage

We assessed the amount of coverage obtained from the total reads acquired from each group. Sequencing coverage was calculated by assessing the percentage of the mappable genome that was covered by a fragment depth of 20x.

Figure 8: Total amount of sequencing and the resulting coverage. The X axis shows the number of lanes of sequencing and Y axis is the percentage of mappable genome coverage at 20x. The red line represents the expected median coverage based on the black solid line, which represents the median percentage of coverage for 10 lanes. The black dotted lines represent the variation for multiple iterations of n lanes on the x axis

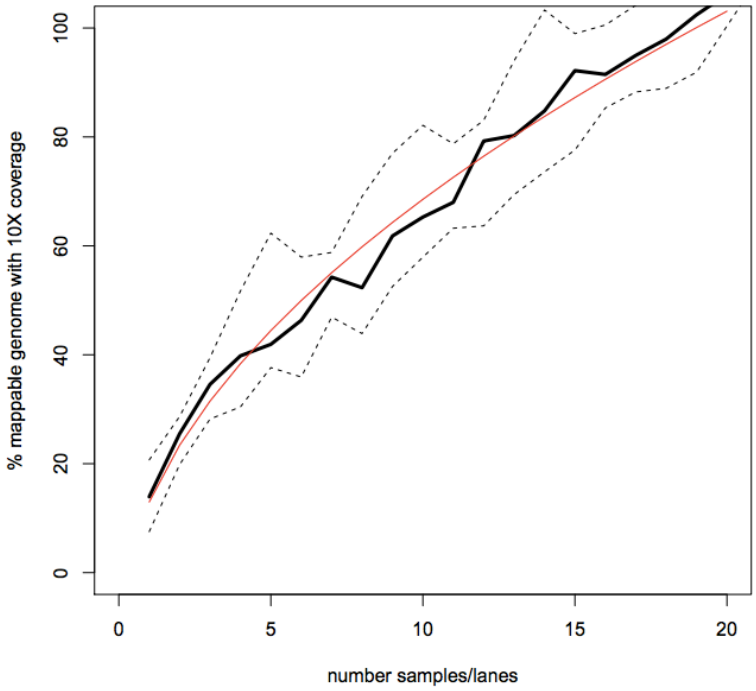

V) Technical Validation

In order to technically validate our sequencing we used regions with very high and very low read counts, designed specific primers for those regions and quantified reads using real time PCR on leftover DNA from the MBD-enrichment.

Figure 9: Sequencing Validation, technical replication: Real time PCR values were normalized using three control regions which had consistent read counts across all samples. The sequencing read counts were log transformed. Three control samples and 3 suicide samples showing variable read counts for a region on chromosome 4 showed a strong negative correlation (r=-0.81, t=0.025) between read count and cycle number. This was repeated for 2 other regions, both showing the expected negative correlation, one being statistically significant (r=-0.74, t=0.047) the other showing a trend (r= -0.61, t=0.09)

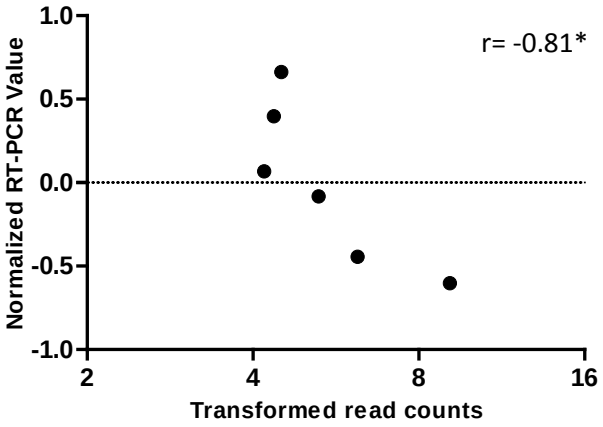

Figure 10: Reads to chromosome and DMRs to chromosome correlations: Read count strongly correlated with chromosome size. Graph a) shows the number of reads that map back to each chromosome is highly proportional to the size of each chromosome (r=0.83 p<0.0001). b) There was no difference in the number of reads that contributed to any given chromosome by either group. c) the number of DMRs were not associated with chromosome size (r=-0.15, p=0.48).

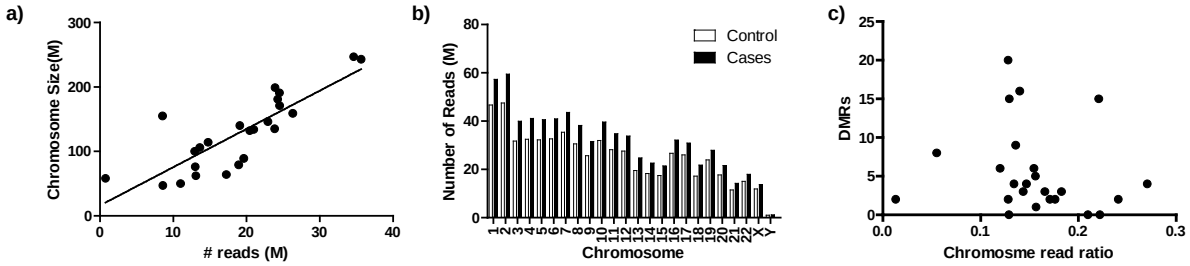

VI) Additional characterization of DNA methylation

In characterizing the results we found two regions that showed an unexpected clustering of differential methylation, the regions are outlined in table 5 below.

Table 5: Cluster regions: Description of cluster regions across the genome. Our data showed 2 regions across the genome where clustering of differentially methylated regions is suggested.

Chromosome	Region	Size of cluster region	# of differences	FDR
10	2095501-21193250	19 Mb	6	5.60E-07
X	101854251-136135250	34Mb	7	7.69E-06

FDR = false discovery rate of hypergeometric p-value

Figure 11: Functional overlap with sites in cluster region

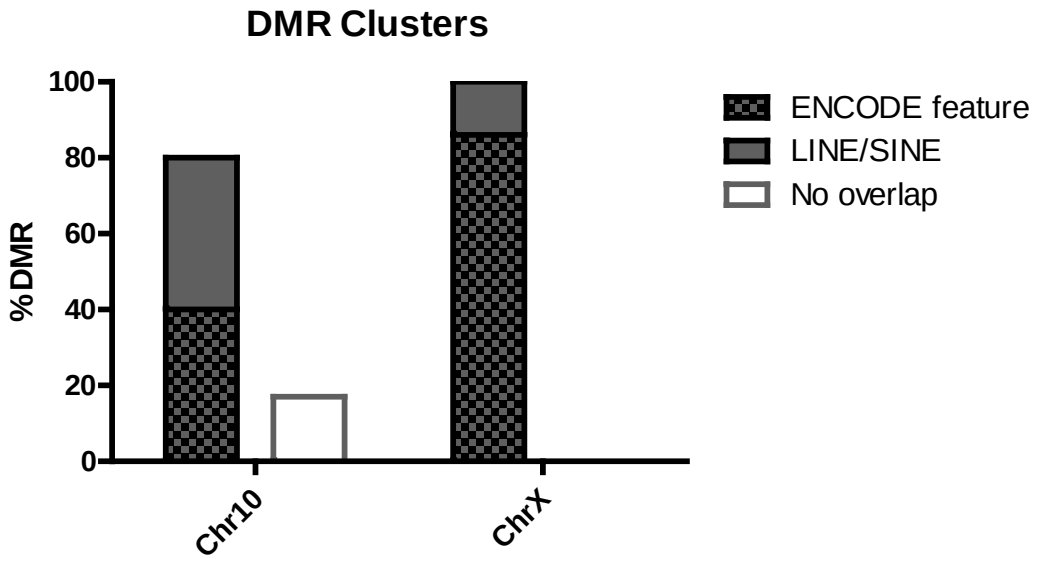

Examination of the cluster regions revealed that almost all the DMRs in these regions fall on some form of regulatory element. The ENCODE feature graphed here include transcription factor binding sites, including insulator elements such as CTCF binding sites, chromatin marks, and DNase hypersensitivity regions. LINEs and SINES are known as transposable elements, generally regulated by DNA methylation. These cluster regions showing differences in methylation levels of these elements suggest a regulatory effect.

To assess whether the differential methylated regions had a functional association we assessed their overlap with 41 ENCODE elements. Of the 41 features examined in this paper, 37 showed significant enrichment with DMRs.

Table 6: ENCODE enrichment

Name	DMR Enrichment pVal	Hypermethylated DMRs pVal	Hypomethylated DRMs Pval
H4K20me1	1.31E-11	1	4.22E-13
H3K9ac	4.15E-10	1	5.71E-12
HDAC6	1.54E-09	1	2.91E-10
CTCF	9.98E-09	1	9.65E-11
EZH2	1.91E-07	1	2.40E-08
JMJD2A	8.27E-07	1	1.58E-07
SIRT6	3.39E-06	1	9.87E-07
SUZ12	4.04E-06	1	1.18E-06
SAP30	9.95E-06	1	1.94E-06
CHD4	1.09E-05	1	3.18E-06
H3K4me3	1.90E-05	0.475610352	3.84E-06
H3K27me3	2.24E-05	1	2.03E-06
H3K4me2	2.42E-05	0.329017223	1.27E-05
H3K36me3	3.75E-05	1	1.10E-05
H3K27ac	3.91E-05	1	2.49E-06
HDAC2	0.00012774	1	3.78E-05
CBP	0.000138162	1	6.11E-05
CHD7	0.000259509	1	0.000114996
P300	0.000311222	1	0.000137979
H3K9me1	0.000461329	1	0.000204781
H3K4me1	0.000481021	1	3.51E-05
H3K79me2	0.000566976	1	0.000170504
CHD1	0.000610197	1	0.000271144
H2A.Z	0.001157393	0.231449607	0.001847849
RNF2	0.001403804	1	0.000626376
H3K4me3B	0.001737147	0.348956736	0.001545302
RBBP5	0.0017713	1	0.000791545
CBX8	0.002142505	1	0.000958744
PCAF	0.002894336	1	0.001930487
PHF8	0.002934809	1	0.001316705
CBX3	0.007169965	1	0.004785701
JARID1A	0.008061677	1	0.005381692
H3K9me3	0.011480984	1	0.005243821
SETDB1	0.015290183	1	0.010219597
NSD2	0.016789584	1	0.011224598
PLU1	0.024939058	1	0.016695901

REST	0.036869391	1	0.024733131
H3K27me3B	0.045286647	0.482840224	0.040265255
CBX2	1	1	1
HDAC1	1	1	1
NCoR	1	1	1
LSD1	0.052582919	1	0.03536986
Pol2(b)	0.107898009	1	0.073291708
H3K9acB	0.614482174	1	0.470299961

Note that information on some elements is captured by more than one marker. Therefore, for the analyses presented in table 6, these elements were considered as the same feature.

To give us a better understanding of the overlap of DMRs and these elements we divided the elements into active or passive regulators based on their known functions.

Table 7: Active ENCODE marks

ENCODE feature	Enrichment p Value	Role
CBP	0.0001	Nuclear cap-binding protein subunit1; Component of the cap-binding complex (CBC), which binds cotranscriptionally to the 5'-cap of pre-mRNAs and is involved in various processes such as pre-mRNA splicing, translation regulation, nonsense-mediated mRNA decay, RNA-mediated gene silencing (RNAi) by microRNAs (miRNAs) and mRNA export
CBX3	0.0048	Seems to be involved in transcriptional silencing in heterochromatin-like complexes. Recognizes and binds histone H3 tails methylated at 'Lys-9', leading to epigenetic repression.
CHD7	0.0001	an ATP-dependent chromatin remodeler homologous to the Drosophila trithorax-group protein Kismet; chromatin remodeling
H2A.Z	0.0018	Positioning of H2A.Z containing nucleosomes around transcription start sites has now been shown to affect the downstream gene expression.[3]
H3K27ac	0.0000	distinguishes active enhancers from poised/inactive enhancers (h3k4me1)
H3K36me3	0.0000	deposited by the methyltransferase Set2; This protein associates with elongating RNA polymerase II, and H3K36Me3 is indicative of actively transcribed genes
H3K4me2	0.0000	Enhancer
H3K4me3	0.0000	mark of promoter region and active gene transcription
H3K4me3B	0.0015	mark of promoter region and active gene transcription
H3K79me2	0.0002	Active gene marker, observed throughout the genome
H3K9ac	0.0000	Open active
LSD1	0.0354	Lysine-specific histone demethylase 1A; Acts as a corepressor by mediating demethylation of H3K4me, a specific tag for epigenetic transcriptional activation
P300	0.0001	E1A binding protein p300; The p300 protein carries out its function by activating transcription, transcriptional coactivator

PCAF	0.0019	Histone acetyltransferase; Functions as a histone acetyltransferase (HAT) to promote transcriptional activation. Has significant histone acetyltransferase activity with core histones (H3 and H4), and also with nucleosome core particles
PHF8	0.0013	Histone lysine demethylase with selectivity for the di- and monomethyl states that plays a key role cell cycle progression; Acts as a transcription activator
RBBP5	0.0008	As part of the MLL1/MLL complex, involved in mono-, di- and trimethylation at 'Lys-4' of histone H3. Histone H3 'Lys-4' methylation represents a specific tag for epigenetic transcriptional activation
REST	0.0247	RE1-silencing transcription factor;Transcriptional repressor which binds neuron-restrictive silencer element (NRSE) and represses neuronal gene transcription in non-neuronal cells. Restricts the expression of neuronal genes by associating with two distinct corepressors, mSin3 and CoREST, which in turn recruit histone deacetylase to the promoters of REST-regulated genes

Table 8: Repressive ENCODE marks.

ENCODE feature	Enrichment p Value	Role
H3K9me3	0.0052	H3K9Me2/3 is a well-characterised marker for heterochromatin, and is therefore strongly associated with gene repression.
H3K27me3	0.0000	modification is depositied by the polycomb complex PRC2;It is a clear marker of gene repression, and is likely bound by other proteins to exert a repressive function. Another polycomb complex, PRC1, can bind H3K27Me3
H3K27me3B	0.0403	Second antibody.
CTCF	0.0000	as a TF, it acts as a repressor, also considered an insulator
H4K20me1	0.0000	Monomethylated H4K20 and H3K9 act cooperatively to mark distinct regions of silent chromatin within the mammalian epigenome
EZH2	0.0000	Histone-lysine N-methyltransferase, gene encodes a member of the Polycomb-group (PcG) family, making it mainly a gene silencer, adds 3 me to k27
CHD1	0.0003	Chromodomain-helicase-DNA-binding protein 1: CHD genes alter gene expression possibly by modification of chromatin structure thus altering access of the transcriptional apparatus to its chromosomal DNA template
HDAC2	0.0000	Histone deacetylases act via the formation of large multiprotein complexes and are responsible for the deacetylation of lysine residues on the N-terminal region of the core histones
HDAC6	0.0000	Histone deacetylases act via the formation of large multiprotein complexes and are responsible for the deacetylation of lysine residues on the N-terminal region of the core histones
JARID1A	0.0054	Lysine-specific demethylase 5A
JMJD2A	0.0000	Lysine-specific demethylase 4A, This nuclear protein functions as a trimethylation-specific demethylase, converting specific trimethylated histone residues to the dimethylated form, and as a transcriptional repressor

PLU1	0.0167	Histone demethylase that demethylates 'Lys-4' of histone H3, thereby playing a central role in histone code;Acts as a transcriptional corepressor for FOXG1B and PAX9
SAP30	0.0000	Histone deacetylase complex subunit; Involved in the functional recruitment of the Sin3-histone deacetylase complex (HDAC) to a specific subset of N-CoR corepressor complexes. Capable of transcription repression by N-CoR (low levels of expression in the brain)
SIRT6	0.0000	NAD-dependent protein deacetylase. Has deacetylase activity towards histone H3K9Ac and H3K56Ac;Deacetylates histone H3K9Ac at NF-kappa-B target promoters and may down-regulate the expression of a subset of NF-kappa-B target genes
SUZ12	0.0000	Polycomb group (PcG) protein. Component of the PRC2/EED-EZH2 complex, which methylates 'Lys-9' (H3K9me) and 'Lys-27' (H3K27me) of histone H3, leading to transcriptional repression of the affected target gene. he PRC2/EED-EZH2 complex may also serve as a recruiting platform for DNA methyltransferases, thereby linking two epigenetic repression systems
H3K9me1	0.0002	repressive mark
CBX8	0.0010	Component of a Polycomb group (PcG) multiprotein PRC1-like complex, a complex class required to maintain the transcriptionally repressive state of many genes, including Hox genes, throughout development. PcG PRC1 complex acts via chromatin remodeling and modification of histones; it mediates monoubiquitination of histone H2A 'Lys-119', rendering chromatin heritably changed in its expressibility
CHD4	0.0000	Component of the histone deacetylase NuRD complex which participates in the remodeling of chromatin by deacetylating histones; Central component of the nucleosome remodeling and histone deacetylase (NuRD) repressor complex.
NSD2	0.0112	Histone-lysine N-methyltransferase; Histone methyltransferase with histone H3 'Lys-27' (H3K27me) methyltransferase activity. Isoform RE-IIBP may act as a transcription regulator that binds DNA and suppresses IL5 transcription through HDAC recruitment.
REST	0.0247	RE1-silencing transcription factor;Transcriptional repressor which binds neuron-restrictive silencer element (NRSE) and represses neuronal gene transcription in non-neuronal cells. Restricts the expression of neuronal genes by associating with two distinct corepressors, mSin3 and CoREST, which in turn recruit histone deacetylase to the promoters of REST-regulated genes
RNF2	0.0006	E3 ubiquitin-protein ligase that mediates monoubiquitination of 'Lys-119' of histone H2A, thereby playing a central role in histone code and gene regulation. H2A 'Lys-119' ubiquitination gives a specific tag for epigenetic transcriptional repression and participates in X chromosome inactivation of female mammals. May be involved in the initiation of both imprinted and random X inactivation

SETDB1	0.0102	Histone-lysine N-methyltransferase; Histone methyltransferase that specifically trimethylates 'Lys-9' of histone H3. H3 'Lys-9' trimethylation represents a specific tag for epigenetic transcriptional repression by recruiting HP1 (CBX1, CBX3 and/or CBX5) proteins to methylated histones. Mainly functions in euchromatin regions, thereby playing a central role in the silencing of euchromatic genes. H3 'Lys-9' trimethylation is coordinated with DNA methylation
NCoR	-	The N-terminal region contains three independent domains that are capable of mediating transcriptional repression
CBX2	-	Chromobox protein homolog 2;

Examining DMRs overlapping ENCODE elements shows a very interesting intergenic overlap with a number of features and sits in a potentially distal regulatory region for the astrocytes enriched ADH1L1.

Figure 12: Distal regulatory regions a) shows the DMRs and its proximity to other genes within a 100kb region. b) a regional close up showing overlap with multiple ENCODE features.

a)

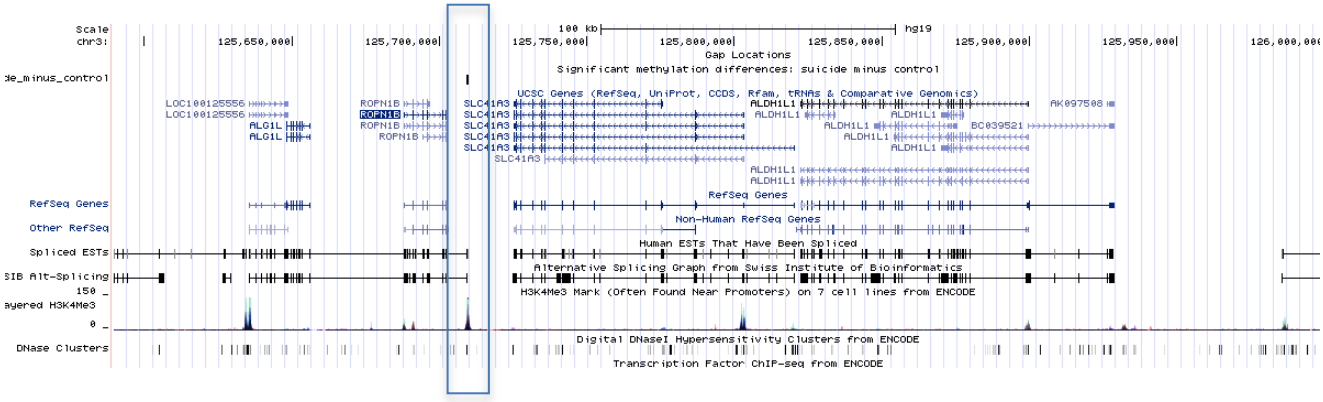

b)

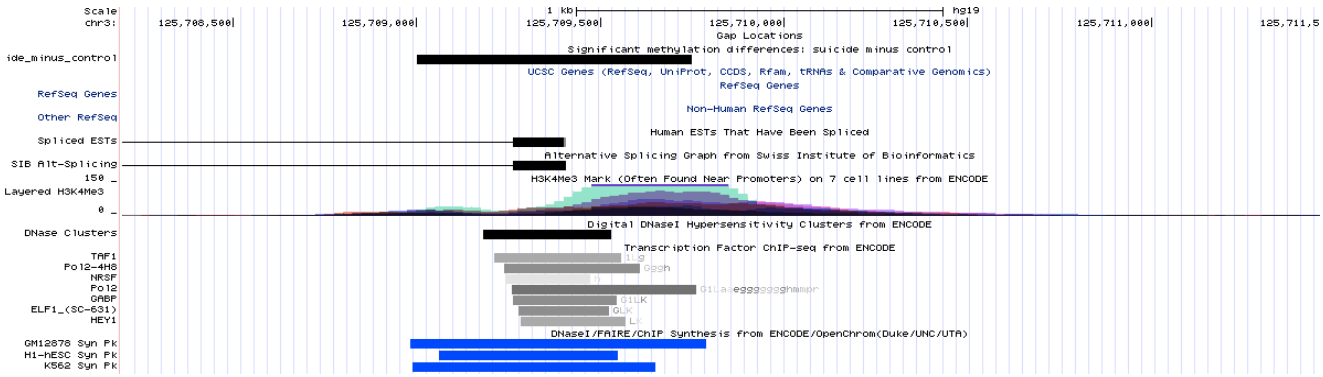

The genes selected for validation were based on their significance and their expression in the brain.

Figure 13: BEGAIN; Brain-enriched guanylate kinase-associated homolog and GRIK2; Glutamate receptor ionotropic kianate. The UCSC screen shot with custom tracks, showing a) overlapping windows with DNA hypermethylation in BEGAIN and b) the region of hypomethylation in GRIK2. Data from Su AI, et al (2004). "A gene atlas of the mouse and human protein-encoding transcriptomes" [6] showing the expression levels of b) BEGAIN and d) GRIK2 in the brain.

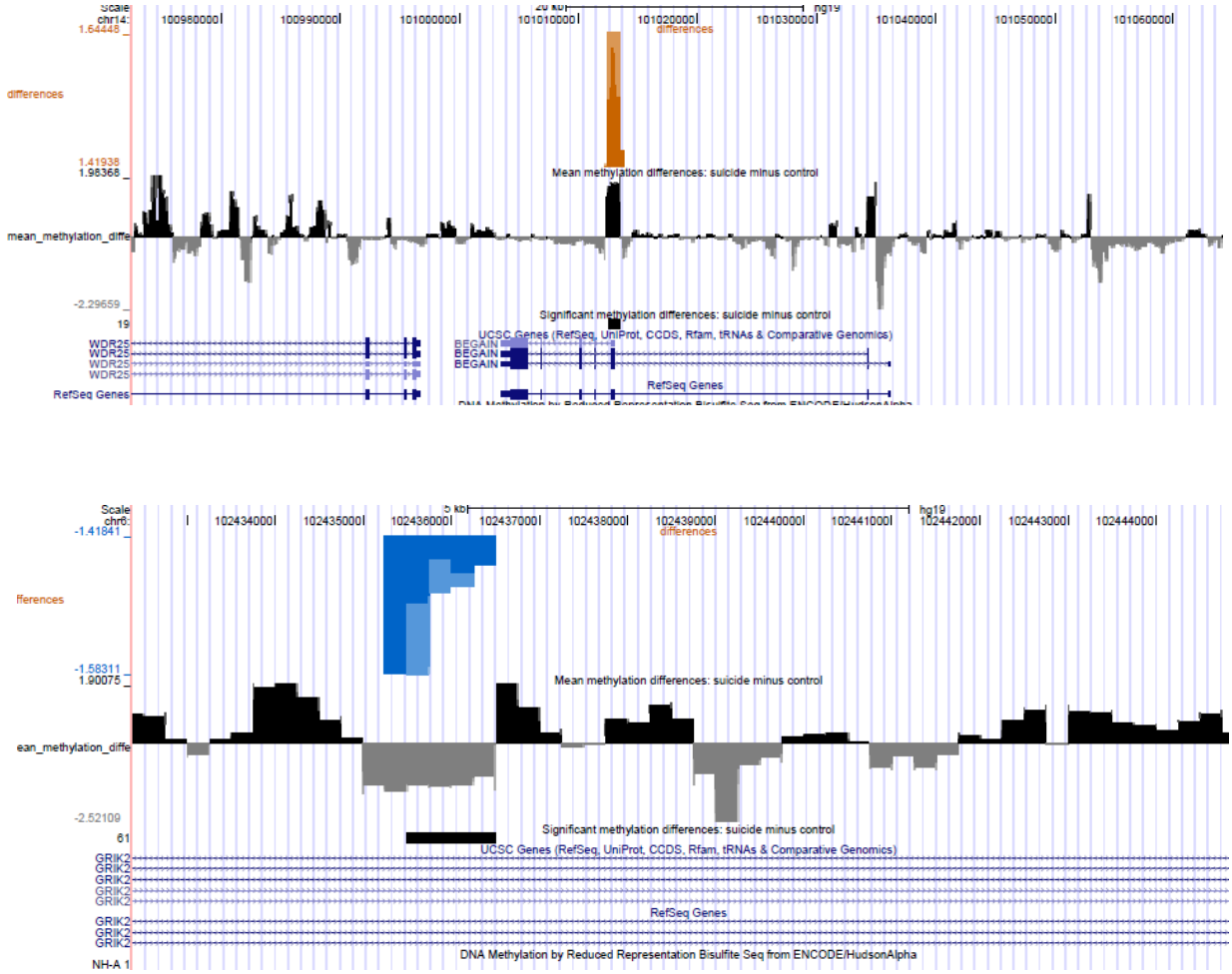

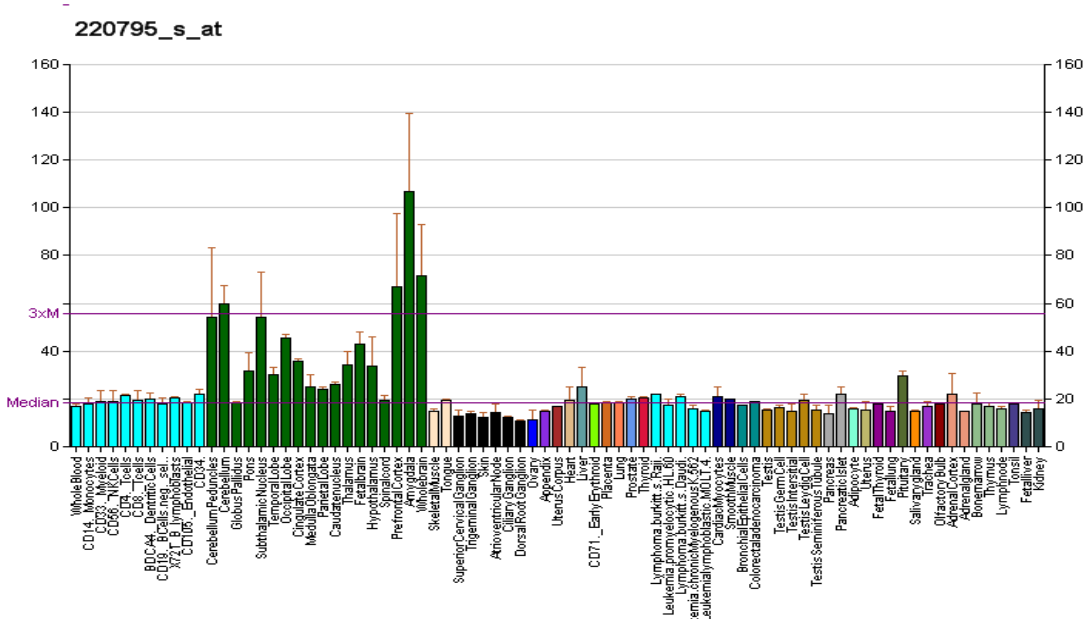
220795_s_at
160
140
120
100
80
60
40
20
0
3xM
Median
WholeBlood
CD14_Monocytes
CD33_Myeloid
CD56_NKCells
CD4_TCells
CD8_TCells
BDCA4_DentrtcCells
CD19_BCells.neg._sel.
X721_B_lymphoblasts
CD105_Endothelial
CD34
CerebellumPeduncles
Cerebellum
Globus Pallidus
Pons
SubthalamicNucleus
TemporalLobe
OccipitalLobe
CingulateCortex
MedullaOblongata
ParietalLobe
CaudateNucleus
Thalamus
Fetalbrain
Hypothalamus
Spinalcord
PrefrontalCortex
Amygdala
WholeBrain
SkeletalMuscle
Tongue
SuperiorCervicalGanglion
TrigeminalGanglion
Skin
AtrioventricularNode
CiliaryGanglion
DorsalRootGanglion
Ovary
Appendix
UterusCorpus
Heart
Liver
CD71_EarlyErythroid
Placenta
Lung
Prostate
Thyroid
Lymphoma.burkitt.s.Raji
Lymphoma.burkitt.s.Daudi
Leukemia.promyelocytic.HL60
Leukemia.chronicMyelogenous.K562
Leukemiallymphoblastic.MOLT.4
CardiacMyocytes
SmoothMuscle
BronchialEpithelialCells
Colorectaladenocarcinoma
Testis
TestisGermCell
TestisInterstitial
TestisLeydigCell
TestisSeminiferousTubule
Pancreas
PancreaticIslet
Adrenocortex
Uterus
FetalThyroid
Fetalllung
Pituitary
Salivarygland
Trachea
OlfactoryBulb
AdrenalCortex
Adrenalgland
Bonemarrow
Thymus
Lymphnode
Tonsil
Fetalliver
Kidney

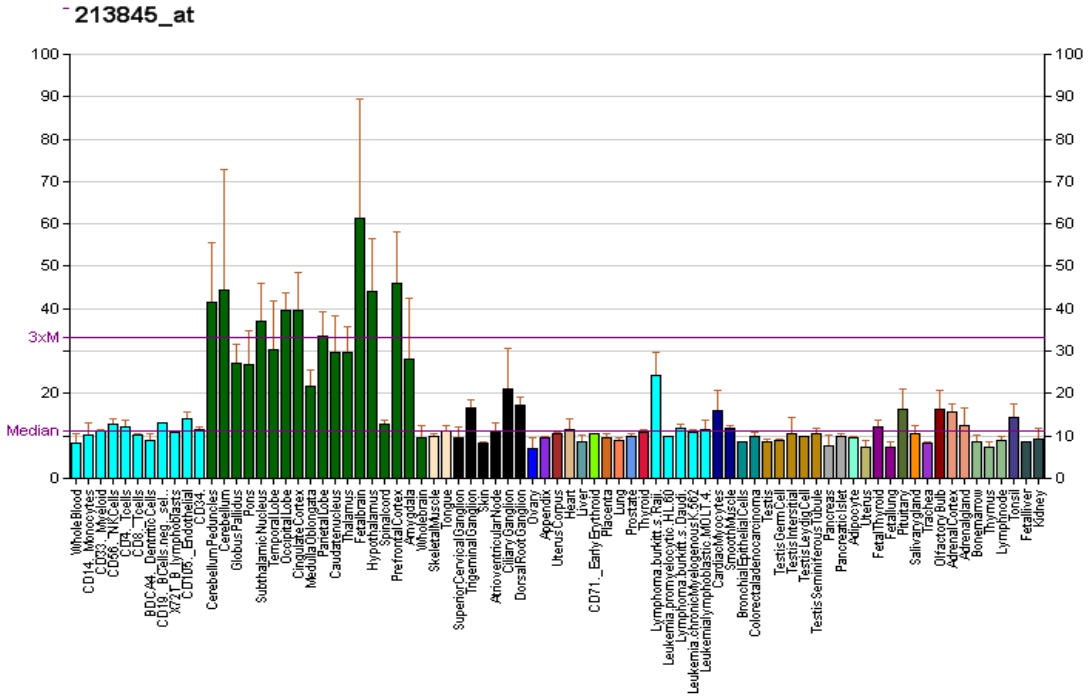
213845_at
100
90
80
70
60
50
40
30
20
10
0
3xM
Median
WholeBlood
CD14_Monocytes
CD33_Myeloid
CD56_NKCells
CD4_TCells
CD8_TCells
BDCA4_DentrtcCells
CD19_BCells.neg._sel.
X721_B_lymphoblasts
CD105_Endothelial
CD34
CerebellumPeduncles
Cerebellum
Globus Pallidus
Pons
SubthalamicNucleus
TemporalLobe
OccipitalLobe
CingulateCortex
MedullaOblongata
ParietalLobe
CaudateNucleus
Thalamus
Fetalbrain
Hypothalamus
Spinalcord
PrefrontalCortex
Amygdala
WholeBrain
SkeletalMuscle
Tongue
SuperiorCervicalGanglion
TrigeminalGanglion
Skin
AtrioventricularNode
CiliaryGanglion
DorsalRootGanglion
Ovary
Appendix
UterusCorpus
Heart
Liver
CD71_EarlyErythroid
Placenta
Lung
Prostate
Thyroid
Lymphoma.burkitt.s.Raji
Lymphoma.burkitt.s.Daudi
Leukemia.promyelocytic.HL60
Leukemia.chronicMyelogenous.K562
Leukemiallymphoblastic.MOLT.4
CardiacMyocytes
SmoothMuscle
BronchialEpithelialCells
Colorectaladenocarcinoma
Testis
TestisGermCell
TestisInterstitial
TestisLeydigCell
TestisSeminiferousTubule
Pancreas
PancreaticIslet
Adrenocortex
Uterus
FetalThyroid
Fetalllung
Pituitary
Salivarygland
Trachea
OlfactoryBulb
AdrenalCortex
Adrenalgland
Bonemarrow
Thymus
Lymphnode
Tonsil
Fetalliver
Kidney

Table 9a: Bs-Seq CpG summary *GRIK2*: Mixed model regression analysis of cases and controls across the 13 CpGs found in the region of differential methylation from MBD-Seq.

Pairwise Comparisons[a]

GRIK2_452bp_CpG#			Mean Difference (I-J)	Std. Error	df	Sig.[c]	95% Confidence Interval for Difference[c]	
							Lower Bound	Upper Bound
1	Control	Suicide	.222*	.056	57.875	.000	.109	.335
	Suicide	Control	-.222*	.056	57.875	.000	-.335	-.109
2	Control	Suicide	.231*	.064	55.550	.001	.103	.359
	Suicide	Control	-.231*	.064	55.550	.001	-.359	-.103
3	Control	Suicide	.227*	.066	52.356	.001	.094	.359
	Suicide	Control	-.227*	.066	52.356	.001	-.359	-.094
4	Control	Suicide	.249*	.068	49.046	.001	.113	.385
	Suicide	Control	-.249*	.068	49.046	.001	-.385	-.113
5	Control	Suicide	.248*	.070	46.248	.001	.107	.390
	Suicide	Control	-.248*	.070	46.248	.001	-.390	-.107
6	Control	Suicide	.262*	.073	44.029	.001	.115	.408
	Suicide	Control	-.262*	.073	44.029	.001	-.408	-.115
7	Control	Suicide	.259*	.078	41.824	.002	.103	.416
	Suicide	Control	-.259*	.078	41.824	.002	-.416	-.103
8	Control	Suicide	.238*	.090	39.201	.011	.057	.419
	Suicide	Control	-.238*	.090	39.201	.011	-.419	-.057
9	Control	Suicide	.268*	.125	35.264	.039	.015	.521
	Suicide	Control	-.268*	.125	35.264	.039	-.521	-.015
10	Control	Suicide	.216	.262	26.317	.416	-.322	.755
	Suicide	Control	-.216	.262	26.317	.416	-.755	.322
11	Control	Suicide	-.202	.537	17.264	.712	-1.333	.930
	Suicide	Control	.202	.537	17.264	.712	-.930	1.333
12	Control	Suicide	.021	.069	23.036	.765	-.122	.164
	Suicide	Control	-.021	.069	23.036	.765	-.164	.122
13	Control	Suicide	.049	.118	24.153	.682	-.195	.293
	Suicide	Control	-.049	.118	24.153	.682	-.293	.195

Based on estimated marginal means

*. The mean difference is significant at the .05 level.

a. Dependent Variable: GRIK2_452bp_Meth.

c. Adjustment for multiple comparisons: Least Significant Difference (equivalent to no adjustments).

Table 9b: Correlation matrix GRIK2: Correlations across all CpGs, significant correlations with spearman rho above or equal to 0.50 are highlighted in purple. This statistical cluster was used for correlations with *GRIK2* gene expression.

Correlations Spearman's rho

		CpG1	CpG2	CpG3	CpG4	CpG5	CpG6	CpG7	CpG8	CpG9	CpG10	CpG11	CpG12	CpG13
CpG1	Correlation	1.000	.970**	.998**	.929**	.855**	.810**	.854**	.851**	.826**	.702**	-.728**	.032	.176
	Sig. (2-		.000	.000	.000	.000	.000	.000	.000	.000	.000	.000	.849	.296
	N	37	37	37	37	37	37	37	37	37	37	37	37	37
CpG2	Correlation	.970**	1.000	.971**	.901**	.825**	.780**	.825**	.822**	.795**	.667**	-.689**	-.040	.141
	Sig. (2-	.000		.000	.000	.000	.000	.000	.000	.000	.000	.000	.812	.404
	N	37	37	37	37	37	37	37	37	37	37	37	37	37
CpG3	Correlation	.998**	.971**	1.000	.931**	.857**	.813**	.856**	.853**	.828**	.704**	-.730**	.019	.160
	Sig. (2-	.000	.000		.000	.000	.000	.000	.000	.000	.000	.000	.911	.345
	N	37	37	37	37	37	37	37	37	37	37	37	37	37
CpG4	Correlation	.929**	.901**	.931**	1.000	.936**	.886**	.936**	.926**	.904**	.771**	-.798**	.070	.208
	Sig. (2-	.000	.000	.000		.000	.000	.000	.000	.000	.000	.000	.682	.217
	N	37	37	37	37	37	37	37	37	37	37	37	37	37
CpG5	Correlation	.855**	.825**	.857**	.936**	1.000	.959**	1.000**	.999**	.964**	.837**	-.725**	.116	.103
	Sig. (2-	.000	.000	.000	.000		.000	.000	.000	.000	.000	.000	.496	.545
	N	37	37	37	37	37	37	37	37	37	37	37	37	37
CpG6	Correlation	.810**	.780**	.813**	.886**	.959**	1.000	.959**	.959**	.922**	.793**	-.666**	.141	.124
	Sig. (2-	.000	.000	.000	.000	.000		.000	.000	.000	.000	.000	.406	.464
	N	37	37	37	37	37	37	37	37	37	37	37	37	37
CpG7	Correlation	.854**	.825**	.856**	.936**	1.000**	.959**	1.000	.999**	.963**	.837**	-.725**	.114	.099
	Sig. (2-	.000	.000	.000	.000	.000	.000		.000	.000	.000	.000	.503	.559
	N	37	37	37	37	37	37	37	37	37	37	37	37	37
CpG8	Correlation	.851**	.822**	.853**	.926**	.999**	.959**	.999**	1.000	.963**	.838**	-.716**	.108	.090
	Sig. (2-	.000	.000	.000	.000	.000	.000	.000		.000	.000	.000	.524	.595
	N	37	37	37	37	37	37	37	37	37	37	37	37	37
CpG9	Correlation	.826**	.795**	.828**	.904**	.964**	.922**	.963**	.963**	1.000	.797**	-.684**	.029	.047
	Sig. (2-	.000	.000	.000	.000	.000	.000	.000	.000		.000	.000	.863	.782
	N	37	37	37	37	37	37	37	37	37	37	37	37	37
CpG10	Correlation	.702**	.667**	.704**	.771**	.837**	.793**	.837**	.838**	.797**	1.000	-.605**	.010	.043
	Sig. (2-	.000	.000	.000	.000	.000	.000	.000	.000	.000		.000	.955	.801
	N	37	37	37	37	37	37	37	37	37	37	37	37	37
CpG11	Correlation	-.728**	-.689**	-.730**	-.798**	-.725**	-.666**	-.725**	-.716**	-.684**	-.605**	1.000	-.206	-.249
	Sig. (2-	.000	.000	.000	.000	.000	.000	.000	.000	.000	.000		.221	.137
	N	37	37	37	37	37	37	37	37	37	37	37	37	37
CpG12	Correlation	.032	-.040	.019	.070	.116	.141	.114	.108	.029	.010	-.206	1.000	.209
	Sig. (2-	.849	.812	.911	.682	.496	.406	.503	.524	.863	.955	.221		.216
	N	37	37	37	37	37	37	37	37	37	37	37	37	37
CpG13	Correlation	.176	.141	.160	.208	.103	.124	.099	.090	.047	.043	-.249	.209	1.000
	Sig. (2-	.296	.404	.345	.217	.545	.464	.559	.595	.782	.801	.137	.216	
	N	37	37	37	37	37	37	37	37	37	37	37	37	37

**. Correlation is significant at the 0.01 level (2-tailed).

Table 9c: Bs-Seq CpG summary *BEGAIN* Mixed model regression analysis of cases and controls across the 13 CpGs found in the region of differential methylation from MBD-Seq

Pairwise Comparisons

BEGAIN_474bp_CpG#			Mean Difference (I-J)	Std. Error	df	Sig.[c]	95% Confidence Interval for Difference[c]	
							Lower Bound	Upper Bound
1	Control	Suicide	-.294*	.118	27.896	.019	-.535	-.053
	Suicide	Control	.294*	.118	27.896	.019	.053	.535
2	Control	Suicide	-.379*	.095	39.144	.000	-.572	-.186
	Suicide	Control	.379*	.095	39.144	.000	.186	.572
3	Control	Suicide	-.339*	.087	47.054	.000	-.515	-.163
	Suicide	Control	.339*	.087	47.054	.000	.163	.515
4	Control	Suicide	-.279*	.074	56.863	.000	-.428	-.130
	Suicide	Control	.279*	.074	56.863	.000	.130	.428
5	Control	Suicide	-.263*	.085	51.869	.003	-.435	-.092
	Suicide	Control	.263*	.085	51.869	.003	.092	.435
6	Control	Suicide	-.313*	.084	50.765	.001	-.482	-.143
	Suicide	Control	.313*	.084	50.765	.001	.143	.482
7	Control	Suicide	-.234*	.076	56.920	.003	-.386	-.083
	Suicide	Control	.234*	.076	56.920	.003	.083	.386
8	Control	Suicide	-.227*	.085	55.615	.010	-.398	-.057
	Suicide	Control	.227*	.085	55.615	.010	.057	.398
9	Control	Suicide	-.322*	.072	56.399	.000	-.466	-.178
	Suicide	Control	.322*	.072	56.399	.000	.178	.466
10	Control	Suicide	-.247*	.070	58.591	.001	-.387	-.107
	Suicide	Control	.247*	.070	58.591	.001	.107	.387
11	Control	Suicide	-.301*	.068	59.147	.000	-.437	-.165
	Suicide	Control	.301*	.068	59.147	.000	.165	.437
12	Control	Suicide	-.347*	.070	60.643	.000	-.486	-.208
	Suicide	Control	.347*	.070	60.643	.000	.208	.486
13	Control	Suicide	-.263*	.076	60.523	.001	-.415	-.111
	Suicide	Control	.263*	.076	60.523	.001	.111	.415
14	Control	Suicide	-.330*	.078	57.186	.000	-.486	-.173
	Suicide	Control	.330*	.078	57.186	.000	.173	.486
15	Control	Suicide	-.229*	.074	55.845	.003	-.376	-.081
	Suicide	Control	.229*	.074	55.845	.003	.081	.376
16	Control	Suicide	-.189*	.074	55.384	.014	-.338	-.040
	Suicide	Control	.189*	.074	55.384	.014	.040	.338
17	Control	Suicide	-.289*	.085	54.393	.001	-.459	-.120
	Suicide	Control	.289*	.085	54.393	.001	.120	.459
18	Control	Suicide	-.321*	.085	50.954	.000	-.492	-.151
	Suicide	Control	.321*	.085	50.954	.000	.151	.492
19	Control	Suicide	-.200*	.083	45.053	.020	-.367	-.032
	Suicide	Control	.200*	.083	45.053	.020	.032	.367
20	Control	Suicide	-.282*	.101	44.434	.008	-.486	-.079
	Suicide	Control	.282*	.101	44.434	.008	.079	.486

21	Control	Suicide	-.158	.089	43.918	.082	-.337	.021
	Suicide	Control	.158	.089	43.918	.082	-.021	.337
22	Control	Suicide	-.265*	.096	45.440	.008	-.458	-.072
	Suicide	Control	.265*	.096	45.440	.008	.072	.458
23	Control	Suicide	-.179	.090	49.518	.053	-.360	.003
	Suicide	Control	.179	.090	49.518	.053	-.003	.360
24	Control	Suicide	-.288*	.081	54.966	.001	-.450	-.127
	Suicide	Control	.288*	.081	54.966	.001	.127	.450
25	Control	Suicide	-.257*	.077	56.962	.002	-.412	-.102
	Suicide	Control	.257*	.077	56.962	.002	.102	.412
26	Control	Suicide	-.244*	.094	49.336	.012	-.432	-.056
	Suicide	Control	.244*	.094	49.336	.012	.056	.432
27	Control	Suicide	-.280*	.110	38.160	.015	-.503	-.058
	Suicide	Control	.280*	.110	38.160	.015	.058	.503
28	Control	Suicide	-.360*	.115	36.178	.003	-.593	-.127
	Suicide	Control	.360*	.115	36.178	.003	.127	.593
29	Control	Suicide	-.090	.112	37.867	.428	-.317	.137
	Suicide	Control	.090	.112	37.867	.428	-.137	.317
30	Control	Suicide	-.215*	.097	46.944	.031	-.410	-.021
	Suicide	Control	.215*	.097	46.944	.031	.021	.410
31	Control	Suicide	-.224*	.094	52.014	.021	-.414	-.035
	Suicide	Control	.224*	.094	52.014	.021	.035	.414
32	Control	Suicide	-.158	.109	41.999	.154	-.377	.062
	Suicide	Control	.158	.109	41.999	.154	-.062	.377
33	Control	Suicide	-.023	.124	32.058	.852	-.277	.230
	Suicide	Control	.023	.124	32.058	.852	-.230	.277
34	Control	Suicide	.030	.051	26.692	.560	-.075	.135
	Suicide	Control	-.030	.051	26.692	.560	-.135	.075

Based on estimated marginal means

*. The mean difference is significant at the .05 level.

a. Dependent Variable: BEGAIN_474bp_Meth.

c. Adjustment for multiple comparisons: Least Significant Difference (equivalent to no adjustments).

Table 9c: Correlation Matrix *BEGAIN*: Correlations across all CpGs, significant correlations with spearman rho above or equal to 0.50 are highlighted in purple. A noticeable absence in correlations occur at CpG 29, biologically this CpG and the last 4 are physically removed (~50bps) from the first 28 CpGs, which are biologically and statistically, tightly clusters. This first cluster was used in the correlations with expression data.

Correlations

		CpG1	CpG2	CpG3	CpG4	CpG5	CpG6	CpG7	CpG8	CpG9	CpG10	CpG11	CpG12	CpG13	CpG14	CpG15	CpG16	CpG17	CpG18	CpG19	CpG20	CpG21	CpG22	CpG23	CpG24	CpG25	CpG26	CpG27	CpG28	CpG29	CpG30	CpG31	CpG32	CpG33	CpG34
CpG1	Pearson Correlation	1	.814**	.793**	.925**	.904**	.626**	.519*	.514*	.844**	.936**	.781**	.904**	.822**	.803**	.671**	.553**	.816**	.768**	.568**	.794**	.529*	.811**	.494*	.831**	.731**	.659**	.423	.856**	.281	.680**	.632**	.584**	.409	.192
	Sig. (2-tailed)		.000	.000	.000	.000	.002	.016	.017	.000	.000	.000	.000	.000	.000	.001	.009	.000	.000	.007	.000	.014	.000	.023	.000	.000	.001	.056	.000	.217	.001	.002	.009	.082	.431
	N	21	21	21	21	21	21	21	21	21	21	21	21	21	21	21	21	21	21	21	21	21	21	21	21	21	21	21	21	21	21	21	19	19	19
CpG2	Pearson Correlation	.814**	1	.979**	.926**	.900**	.467*	.438*	.529*	.739**	.835**	.600**	.720**	.823**	.689**	.605**	.421	.709**	.679**	.527*	.620**	.377	.615**	.311	.621**	.657**	.706**	.358	.779**	.362	.575**	.481*	.394	.184	-.203
	Sig. (2-tailed)	.000		.000	.000	.000	.033	.047	.014	.000	.000	.004	.000	.000	.001	.004	.057	.000	.001	.014	.003	.092	.003	.170	.003	.001	.000	.111	.000	.107	.006	.027	.095	.427	.404
	N	21	21	21	21	21	21	21	21	21	21	21	21	21	21	21	21	21	21	21	21	21	21	21	21	21	21	21	21	21	21	21	19	19	19
CpG3	Pearson Correlation	.793**	.979**	1	.911**	.881**	.469*	.475*	.548**	.721**	.805**	.588**	.693**	.787**	.670**	.599**	.415*	.693**	.663**	.506*	.578**	.352	.575**	.327	.609**	.657**	.725**	.333	.732**	.300	.529**	.442*	.399	.200	-.219
	Sig. (2-tailed)	.000	.000		.000	.000	.018	.016	.005	.000	.000	.002	.000	.000	.000	.002	.039	.000	.000	.010	.002	.084	.003	.110	.001	.000	.000	.104	.000	.145	.007	.027	.059	.359	.340
	N	21	21	25	25	25	25	25	25	25	25	25	25	25	25	25	25	25	25	25	25	25	25	25	25	25	25	25	25	25	25	25	23	23	21
CpG4	Pearson Correlation	.925**	.926**	.911**	1	.924**	.513**	.506**	.567**	.765**	.830**	.626**	.769**	.783**	.695**	.607**	.493**	.763**	.721**	.565**	.675**	.433*	.656**	.404*	.700**	.710**	.619**	.407*	.767**	.298	.616**	.531**	.482**	.309	-.152
	Sig. (2-tailed)	.000	.000	.000		.000	.002	.002	.000	.000	.000	.000	.000	.000	.000	.000	.003	.000	.000	.000	.000	.010	.000	.018	.000	.000	.000	.017	.000	.087	.000	.001	.005	.085	.422
	N	21	21	25	34	34	34	34	34	34	34	34	34	34	34	34	34	34	34	34	34	34	34	34	34	34	34	34	34	34	34	34	32	32	30
CpG5	Pearson Correlation	.904**	.900**	.881**	.924**	1	.469**	.524**	.579**	.813**	.802**	.616**	.747**	.821**	.756**	.614**	.471**	.809**	.786**	.551**	.732**	.476**	.667**	.462**	.734**	.733**	.673**	.502**	.696**	.229	.663**	.566**	.595**	.333	-.063
	Sig. (2-tailed)	.000	.000	.000	.000		.005	.001	.000	.000	.000	.000	.000	.000	.000	.000	.005	.000	.000	.001	.000	.004	.000	.006	.000	.000	.000	.003	.000	.192	.000	.000	.000	.063	.743
	N	21	21	25	34	34	34	34	34	34	34	34	34	34	34	34	34	34	34	34	34	34	34	34	34	34	34	34	34	34	34	34	32	32	30
CpG6	Pearson Correlation	.626**	.467*	.469*	.513**	.469**	1	.818**	.860**	.673**	.689**	.587**	.721**	.612**	.700**	.885**	.912**	.711**	.653**	.841**	.717**	.814**	.699**	.855**	.687**	.642**	.583**	.686**	.517**	.425*	.663**	.643**	.587**	.154	.130
	Sig. (2-tailed)	.002	.033	.018	.002	.005		.000	.000	.000	.000	.000	.000	.000	.000	.000	.000	.000	.000	.000	.000	.000	.000	.000	.000	.000	.000	.000	.002	.012	.000	.000	.000	.399	.495
	N	21	21	25	34	34	34	34	34	34	34	34	34	34	34	34	34	34	34	34	34	34	34	34	34	34	34	34	34	34	34	34	32	32	30
CpG7	Pearson Correlation	.519*	.438*	.475*	.506**	.524**	.818**	1	.866**	.713**	.605**	.548**	.674**	.649**	.738**	.874**	.856**	.725**	.723**	.782**	.680**	.762**	.639**	.848**	.684**	.666**	.581**	.804**	.555**	.408*	.606**	.630**	.585**	.094	.145
	Sig. (2-tailed)	.016	.047	.016	.002	.001	.000		.000	.000	.000	.001	.000	.000	.000	.000	.000	.000	.000	.000	.000	.000	.000	.000	.000	.000	.000	.000	.001	.017	.000	.000	.000	.607	.445
	N	21	21	25	34	34	34	34	34	34	34	34	34	34	34	34	34	34	34	34	34	34	34	34	34	34	34	34	34	34	34	34	32	32	30
CpG8	Pearson Correlation	.514*	.529*	.548**	.567**	.579**	.860**	.866**	1	.711**	.630**	.549**	.673**	.690**	.722**	.879**	.861**	.720**	.713**	.720**	.685**	.704**	.634**	.841**	.679**	.677**	.610**	.699**	.485**	.430*	.653**	.649**	.667**	-.074	.031
	Sig. (2-tailed)	.017	.014	.005	.000	.000	.000	.000		.000	.000	.001	.000	.000	.000	.000	.000	.000	.000	.000	.000	.000	.000	.000	.000	.000	.000	.000	.004	.011	.000	.000	.000	.687	.870
	N	21	21	25	34	34	34	34	34	34	34	34	34	34	34	34	34	34	34	34	34	34	34	34	34	34	34	34	34	34	34	34	32	32	30
CpG9	Pearson Correlation	.844**	.739**	.721**	.765**	.813**	.673**	.713**	.711**	1	.903**	.844**	.937**	.918**	.975**	.736**	.722**	.945**	.966**	.650**	.935**	.646**	.922**	.722**	.934**	.897**	.832**	.697**	.782**	.350*	.860**	.787**	.832**	.262	.205
	Sig. (2-tailed)	.000	.000	.000	.000	.000	.000	.000	.000		.000	.000	.000	.000	.000	.000	.000	.000	.000	.000	.000	.000	.000	.000	.000	.000	.000	.000	.000	.042	.000	.000	.000	.147	.276
	N	21	21	25	34	34	34	34	34	34	34	34	34	34	34	34	34	34	34	34	34	34	34	34	34	34	34	34	34	34	34	34	32	32	30
CpG10	Pearson Correlation	.936**	.835**	.805**	.830**	.802**	.689**	.605**	.630**	.903**	1	.813**	.912**	.896**	.887**	.721**	.666**	.869**	.860**	.677**	.860**	.570**	.909**	.613**	.874**	.851**	.798**	.568**	.821**	.373*	.778**	.686**	.681**	.269	.089
	Sig. (2-tailed)	.000	.000	.000	.000	.000	.000	.000	.000	.000		.000	.000	.000	.000	.000	.000	.000	.000	.000	.000	.000	.000	.000	.000	.000	.000	.000	.000	.030	.000	.000	.000	.136	.639
	N	21	21	25	34	34	34	34	34	34	34	34	34	34	34	34	34	34	34	34	34	34	34	34	34	34	34	34	34	34	34	34	32	32	30
CpG11	Pearson Correlation	.781**	.600**	.588**	.626**	.616**	.587**	.548**	.549**	.844**	.813**	1	.877**	.745**	.843**	.607**	.574**	.805**	.810**	.465**	.822**	.438*	.826**	.549**	.819**	.781**	.694**	.484**	.665**	.045	.728**	.673**	.718**	.161	.209
	Sig. (2-tailed)	.000	.004	.002	.000	.000	.000	.001	.001	.000	.000		.000	.000	.000	.000	.000	.000	.000	.006	.000	.010	.000	.001	.000	.000	.000	.004	.000	.802	.000	.000	.000	.379	.268
	N	21	21	25	34	34	34	34	34	34	34	34	34	34	34	34	34	34	34	34	34	34	34	34	34	34	34	34	34	34	34	34	32	32	30
CpG12	Pearson Correlation	.904**	.720**	.693**	.769**	.747**	.721**	.674**	.673**	.937**	.912**	.877**	1	.862**	.912**	.749**	.748**	.887**	.889**	.652**	.927**	.639**	.933**	.672**	.929**	.880**	.783**	.610**	.832**	.333	.821**	.761**	.742**	.255	.281
	Sig. (2-tailed)	.000	.000	.000	.000	.000	.000	.000	.000	.000	.000	.000		.000	.000	.000	.000	.000	.000	.000	.000	.000	.000	.000	.000	.000	.000	.000	.000	.054	.000	.000	.000	.159	.132
	N	21	21	25	34	34	34	34	34	34	34	34	34	34	34	34	34	34	34	34	34	34	34	34	34	34	34	34	34	34	34	34	32	32	30
CpG13	Pearson Correlation	.822**	.823**	.787**	.783**	.821**	.612**	.649**	.690**	.918**	.896**	.745**	.862**	1	.886**	.891**	.866**	.900**	.896**	.672**	.870**	.668**	.862**	.687**	.913**	.873**	.827**	.654**	.730**	.482**	.859**	.787**	.785**	.275	.124
	Sig. (2-tailed)	.000	.000	.000	.000	.000	.000	.000	.000	.000	.000	.000	.000		.000	.000	.000	.000	.000	.000	.000	.000	.000	.000	.000	.000	.000	.000	.000	.004	.000	.000	.000	.128	.514
	N	21	21	25	34	34	34	34	34	34	34	34	34	34	34	34	34	34	34	34	34	34	34	34	34	34	34	34	34	34	34	34	32	32	30
CpG14	Pearson Correlation	.803**	.689**	.670**	.695**	.756**	.700**	.738**	.722**	.975**	.887**	.843**	.912**	.886**	1	.737**	.718**	.952**	.959**	.663**	.904**	.668**	.920**	.757**	.911**	.908**	.837**	.739**	.772**	.367*	.838**	.810**	.838**	.255	.200
	Sig. (2-tailed)	.000	.001	.000	.000	.000	.000	.000	.000	.000	.000	.000	.000	.000		.000	.000	.000	.000	.000	.000	.000	.000	.000	.000	.000	.000	.000	.000	.033	.000	.000	.000	.159	.290
	N	21	21	25	34	34	34	34	34	34	34	34	34	34	34	34	34	34	34	34	34	34	34	34	34	34	34	34	34	34	34	34	32	32	30
CpG15	Pearson Correlation	.671**	.605**	.599**	.607**	.614**	.885**	.874**	.879**	.736**	.721**	.607**	.749**	.891**	.737**	1	.893**	.735**	.703**	.866**	.750**	.769**	.713**	.836**	.713**	.681**	.634**	.779**	.574**	.415*	.684**	.666**	.603**	.058	.056
	Sig. (2-tailed)	.001	.004	.002	.000	.000	.000	.000	.000	.000	.000	.000	.000	.000	.000		.000	.000	.000	.000	.000	.000	.000	.000	.000	.000	.000	.000	.000	.015	.000	.000	.000	.753	.770
	N	21	21	25	34	34	34	34	34	34	34	34	34	34	34	34	34	34	34	34	34	34	34	34	34	34	34	34	34	34	34	34	32	32	30
CpG16	Pearson Correlation	.553**	.421	.415*	.493**	.471**	.912**	.856**	.861**	.722**	.666**	.574**	.748**	.866**	.718**	.893**	1	.719**	.720**	.830**	.768**	.793**	.748**	.882**	.751**	.718**	.658**	.753**	.513**	.395*	.707**	.656**	.651**	.097	.188
	Sig. (2-tailed)	.009	.057	.039	.003	.005	.000	.000	.000	.000	.000	.000	.000	.000	.000	.000		.000	.000	.000	.000	.000	.000	.000	.000	.000	.000	.000	.002	.021	.000	.000	.000	.598	.319
	N	21	21	25	34	34	34	34	34	34	34	34	34	34	34	34	34	34	34	34	34	34	34	34	34	34	34	34	34	34	34	34	32	32	30
CpG17	Pearson Correlation	.816**	.709**	.693**	.763**	.809**	.711**	.725**	.720**	.945**	.869**	.805**	.887**	.900**	.952**	.735**	.719**	1	.932**	.686**	.894**	.707**	.896**	.743**	.915**	.915**	.834**	.684**	.739**	.346*	.893**	.829**	.824**	.330	.132
	Sig. (2-tailed)	.000	.000	.000	.000	.000	.000	.000	.000	.000	.000	.000	.000	.000	.000	.000	.000		.000	.000	.000	.000	.000	.000	.000	.000	.000	.000	.000	.045	.000	.000	.000	.065	.485
	N	21	21	25	34	34	34	34	34	34	34	34	34	34	34	34	34	34	34	34	34	34	34	34	34	34	34	34	34	34	34	34	32	32	30
CpG18	Pearson Correlation	.768**	.679**	.663**	.721**	.786**	.653**	.723**	.713**	.966**	.860**	.810**	.889**	.896**	.959**	.703**	.720**	.932**	1	.649**	.923**	.637**	.889**	.739**	.907**	.931**	.852**	.736**	.758**	.290	.855**	.759**	.825**	.249	.206
	Sig. (2-tailed)	.000	.001	.000	.000	.000	.000	.000	.000	.000	.000	.000	.000	.000	.000	.000	.000	.000		.000	.000	.000	.000	.000	.000	.000	.000	.000	.000	.093	.000	.000	.000	.169	.275
	N	21	21	25	34	34	34	34	34	34	34	34	34	34	34	34	34	34	34	34	34	34	34	34	34	34	34	34	34	34	34	34	32	32	30
CpG19	Pearson Correlation	.568**	.527*	.506*	.565**	.551**	.841**	.782**	.720**	.650**	.677**	.465**	.652**	.672**	.663**	.866**	.830**	.686**	.649**	1	.697**	.878**	.644**	.814**	.651**	.619**	.571**	.839**	.577**	.535**	.669**	.642**	.514**	.335	-.042
	Sig. (2-tailed)	.007	.014	.010	.000	.001	.000	.000	.000	.000	.000	.006	.000	.000	.000	.000	.000	.000	.000		.000	.000	.000	.000	.000	.000	.000	.000	.000	.001	.000	.000	.003	.061	.824
	N	21	21	25	34	34	34	34	34	34	34	34	34	34	34	34	34	34	34	34	34	34	34	34	34	34	34	34	34	34	34	34	32	32	30
CpG20	Pearson Correlation	.794**	.620**	.578**	.675**	.732**	.717**	.680**	.685**	.935**	.860**	.822**	.927**	.870**	.904**	.750**	.768**	.894**	.923**	.697**	1	.673**	.959**	.748**	.917**	.900**	.808**	.708**	.728**	.303	.880**	.766**	.800**	.207	.294
	Sig. (2-tailed)	.000	.003	.002	.000	.000	.000	.000	.000	.000	.000	.000	.000	.000	.000	.000	.000	.000	.000	.000		.000	.000	.000	.000	.000	.000	.000	.000	.082	.000	.000	.000	.255	.115
	N	21	21	25	34	34	34	34	34	34	34	34	34	34	34	34	34	34	34	34	34	34	34	34	34	34	34	34	34	34	34	34	32	32	30
CpG21	Pearson Correlation	.529*	.377	.352	.433*	.476**	.814**	.762**	.704**	.646**	.570**	.438*	.639**	.668**	.668**	.769**	.793**	.707**	.637**	.878**	.673**	1	.626**	.876**	.701**	.613**	.551**	.798**	.481**	.577**	.725**	.728**	.652**	.464**	.217
	Sig. (2-tailed)	.014	.092	.084	.010	.004	.000	.000	.000	.000	.000	.010	.000	.000	.000	.000	.000	.000	.000	.000	.000		.000	.000	.000	.000	.001	.000	.004	.000	.000	.000	.000	.008	.248
	N	21	21	25	34	34	34	34	34	34	34	34	34	34	34	34	34	34	34	34	34	34	34	34	34	34	34	34	34	34	34	34	32	32	30
CpG22	Pearson Correlation	.811**	.615**	.575**	.656**	.667**	.699**	.639**	.634**	.922**	.909**	.826**	.933**	.862**	.920**	.713**	.748**	.896**	.889**	.644**	.959**	.626**	1	.707**	.936**	.896**	.807**	.637**	.766**	.360*	.861**	.769**	.762**	.166	.289
	Sig. (2-tailed)	.000	.003	.003	.000	.000	.000	.000	.000	.000	.000	.000	.000	.000	.000	.000	.000	.000	.000	.000	.000	.000		.000	.000	.000	.000	.000	.000	.037	.000	.000	.000	.362	.121
	N	21	21	25	34	34	34	34	34	34	34	34	34	34	34	34	34	34	34	34	34	34	34	34	34	34	34	34	34	34	34	34	32	32	30
CpG23	Pearson Correlation	.494*	.311	.327	.404*	.462**	.855**	.848**	.841**	.722**	.613**	.549**	.672**	.687**	.757**	.836**	.882**	.743**	.739**	.814**	.748**	.876**	.707**	1	.740**	.697**	.636**	.865**	.412*	.463**	.722**	.720**	.742**	.135	.236
	Sig. (2-tailed)	.023	.170	.110	.018	.006	.000	.000	.000	.000	.000	.001	.000	.000	.000	.000	.000	.000	.000	.000	.000	.000	.000		.000	.000	.000	.000	.016	.006	.000	.000	.000	.460	.210
	N	21	21	25	34	34	34	34	34	34	34	34	34	34	34	34	34	34	34	34	34	34	34	34	34	34	34	34	34	34	34	34	32	32	30
CpG24	Pearson Correlation	.831**	.621**	.609**	.700**	.734**	.687**	.684**	.679**	.934**	.874**	.819**	.929**	.913**	.911**	.713**	.751**	.915**	.907**	.651**	.917**	.701**	.936**	.740**	1	.890**	.793**	.668**	.756**	.384*	.889**	.840**	.833**	.308	.253
	Sig. (2-tailed)	.000	.003	.001	.000	.000	.000	.000	.000	.000	.000	.000	.000	.000	.000	.000	.000	.000	.000	.000	.000	.000	.000	.000		.000	.000	.000	.000	.025	.000	.000	.000	.087	.178
	N	21	21	25	34	34	34	34	34	34	34	34	34	34	34	34	34	34	34	34	34	34	34	34	34	34	34	34	34	34	34	34	32	32	30
CpG25	Pearson Correlation	.731**	.657**	.657**	.710**	.733**	.642**	.666**	.677**	.897**	.851**	.781**	.880**	.873**	.908**	.681**	.718**	.915**	.931**	.619**	.900**	.613**	.896**	.697**	.890**	1	.924**	.648**	.732**	.259	.827**	.698**	.758**	.194	.162
	Sig. (2-tailed)	.000	.001	.000	.000	.000	.000	.000	.000	.000	.000	.000	.000	.000	.000	.000	.000	.000	.000	.000	.000	.000	.000	.000	.000		.000	.000	.000	.139	.000	.000	.000	.287	.337
	N	21	21	25	34	34	34	34	34	34	34	34	34	34	34	34	34	34	34	34	34	34	34	34	34	34	34	34	34	34	34	34	32	32	30
CpG26	Pearson Correlation	.659**	.706**	.725**	.619**	.673**	.583**	.581**	.610**	.832**	.798**	.694**	.783**	.827**	.837**	.634**	.658**	.834**	.852**	.571**	.808**	.551**	.807**	.636**	.793**	.924**	1	.573**	.593**	.204	.769**	.608**	.730**	.168	.100
	Sig. (2-tailed)	.001	.000	.000	.000	.000	.000	.000	.000	.000	.000	.000	.000	.000	.000	.000	.000	.000	.000	.000	.000	.001	.000	.000	.000	.000		.000	.000	.246	.000	.000	.000	.363	.601
	N	21	21	25	34	34	34	34	34	34	34	34	34	34	34	34	34	34	34	34	34	34	34	34	34	34	34	34	34	34	34	34	32	32	30
CpG27	Pearson Correlation	.423	.358	.333	.407*	.502**	.686**	.804**	.669**	.697**	.568**	.484**	.610**	.654**	.739**	.779**	.753**	.684**	.736**	.839**	.708**	.798**	.637**	.865**	.668**	.648**	.573**	1	.527**	.501**	.652**	.669**	.618**	.212	.120
	Sig. (2-tailed)	.056	.111	.104	.017	.003	.000	.000	.000	.000	.000	.004	.000	.000	.000	.000	.000	.000	.000	.000	.000	.000	.000	.000	.000	.000	.000		.001	.003	.000	.000	.000	.245	.527
	N	21	21	25	34	34	34	34	34	34	34	34	34	34	34	34	34	34	34	34	34	34	34	34	34	34	34	34	34	34	34	34	32	32	30
CpG28	Pearson Correlation	.856**	.779**	.732**	.767**	.696**	.517**	.555**	.485**	.782**	.821**	.665**	.832**	.730**	.772**	.574**	.513**	.739**	.758**	.577**	.728**	.481**	.766**	.412*	.756**	.732**	.593**	.527**	1	.448**	.611**	.615**	.456**	.304	.051
	Sig. (2-tailed)	.000	.000	.000	.000	.000	.002	.001	.004	.000	.000	.000	.000	.000	.000	.000	.002	.000	.000	.000	.000	.004	.000	.016	.000	.000	.000	.001		.008	.000	.000	.009	.091	.790
	N	21	21	25	34	34	34	34	34	34	34	34	34	34	34	34	34	34	34	34	34	34	34	34	34	34	34	34	34	34	34	34	32	32	30
CpG29	Pearson Correlation	.281	.362	.300	.298	.229	.425*	.408*	.430*	.350*	.373*	.045	.333	.482**	.367*	.415*	.395*	.346*	.290	.535**	.303	.577**	.360*	.463**	.384*	.259	.204	.501**	.448**	1	.412*	.548**	.267	.210	.028
	Sig. (2-tailed)	.217	.107	.145	.087	.192	.012	.017	.011	.042	.030	.802	.054	.004	.033	.015	.021	.045	.093	.001	.082	.000	.037	.006	.025	.139	.246	.003	.008		.016	.001	.140	.249	.882
	N	21	21	25	34	34	34	34	34	34	34	34	34	34	34	34	34	34	34	34	34	34	34	34	34	34	34	34	34	34	34	34	32	32	30
CpG30	Pearson Correlation	.680**	.575**	.529**	.616**	.663**	.663**	.606**	.653**	.860**	.778**	.728**	.821**	.859**	.858**	.684**	.707**	.893**	.855**	.669**	.880**	.725**	.861**	.722**	.889**	.827**	.769**	.652**	.611**	.412*	1	.924**	.870**	.325	.171
	Sig. (2-tailed)	.001	.006	.007	.000	.000	.000	.000	.000	.000	.000	.000	.000	.000	.000	.000	.000	.000	.000	.000	.000	.000	.000	.000	.000	.000	.000	.000	.000	.016		.000	.000	.069	.367
	N	21	21	25	34	34	34	34	34	34	34	34	34	34	34	34	34	34	34	34	34	34	34	34	34	34	34	34	34	34	34	34	32	32	30
CpG31	Pearson Correlation	.632**	.481*	.442*	.531**	.566**	.643**	.630**	.649**	.787**	.686**	.673**	.761**	.787**	.810**	.666**	.656**	.829**	.759**	.642**	.766**	.728**	.769**	.720**	.840**	.698**	.608**	.669**	.615**	.548**	.924**	1	.880**	.345	.174
	Sig. (2-tailed)	.002	.027	.027	.001	.000	.000	.000	.000	.000	.000	.000	.000	.000	.000	.000	.000	.000	.000	.000	.000	.000	.000	.000	.000	.000	.000	.000	.000	.001	.000		.000	.053	.357
	N	21	21	25	34	34	34	34	34	34	34	34	34	34	34	34	34	34	34	34	34	34	34	34	34	34	34	34	34	34	34	34	32	32	30
CpG32	Pearson Correlation	.584**	.394	.399	.482**	.595**	.587**	.585**	.667**	.832**	.681**	.718**	.742**	.785**	.838**	.603**	.651**	.824**	.825**	.514**	.800**	.652**	.762**	.742**	.833**	.758**	.730**	.618**	.456**	.267	.870**	.880**	1	.312	.328
	Sig. (2-tailed)	.009	.095	.059	.005	.000	.000	.000	.000	.000	.000	.000	.000	.000	.000	.000	.000	.000	.000	.003	.000	.000	.000	.000	.000	.000	.000	.000	.009	.140	.000	.000		.083	.077
	N	19	19	23	32	32	32	32	32	32	32	32	32	32	32	32	32	32	32	32	32	32	32	32	32	32	32	32	32	32	32	32	32	32	30
CpG33	Pearson Correlation	.409	.184	.200	.309	.333	.154	.094	-.074	.262	.269	.161	.255	.275	.255	.058	.097	.330	.249	.335	.207	.464**	.166	.135	.308	.194	.168	.212	.304	.210	.325	.345	.312	1	.173
	Sig. (2-tailed)	.082	.427	.359	.085	.063	.399	.607	.687	.147	.136	.379	.159	.128	.159	.753	.598	.065	.169	.061	.255	.008	.362	.460	.087	.287	.363	.245	.091	.249	.069	.053	.083		.360
	N	19	19	23	32	32	32	32	32	32	32	32	32	32	32	32	32	32	32	32	32	32	32	32	32	32	32	32	32	32	32	32	32	32	30
CpG34	Pearson Correlation	.192	-.203	-.219	-.152	-.063	.130	.145	.031	.205	.089	.209	.281	.124	.200	.056	.188	.132	.206	-.042	.294	.217	.289	.236	.253	.182	.100	.120	.051	.028	.171	.174	.328	.173	1
	Sig. (2-tailed)	.431	.404	.340	.422	.743	.495	.445	.870	.276	.639	.268	.132	.514	.290	.770	.319	.485	.275	.824	.115	.248	.121	.210	.178	.337	.601	.527	.790	.882	.367	.357	.077	.360	
	N	19	19	21	30	30	30	30	30	30	30	30	30	30	30	30	30	30	30	30	30	30	30	30	30	30	30	30	30	30	30	30	30	30	30
Epression	Pearson Correlation	.338	.234	.193	.064	.124	.100	.318	.233	-.038	-.006	-.181	.041	.101	-.049	.331	.211	-.067	-.029	.288	.001	.330	-.074	.261	.016	-.024	-.087	.395	.030	.347	-.081	.037	.076	.187	.237
	Sig. (2-tailed)	.339	.515	.593	.806	.636	.703	.214	.368	.885	.981	.486	.875	.699	.852	.195	.416	.798	.912	.262	.996	.195	.777	.311	.952	.927	.739	.117	.908	.172	.757	.887	.798	.488	.376
	N	10	10	10	17	17	17	17	17	17	17	17	17	17	17	17	17	17	17	17	17	17	17	17	17	17	17	17	17	17	17	17	16	16	16
Group	Pearson Correlation	.578**	.665**	.637**	.492**	.477**	.380*	.436*	.400*	.584**	.478**	.564**	.598**	.459**	.557**	.449**	.381*	.487**	.548**	.431*	.487**	.339	.476**	.337	.501**	.455**	.422*	.512**	.609**	.185	.383*	.359*	.302	.069	-.117
	Sig. (2-tailed)	.006	.001	.001	.003	.004	.026	.010	.019	.000	.004	.001	.000	.006	.001	.008	.026	.003	.001	.011	.003	.050	.004	.051	.003	.007	.013	.002	.000	.294	.025	.037	.093	.707	.538
	N	21	21	25	34	34	34	34	34	34	34	34	34	34	34	34	34	34	34	34	34	34	34	34	34	34	34	34	34	34	34	34	32	32	30

**. Correlation is significant at the 0.01 level (2-tailed).

*. Correlation is significant at the 0.05 level (2-tailed).

c. Cannot be computed because at least one of the variables is constant.

Table 10: Complete list of in-gene DMRs

Chromosome	Gene Name	Meth Status	ENCODE Overlap	Regions	Strand	Avg Log_2 Fold change	Avg Adj P value	# of Win	Function
14	*BEGAIN*	↑	Both	exonic	-	1.75	0.00	3	Involved in sustaning PSD
X	*ARMCX5*	↓	Both	exonic	+	3.57	0.00	1	Cellular aging and survival
4	*AC118282.5*	↓	Dnase	intronic		2.78	0.01	1	uncharacterized protein
1	*COL24A1*	↓	None	intronic	-	1.77	0.01	1	Cell adhesion
3	ROPN1B	↑	Both	downstream of TES	-	1.04	0.01	2	signal transduction
1	*COL24A1*	↓	None	intronic	-	1.59	0.03	2	ECM, cellular adhesion
4	*C4orf37*	↑	None	intronic	-	1.08	0.04	6	Unknown function
X	*GPR101*	↓	H3K4me3	exonic	-	2.59	0.04	1	G-coupled protein receptor
1	*LCE3C*	↓	None	upstream	+	1.04	0.06	3	keratinization
X	*BGN*	↓	Both	intronic	+	1.40	0.07	1	protein binding
6	*GRIK2*	↓	None	intronic	+	1.44	0.09	2	Glutamate ionotropic kianate receptor
3	*PVRL3*	↑	None	intronic	+	2.96	0.08	1	Adhesion molecule at adhesion junctions
7	*ISPD*	↓	None	intronic	-	1.04	0.09	2	Isoprenoid biosynthetic process
8	*CNBD1*	↑	None	intronic	+	1.00	0.10	1	Binds cyclic nucelotides
10	*NEBL*	↓	None	intronic	-	2.00	0.11	2	Actin-binding related protein
16	*ACSM3*	↓	H3K4me3	intronic	-	1.68	0.15	2	acyl-CoA synthetase
3	*TXNRD3*	↑	None	intronic	-	2.82	0.16	1	Thioredoxin reductase, cell growth and survival
6	*PKHD1*	↑	None	intronic	-	1.57	0.17	1	Regulation of cell division
4	*DAPP1*	↓	H3K4me3	Intronic	+	2.68	0.18	1	signal transduction

Some of these genes have multiple windows of methylation differences; altogether this list represents 34 DMRs of the total 115 (~30%). *Meth status* refers to whether the regions shows an increase (↑) or decrease (↓) in methylation. *ENCODE overlap* refers to number of ENCODE features overlaping with the DMR, if one the specific feature or no overlap. *Region* describes the general genomic region where the DMR is found for that gene. *Strand* refers to the location of the genes, either on the sense (+) or antisense (−) strand. *Avg log_2 fold change* is the absolute difference of methylation at that site, it is averaged to account for the multiple windows (DMRs) found in the gene. *Avg Adj p value* is the significance of the fold change adjusted to correct for multiple testing, averaged as before. *# of win* is the

number of windows found within that gene; a window represents a differentially methylated region. *Function* is a brief functional description of the gene. The list is ranked by DMR containing windows, and then lowest avg adj p value and avg $\log_2$ fold change.

Figure 14: Fluorescent assisted Cell sorting (FACs)

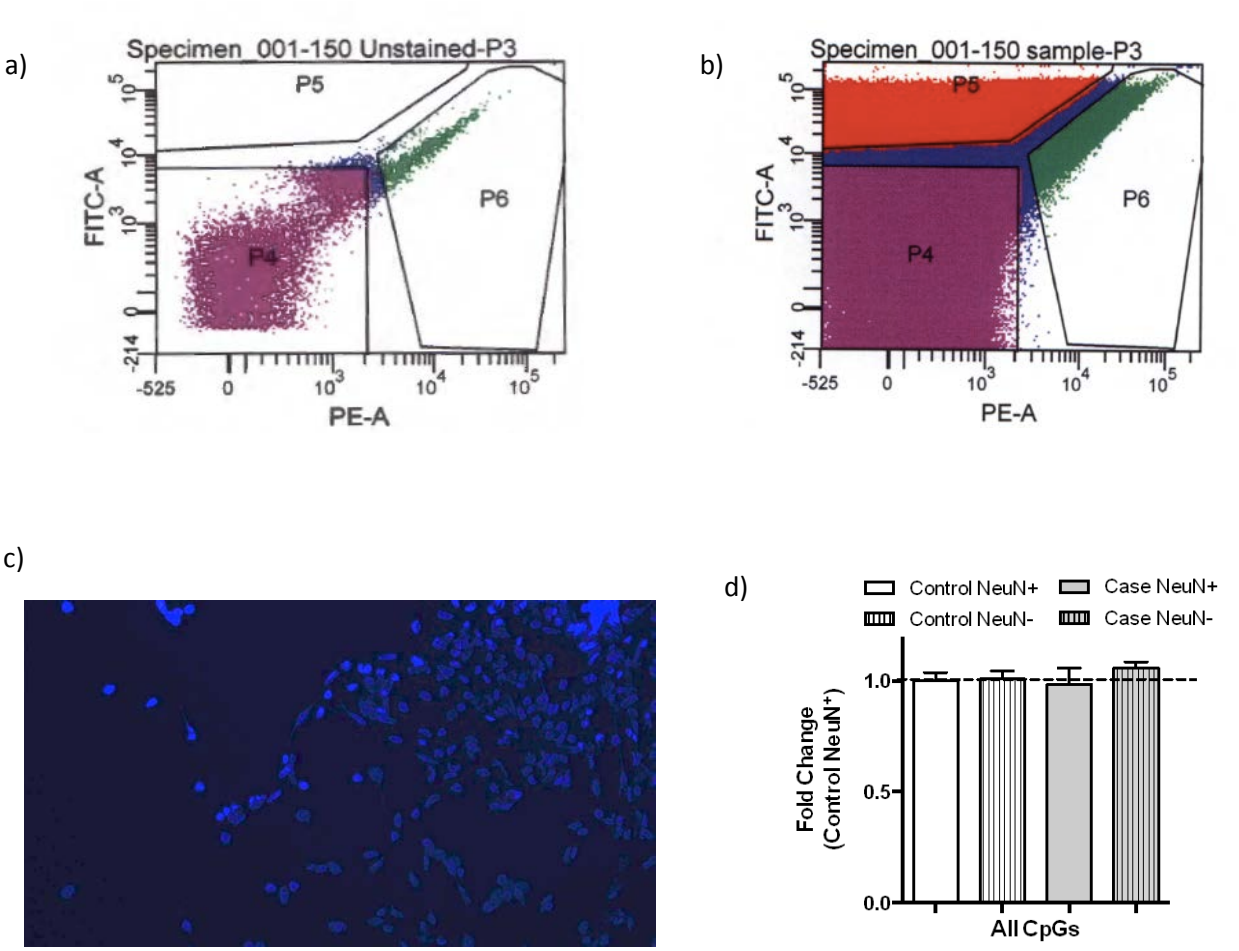

FACs was used to separate neuronal and non-neuronal cell types a) Unstained specimen refers to the non-neuronal cell type as neuronal cells were tagged using NeuN; a protein specific to the nuclear membrane of neurons. This scatterplot shows these cells are filtered by P4. b) Running the sample with gates P4 to identify unstained non-neuronal samples, P5 to identify neuronal samples stained with Alexa 488 secondary and P6 for discarding unidentified wastes particles. c) DAPI stained nuclei post sort to assure collection was successful. d) e) GRIK2 FAC sorted samples show no difference in the contribution of methylation from either cell fraction in either group (n=9 for all 4 groups, avg. 17 clones/sample, Kruskal-Wallis F (4, 37) = 3.481, P = 0.323).

Figure 15: Chromatin State Segmentation using HMM from ENCODE at BEGAIN 474bp Amplicon shows both enhancer and promoter potential.

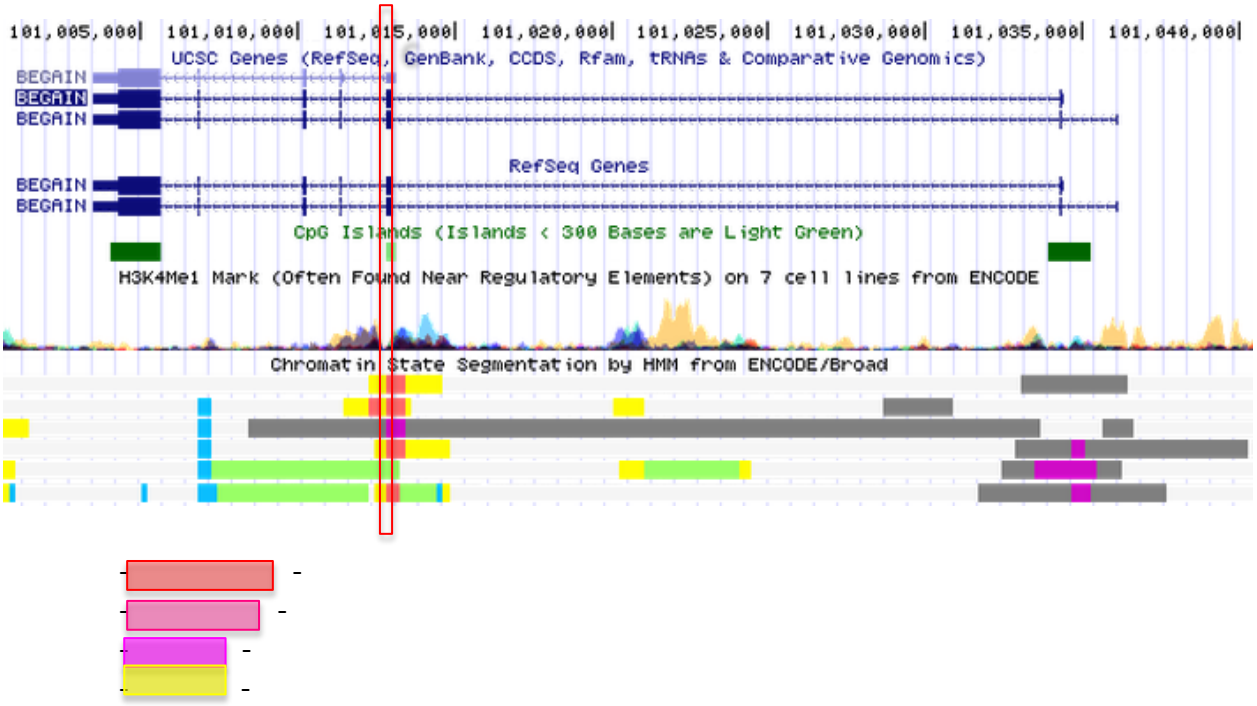

According to in-silico data produced by the ENCODE project this 474 bp region of BEGAIN has the biological infrastructure to act as both a promoter and enhancer.

Figure 15: Luciferase Activity

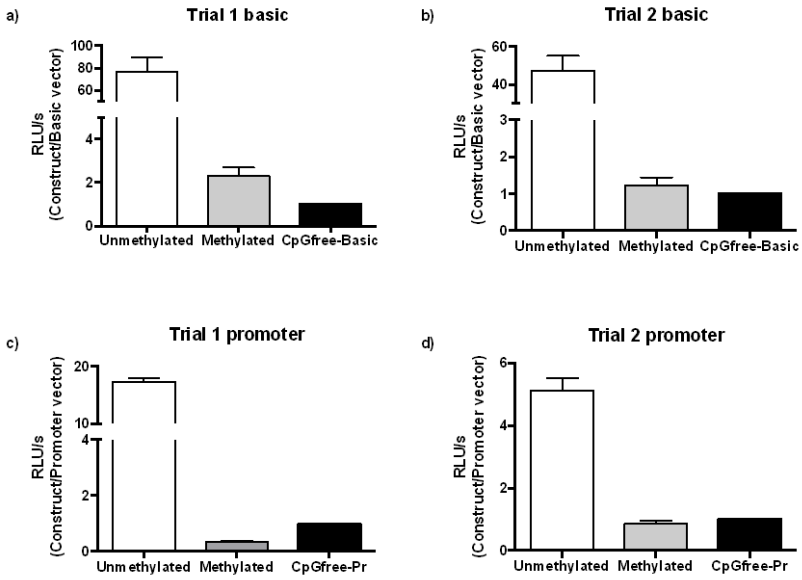

Functional cell assays were repeated independent for both the basic construct (a and b) containing no endogenous promoter) and the promoter constructs (c and d). Each independent trial was conducted in quintuplicate and presented as a fold change to the control vector. Statistical results for independent trials show overall differences between unmethylated and methylated or vector condition (in all case Kruskal-Wallis p value <0.001), however statistical power is weak; therefore results are present in text as a combination of trials. Here we show consistency between independent trials.

Supplemental Methods

I) Histological sectioning

Sectioning was performed at 4°C, and sections were snap frozen in isopentene at −80°C. Experienced histopathologists using reference neuroanatomical maps identified and dissected the neuroanatomical regions. In all cases, 1-cm^3 human tissue blocks were paraffin embedded, cryostat sectioned, slide mounted, and examined for any signs of disease by 2 independent neuropathologists in at least 3 different brain regions. All sections were cryostat cut at 15 μm.

II) Gene expression analysis

RNA was extracted from the prefrontal cortex using Qiagen RNeasy kit (Hilden, Germany Cat. #74104). Both nanodrop and Agilent 2100 BioAnalyzer were used to assess the quality and quantity of all extracted RNA. RNA Integrity Numbers (RIN) were not significantly different between cases (n=76) and controls (n=45) (control 6.1 (±0.13), case 6.2 (±0.10), p=0.67). cDNA for real time quantitation was synthesized using M-MLV reverse transcriptase from Invitrogen (28025-013, Life technologies) and 16mer oligo (dT) for primer the poly-A tail inherent to mRNA. The cDNA product was verified by agarose gel. We used Taqman probes (ABI, Life technologies Carlsbad, California, U.S.) to quantify gene expression levels by real-time PCR (RT-PCR). *GFAP* (Hs00*) ALDH1L1* (Hs00201836_m1), *RBFOX3* (Hs01370653_m1), *GJA1* (Hs00748445_s1), *GJB6* (Hs00917676_m1), *SOX9* (Hs00165814_m1), *GLUL* (Hs01013055_g1), and *SLC1A3* (Hs00904824_m1). We assessed transcript levels by relative quantification (RQ) using the endogenous control *ATCB (4310881E).* RQ values were assessed using RQ manage from ABI.

III) MBD methylation pulldown, library preparation and sequencing (MBD-Seq)

DNA was extracted using the Qiagen QIAamp (Cat.# 51304) from prefrontal cortex, and all DNA was quality assessed using the Agilent 2100 Bioanalyzer. Equal concentrations of DNA were sheared by sonication using the Cole Parmer Ultrasonic processor. DNA was pulse sonicated on ice, 4 rounds of 30 seconds with the sonicating probe on and 30 seconds rest, to obtain fragment sizes between 200-500bps. To enrich for methylated regions of DNA, we followed the MethylMiner™ Methylated DNA Enrichment Kit (ME10025, Life Technologies) protocol, which uses the MBD-biotin protein. We made the following changes: the elution step was carried out with proteinase K (Qiagen Cat.# 19131) at 62° for 2hrs to isolate all methylated DNA from magnetic beads. The DNA was extracted from protein by phenol/chloroform extraction and ethanol precipitation. The pellet was resuspended in 30 μL of water to provide the correct starting volume for creation of Illumina ChIP libraries for downstream sequencing. MBD-DNA was subjected to an Illunima (San Diego, California, U.S.) library preparationThe libraries were amplified with single read sequencing primers and Phusion DNA polymerase using the following thermocycling profile: 30 seconds at 98°C, then 15 cycles of (10 seconds at 98°C, 30 sec at 65°C, 30 seconds at 72°C), 5 minutes at 72°C and hold at 4°C. The amplified libraries were purified using AMPure magnetic beads (Beckman Coulter, Brea, CA.), to reduce loss and eliminate primer and adapter dimer.

The ChIP fragments undergo end repair using Polymerase I Klenow fragment to digest 3’ overhangs and adding a phosphate group to the 5’ –hydroxyl terminus of the double stranded DNA. A polyadenosine tail is then added to the

repaired ends using Klenow Fragment with no 3'-5' exonuclease activity. Sequencing adaptors were added to the poly (A) tail using Quick T4 DNA Ligase. The adaptors were diluted 1:30 to adjust for the smaller quantity of DNA resulting from the pulldown. Excess adaptors are known to interfere with sequencing. The libraries were then size selected using E-gel size select gels capturing fragment of ~200bp.

IV) MBD-Seq analysis

DNA libraries were sequenced at the Genome Quebec and McGill University Innovation Center using Illumina 36 base pair single read sequencing on the Genome Analyser II and using one sample per lane. Raw reads were aligned to the human genome (assembly hg19) using BWA (http://bio-bwa.sourceforge.net/). Reads with non-unique alignments and reads with duplicate alignments were omitted from analysis. DMRs were assessed using individual samples in the DESeq software package and methylation levels within each window were estimated as described in Down et al. [7]. The genome was tiled using overlapping 500 bp windows at every 250 bp (e.g. the first 1500 bp of chr1 are tiled with the following intervals: 1-500, 250-750, 500-1000, 750-1250, 1000-1500, 1250-1750). Windows containing no 36bp genomically unique sequences were omitted from analysis. Such windows were called "unmappable" (list obtained from http://www.rglab.org/). Each window was assigned a read count equal to the number of reads that intersected the window, following in-silico extension of each read by 400bp to reflect the average sequenced DNA fragment length. Around 80% of the mappable windows overlapped with at least 20 reads when reads were pooled among all samples.

Differentially methylated regions (DMRs) were identified using the negative binomial test implement in the DESeq software package [8] to compare window read counts between cases and controls. To be called a DMR, the log2-fold read count difference between cases and controls had to be at least 1, there had to be an average of at least 3 reads per sample in cases or controls, and the multiple-testing adjusted p-value (i.e. false discovery rate) obtained from the negative binomial test had to be less than 0.2.

Methylation levels within each window were estimated as described in Down et al. [7]. Assuming an average DNA fragment length of 500bp, we obtained 20x coverage per base of 80% of the mappable genome (uniquely mappable with 36bp of sequence; http://www.rglab.org/).

All false discovery rates were calculated using the Benjamini –Hochberg algorithm.

V) Astrocyte-related Genes

Genes with astrocyte-related functions were identified by selecting relevant gene sets from the Gene Ontology [9] and from a list of genes with astrocyte-specific function identified by Cahoy et al. [10]. Gene Ontology gene sets labeled with the following functions were included: lactate transport, inflammation, glutamate homeostasis, ion homeostasis, water homeostasis, glycogen storage, oxidative stress, glutathione metabolism and calcium signalling.

VI) ENCODE DNase I hypersensitivity, histone modification and DNA binding profiles

DNase I hypersensitivity sites were obtained from the ENCODE analyses distributed with the UCSC Genome Browser (http://genome.ucsc.edu/cgi-bin/hgTrackUi?hgsid=302751301&g=wgEncodeRegDnaseClustered). The

sites were obtained from assays applied to a large number of cell types. We thus merged the sites for all of the cell types (with Integ Cluster scores > 100) into a single set of sites.
Enrichment of sites/peaks with DMRs was determined by partitioning the genome into 250bp windows and then applying Fisher's exact test to determine whether or not the number of windows overlapping with DMRs and peaks were statistically significantly more than expected by chance.
Several histone mark profiles and DNA binding sites of DNA binding proteins relevant to epigenetics were obtained from the ENCODE analyses (http://encodeproject.org/ENCODE/dataMatrix/encodeChipMatrixHuman.html).
These include:
CBP, CBX2, CBX3, CBX8, CHD1, CHD4, CHD7, CTCF, EZH2, H2A.Z, H3K27ac, H3K27me3, H3K27me3B, H3K36me3, H3K36me3B, H3K4me1, H3K4me2, H3K4me3, H3K4me3B, H3K79me2, H3K9ac, H3K9acB, H3K9me1, H3K9me3, H4K20me1, HDAC1, HDAC2, HDAC6, JARID1A, JMJD2A, LSD1, NCoR, NSD2, P300, p300, PCAF, PHF8, PLU1, Pol2(b), RBBP5, REST, RNF2, SAP30, SETDB1, SIRT6, SUZ12.

Sets of peaks (with detection p < 10E-20) derived from multiple cell types for a single histone mark or DNA binding protein were merged into a single set of peaks.

VII) High Resolution melting

DNA was bisulfite converted using EpiTect Bisulfite kit from Qiagen (Cat.# 59104). Briefly, DNA extracted from brain tissue was treated with sodium bisulfite, cycling between 95°C and 60°C for 5hrs. These conditions result in deamination of the cytosine into a uracil, except in the presence of 5-methylcytosine. Real time PCR primers were designed using Methyl Primer Express Software V1.0 (Applied Biosystems) to produced amplicons of ~200bp. ABI Melt Doctor was used to assess differences in melt temperature of methylated and non-methylated cytosines of DNA amplicons. Post PCR, the reactions are slowly heated in the 7900HT Fast Real-Time system from ABI, which captures extensive fluorescent data points per change in temperature, with high precision [11]. Analysis of data points was conducted using an in-house script. The in house script used estimates the midpoint between the temperature at which the DNA begins to denature (take-off) as seen by a sudden decrease in fluorescence, and the temperature at which the DNA is completely denatured (touch-down), signaled by fluorescence levels stabilizing. The melting curve is normalized so that normalized fluorescence begins at a value of 1 and at take-off begins to decrease until it reaches 0 at touch-down. The temperature at which normalized fluorescence reaches a value of 0.5 corresponds with the temperature at which half of the DNA is denatured and therefore to the melting temperature of the DNA. As DNA methylation of a given genomic region increases, melting temperature of that similarly increases because methylated cytosines are protected from conversion to uracil during bisulfite treatment. Primers for *GRIK2* forward 5'-GTGTTATTTTGGAAATTATTTAAAGA-3' and reverse 5'-CCTAAACTTATCAATTCTCACAA-3' and *BEGAIN* forward 5'-GAGTTTGTGTGTGGTGTAGGATAGT-3' and reverse 5'-AACCTACRAACCTTAATTT CCCC-3'

VIII) Site-specific Bisulfite Sequencing

DNA was bisulfite converted as described in the previous section and regions of interest were isolated by PCR with primers design as before. The PCR product was cloned into pCR™2.1-TOPO® TA vector (Life Technologies, Invitrogen) and 20 colonies per sample were sequenced using Sanger sequencing, and M13R as the sequencing primer. Only high quality sequences were kept. An average of 17 clones per sample for *GRIK2* and 11 for *BEGAIN* had quality Sanger sequences. Combining samples for *GRIK2* gave an average of 350 clones analysed per CpG site while *BEGAIN* averaged around 200 clones, providing more than adequate depth for each group. The sequences were oriented and aligned to the methylated reference using SeqMan Pro™ (DNAstar Inc. 2012, Wisconson, USA). A mixed model regression and pairwise comparisons were used to analyze for site-specific methylation levels at each CpG. Cloning primers for *GRIK2*, forward 5'- TGTGAGAATTGATAAGTTTAGGG-3', reverse 5'-ATTTAAACAATACAACCCCAAA-3' and *BEGAIN* 5'- GTTTGTGTGTGGTGTAGGATAGT-3' and reverse 5'-AATCACCTATACCACCCAAAA-3'. The same procedure and primers were used on FAC sorted cell for cell specific methylation levels.

IX) Nuclei isolation and Fluorescent assisted cell-sorting (FACs)

We extracted 150 mg of brain sample and homogenize by douncing in 5ml of lysis buffer. A sucrose gradient is created by adding the homogenate to 9mls of sucrose solution, entire solution is then ultracentrafuged for 2 hours and 3 minutes at 24 400 rpm. All debris and supernatant are removed with vacuum. Pellet is then gently dissociated from tube with 500 ul of PBS. Neuronal nuclei are then immunotagged with 1.2ul anti-NeuN (Ms) (Millipore Cat# MAB377) and 1.0ul anti-Ms IgG (Alexa 488) (Millipore Cat# 16-240) in 300 ul of 1X PBS, 100ul of blocking mix containing 0.5% BSA and 10% normal goat serum in 1X PBS. A negative control is prepared for each sample as above excluding NeuN. Solutions without nuclei are mixed and incubate them at room temperature for 5 minutes in the dark. Nuclei is then added to solution and incubated while rotating at 4° in the dark for 45min. Isolate neurons via FACS by first filtering the neuronal fraction through a 40um filter (Nitex mesh) to remove clumps, then run the samples with the appropriate settings. Sort neuronal fraction and the non-neuronal fraction in different tubes containing PBS (10ml) and be sure the debris is isolated alone. Post FACS take 10ml of sorted samples and add 2ml of sucrose solution, 50ul of 1M CaCl2, and 30ul of 1M Mg (Ace)2. Invert and incubate on ice for 15 minutes, centrifuge the samples for 15min at 4°C. Vacuum supernatant without disturbing the white pellet. We resuspended the pellet in 200ul of H_2O and stored at -80°C for later use.

X) Functional cell assay

The 474bp sequence of BEGAIN was amplified by PCR from genomic DNA with primers including AvrII and BamHI sites at the 5' and 3' ends, respectively. The amplified fragment was digested by AvrII and BamHI and was inserted into luciferase reporter vectors CpGfree-basic and CpGfree-Promoter. The final constructed vectors were named B-Begain and P-Begain.

These vectors were then transfected in a human neuroblastoma cell line, Be(2)C purchased from ATCC and maintained in Eagle's Minimum Essential Medium (EMEM, ATCC) containing 10% fetal bovine serum, 100 U/ml Penicillin and 100ug/ml Streptomycin in incubator at 37°C with 5% CO2.

The Be(2)C cells were seeded into 48-well plates, transiently co-transfected with 197.5ng of Lucia luciferase reporter vector containing the BEGAIN sequence and 2.5ng or firefly luciferase vector as an internal control. Vectors were transfected into Be(2)C cells using Lipofectamine LTX and PLUS Reagent. Luciferase assay was performed 24 hours after transfection.

Luciferase Reporter Assay

After 24 hour transfection, supernatant from each well was collect, cells were then washed with PBS once, lysed for 15min at room temperature, and luciferase activities were measured using a Dual-Luciferase Reporter Assay System. The reporter assays were performed in quintuplicates. The relative luciferase activity was calculated by Lucia luciferase activity / firefly luciferase activity. Data were presented as fold change to control vector. This experiment was repeated twice independently.

Supplemental references

1. **Ernst C, Nagy C, Kim S, Yang J, Deng X, Hellstrom I *et al.* Dysfunction of astrocyte connexins 30 and 43 in dorsal lateral prefrontal cortex of suicide completers. *Biological psychiatry* 2011; 70(4): 312-319.**

2. **Kremsky I, Morgan T, Hou X, Li L, Finch C. Age-changes in gene expression in primary mixed glia cultures from young vs. old rat cerebral cortex are modified by interactions with neurons. *Brain, behavior, and immunity* 2012; 26(5): 797-802.**

3. **Morgan T, Xie Z, Goldsmith S, Yoshida T, Lanzrein A, Stone D *et al.* The mosaic of brain glial hyperactivity during normal ageing and its attenuation by food restriction. *Neuroscience* 1999; 89(3): 687-699.**

4. **Nichols N, Day J, Laping N, Johnson S, Finch C. GFAP mRNA increases with age in rat and human brain. *Neurobiology of aging* 1993; 14(5): 421-429.**

5. **Li H, Durbin R. Fast and accurate long-read alignment with Burrows-Wheeler transform. *Bioinformatics (Oxford, England)* 2010; 26(5): 589-595.**

6. **Su AI, Wiltshire T, Batalov S, Lapp H, Ching KA, Block D *et al.* A gene atlas of the mouse and human protein-encoding transcriptomes. *Proc Natl Acad Sci U S A* 2004; 101(16): 6062-6067.**

7. **Down T, Rakyan V, Turner D, Flicek P, Li H, Kulesha E *et al.* A Bayesian deconvolution strategy for immunoprecipitation-based DNA methylome analysis. *Nature biotechnology* 2008; 26(7): 779-785.**

8. **Brenet F, Moh M, Funk P, Feierstein E, Viale A, Socci N *et al.* DNA methylation of the first exon is tightly linked to transcriptional silencing. *PloS one* 2011; 6(1).**

9. **Ashburner M, Ball CA, Blake JA, Botstein D, Butler H, Cherry JM *et al.* Gene ontology: tool for the unification of biology. The Gene Ontology Consortium. *Nature genetics* 2000; 25(1): 25-29.**

10. **Cahoy J, Emery B, Kaushal A, Foo L, Zamanian J, Christopherson K *et al.* A transcriptome database for astrocytes, neurons, and oligodendrocytes: a new resource for understanding brain development and function. *The Journal of neuroscience : the official journal of the Society for Neuroscience* 2008; 28(1): 264-278.**

11. **Wojdacz TK, Dobrovic A. Methylation-sensitive high resolution melting (MS-HRM): a new approach for sensitive and high-throughput assessment of methylation. *Nucleic Acids Res* 2007; 35(6): e41.**

All 115 DMRs

DMR	chr	start	end	foldChange	log2FoldChange	pval	padj	log2MedianChange
1	1	86405501	86406000	3.05095551	-1.6093	7.99E-07	0.02789	1.498454
2	1	86405751	86406250	2.97849354	-1.5746	1.31E-06	0.03859	1.498454
3	1	86406001	86406500	3.41891332	-1.7735	1.78E-07	0.00996	1.498454
4	1	104573751	104574250	0.25153372	1.99118	9.88E-07	0.03258	-2.4975
5	1	104574001	104574500	0.25145231	1.99164	1.60E-10	3.79E-05	-3.08328
6	1	104574251	104574750	0.2464986	2.02035	9.89E-11	2.51E-05	-2.47486
7	1	104574501	104575000	0.25477361	1.97271	2.55E-10	5.69E-05	-1.96963
8	1	121357501	121358000	4.13472271	-2.0478	1.55E-09	0.00026	0.639668
9	1	121357751	121358250	10.0698395	-3.332	3.05E-15	1.70E-09	0.326501
10	1	121482751	121483250	3.77751252	-1.9174	1.13E-05	0.17833	-0.20401
11	1	121483501	121484000	10.015064	-3.3241	2.90E-21	4.04E-15	0.498119
12	1	143282751	143283250	3.2417932	-1.6968	9.93E-07	0.03266	-0.23133
13	1	143283501	143284000	4.46846043	-2.1598	6.62E-06	0.12196	0.349584
14	1	152564501	152565000	2.02783514	-1.0199	4.99E-06	0.10054	0.517747
15	1	152564751	152565250	2.0808554	-1.0572	1.05E-06	0.03365	0.517747
16	1	152565001	152565500	2.08141453	-1.0576	1.23E-06	0.03689	0.373124
17	2	48276001	48276500	0.15461536	2.69324	6.03E-06	0.11351	-0.69067
18	2	48276251	48276750	0.1705776	2.5515	8.69E-06	0.14811	-0.69067
19	2	90372751	90373250	13.2449811	-3.7274	1.65E-13	7.67E-08	0.505235
20	2	90373001	90373500	12.6252763	-3.6582	1.14E-12	4.75E-07	0.505235
21	3	110987501	110988000	0.12828558	2.96257	3.49E-06	0.07726	-1.07155
22	3	125709001	125709500	2.10855999	-1.0763	3.94E-07	0.01738	1.085346
23	3	125709251	125709750	2.0037744	-1.0027	1.70E-07	0.00988	1.628266
24	3	126358751	126359250	0.14136375	2.82252	9.33E-06	0.15709	-0.25457
25	3	166368251	166368750	0.49610632	1.01128	5.67E-06	0.10796	-1.30415
26	3	166368501	166369000	0.47729861	1.06704	2.30E-06	0.05627	-1.3156
27	4	49109251	49109750	11.4949709	-3.5229	6.94E-08	0.00493	0.39689
28	4	49109501	49110000	8.76030667	-3.131	5.53E-08	0.00417	0.505235
29	4	49109751	49110250	6.86155765	-2.7785	1.26E-07	0.00776	0.622633
30	4	49114251	49114750	5.04140375	-2.3338	5.39E-06	0.10506	0.736966
31	4	49323001	49323500	3.57088712	-1.8363	4.33E-12	1.51E-06	0.277368
32	4	49323751	49324250	3.92703934	-1.9734	5.33E-07	0.02102	0.409391
33	4	49512251	49512750	2.36637609	-1.2427	4.89E-06	0.09942	-0.20687
34	4	98110251	98110750	0.47323346	1.07938	5.17E-07	0.02064	-0.8026
35	4	98110501	98111000	0.47868434	1.06285	8.31E-07	0.02882	-1.02432
36	4	98110751	98111250	0.46465304	1.10577	5.52E-07	0.02138	-0.9871
37	4	98133001	98133500	0.47376007	1.07777	2.80E-06	0.06572	-1.00737
38	4	98133251	98133750	0.47225529	1.08236	2.27E-06	0.05583	-1.00737
39	4	98133501	98134000	0.47442126	1.07576	3.26E-06	0.07504	-0.86323
40	4	100740751	100741250	6.39291882	-2.6765	1.13E-05	0.17776	0.929611
41	4	125658251	125658750	0.18818492	2.40978	5.13E-06	0.10235	-0.90858
42	4	125658501	125659000	0.25403333	1.97691	3.26E-06	0.07504	-0.20231
43	4	162263251	162263750	0.32996097	1.59963	3.27E-12	1.22E-06	-2.59158
44	4	162263501	162264000	0.33945471	1.55871	3.11E-12	1.19E-06	-2.29576
45	4	162263751	162264250	0.34324215	1.5427	3.73E-12	1.34E-06	-2.19492
46	4	162264001	162264500	0.41070914	1.28381	1.09E-05	0.17476	-1.15587
47	5	33355251	33355750	0.31772807	1.65414	1.23E-06	0.03689	-1.82782
48	5	33355501	33356000	0.32246723	1.63278	3.77E-06	0.08216	-1.90182
49	5	33355751	33356250	0.33099845	1.5951	7.40E-06	0.13224	-1.90182
50	5	62704001	62704500	0.31527151	1.66533	2.87E-06	0.06707	-0.20482
51	6	51517001	51517500	2.96910149	-1.57	1.05E-05	0.16992	1.120752
52	6	102435751	102436250	2.70296061	-1.4345	3.92E-06	0.08406	1.380143
53	6	102436001	102436500	2.71571164	-1.4413	4.62E-06	0.09527	1.186413
54	7	16173251	16173750	2.08355299	-1.059	3.61E-06	0.0792	0.706099
55	7	16173501	16174000	2.03581002	-1.0256	4.99E-06	0.10054	0.598541

56	7	61970251	61970750	9.79787426	-3.2925	3.39E-23	6.26E-17	-0.20401
57	8	88272251	88272750	0.49920061	1.00231	4.70E-06	0.09677	-1.05554
58	10	2095501	2096000	0.48405992	1.04674	6.86E-06	0.12509	-0.42231
59	10	2095751	2096250	0.47611337	1.07062	9.40E-06	0.15755	-0.59525
60	10	9474501	9475000	0.47950743	1.06037	7.92E-06	0.13818	-1.93575
61	10	9474751	9475250	0.4642298	1.10709	3.82E-06	0.0823	-1.93575
62	10	21192501	21193000	3.69587684	-1.8859	7.82E-06	0.13686	1.073249
63	10	21192751	21193250	4.3261072	-2.1131	4.07E-06	0.08633	1.457348
64	10	42400251	42400750	5.59174047	-2.4833	2.33E-10	5.31E-05	-0.66297
65	10	42528001	42528500	6.06142971	-2.5997	2.49E-06	0.06018	0.666576
66	10	42597001	42597500	2.52462796	-1.3361	1.48E-08	0.00153	-0.45618
67	12	77964501	77965000	4.02280586	-2.0082	1.02E-06	0.03308	1.067114
68	12	77964751	77965250	3.31213264	-1.7278	3.87E-06	0.08337	1.261668
69	13	47689501	47690000	0.23161704	2.11019	2.18E-07	0.01166	-0.25457
70	13	47689751	47690250	0.30874042	1.69553	4.23E-06	0.08849	-0.73697
71	13	57975501	57976000	0.42609702	1.23075	4.76E-06	0.09778	-2.21299
72	13	81797501	81798000	0.47954496	1.06026	1.18E-05	0.18435	-0.7997
73	13	105161501	105162000	0.38890489	1.36251	9.81E-06	0.16269	-1.37474
74	14	26004501	26005000	0.2581909	1.95349	6.44E-06	0.11912	-1.66928
75	14	26046501	26047000	0.23337504	2.09928	1.41E-07	0.00861	-2.10818
76	14	26046751	26047250	0.2306089	2.11648	3.67E-07	0.01662	-2.10818
77	14	101012501	101013000	0.29838781	1.74474	4.79E-09	0.00067	-1.54641
78	14	101012751	101013250	0.29713547	1.75081	1.16E-09	0.00021	-1.85394
79	14	101013001	101013500	0.29587549	1.75694	1.42E-08	0.00151	-1.6845
80	16	20778251	20778750	3.2255021	-1.6895	7.36E-06	0.13198	1.75743
81	16	20778751	20779250	3.20527612	-1.6804	1.06E-05	0.1703	1.75743
82	16	46385251	46385750	4.55191531	-2.1865	7.35E-06	0.13198	0.665581
83	16	46391001	46391500	2.3189591	-1.2135	2.21E-06	0.05489	-0.22556
84	16	46395001	46395500	9.81948921	-3.2956	1.30E-14	6.89E-09	-0.31719
85	16	46395251	46395750	9.79597796	-3.2922	9.11E-12	2.90E-06	-0.20482
86	16	46402501	46403000	6.2203099	-2.637	4.90E-09	0.00067	0.975197
87	16	46402751	46403250	3.47786584	-1.7982	3.65E-07	0.01662	1.404755
88	16	46403001	46403500	3.94960582	-1.9817	1.32E-16	9.23E-11	0.68966
89	16	46403251	46403750	5.33087915	-2.4144	6.89E-30	1.54E-23	0.32709
90	16	46403501	46404000	5.48041767	-2.4543	2.47E-30	6.88E-24	0.299225
91	16	46407751	46408250	5.22035417	-2.3841	2.35E-08	0.00216	0.353637
92	16	46408001	46408500	4.47598773	-2.1622	9.37E-07	0.03143	0.201634
93	16	46408251	46408750	4.67346236	-2.2245	1.15E-06	0.03584	0.51307
94	16	46425251	46425750	8.66006543	-3.1144	9.64E-20	8.96E-14	0.309855
95	17	81153251	81153750	2.95705179	-1.5642	9.50E-06	0.15823	0.218346
96	17	81153501	81154000	5.18614581	-2.3747	6.40E-06	0.11847	0.710493
97	18	69807001	69807500	2.92639414	-1.5491	5.54E-06	0.10659	0.728516
98	18	69807251	69807750	2.88779766	-1.53	4.28E-06	0.08941	1.020909
99	19	37784001	37784500	3.96874666	-1.9887	1.74E-07	0.00996	0.500265
100	19	37784251	37784750	3.43624288	-1.7808	8.79E-11	2.39E-05	0.324129
101	19	37784501	37785000	3.43624288	-1.7808	8.79E-11	2.39E-05	0.324129
102	19	37784751	37785250	3.05176576	-1.6096	1.34E-08	0.00145	0.324129
103	21	9695501	9696000	3.04536322	-1.6066	1.28E-08	0.0014	0.366494
104	21	9695751	9696250	5.02185258	-2.3282	8.66E-17	6.44E-11	0.415037
105	21	9696001	9696500	7.52487127	-2.9117	4.01E-19	3.20E-13	0.294905
106	X	101854251	101854750	11.8962319	-3.5724	5.75E-09	0.00075	0.254573
107	X	106749751	106750250	8.50111063	-3.0877	8.41E-08	0.00572	0.718229
108	X	106750001	106750500	4.15217985	-2.0539	1.17E-06	0.03597	0.294905
109	X	136113501	136114000	6.00974955	-2.5873	1.69E-06	0.04475	0.482152
110	X	136134501	136135000	9.50583575	-3.2488	3.11E-07	0.01493	0.39689
111	X	136134751	136135250	13.9506385	-3.8023	7.42E-09	0.00092	0.913288
112	X	136135001	136135500	10.4981169	-3.3921	1.76E-08	0.00177	0.645717
113	X	152765251	152765750	2.64191863	-1.4016	3.04E-06	0.07067	1.04258
114	Y	58883251	58883750	3.32189826	-1.732	3.81E-07	0.01719	0.551174
115	Y	58883501	58884000	3.3714273	-1.7534	2.43E-07	0.01264	0.551174